DISSERTATION

USE OF THE INERTIAL MEASUREMENT UNIT TO ASSESS NORMAL AND ABNORMAL EQUINE HOOF KINEMATICS

Submitted by

Valerie J. Moorman

Department of Clinical Sciences

In partial fulfillment of the requirements

For the Degree of Doctor of Philosophy

Colorado State University

Fort Collins, Colorado

Spring 2013

Doctoral Committee:

Advisor: Christopher E. Kawcak

C. Wayne McIlwraith
Raoul F. Reiser II
Kevin K. Haussler

ABSTRACT

USE OF THE INERTIAL MEASUREMENT UNIT TO ASSESS NORMAL AND ABNORMAL EQUINEHOOF KINEMATICS

Lameness is a major medical concern and results in a large economic impact for both horse owners and the equine industry. In addition, subtle to mild lameness can result in poor performance, which can result in decreased competition winnings. While the subjective lameness examination is the most common tool for lameness evaluation, its sensitivity and repeatability have been shown to be poor, especially for subtle and mild lameness.

This has led to the development of objective methods to supplement the subjective lameness examination, including stationary force platform analysis, optical kinematics, and horse-based inertial sensor systems. Several of these methods have been shown to be sensitive in identifying lameness. However, stationary force platform and optical kinematics are largely confined to experimental settings, are expensive and time-consuming, and require expertise for collecting and analyzing data. Horse-based systems have become widely investigated, as the components are small, light-weight, telemetric, and can be more easily used in a clinical setting. One specific system with poll and pelvis-mounted sensors, allows for real-time identification of asymmetry, which objectively supplements the subjective lameness examination. While this inertial-sensor system has been shown to be sensitive enough to detect subtle lameness at the trot, it cannot accurately detect bilateral forelimb lameness at the trot and has not been investigated for use evaluating other gaits. As previous optical methods have shown that distal limb kinematics are altered with moderate lameness and the hoof is an ideal place to rigidly

mount a small sensor, the kinematics of the hoof should also be investigated to determine if mild lameness can also be detected in this manner.

Inertial measurement units (IMU) combine a three-dimensional accelerometer, three-dimensional rate gyroscope, three-dimensional magnetometer, and thermostat. By the integration of these signals, these sensors allow determination of linear and angular kinematics in a global coordinate system. IMUs have been investigated for their use in assessing equine locomotion, by attaching them to the body of a horse. However, an IMU has not been previously utilized on the hoof of the horse. As emerging IMUs are small, light-weight, and often wireless, they have appropriate characteristics to measure hoof kinematics and may be a useful method of also objectively determining abnormal hoof kinematics associated with lameness.

As optical methods are currently the gold standard for assessing distal limb kinematics, we used these as a standard to which to compare both linear and angular kinematics determined by an IMU. In the first experiment, optical methods were used to validate the IMU in five clinically normal horses. Walk and trot data were collected on a single forelimb and hind-limb, as the horse was led over-ground, and three-dimensional linear and angular kinematics were compared between the two systems. In the second experiment, three grades of lameness were induced in a single forelimb in six clinically normal horses, and following the most severe lameness, peri-neural anesthesia of the medial and lateral palmar nerves was performed to alleviate the lameness. Using optical kinematics, intra- and inter-limb comparisons were made at the walk and trot at baseline, and following lameness and peri-neural anesthesia. Linear variables were assessed in the cranial-caudal and vertical directions, as well as sagittal plane orientation

(Θ). Intra-limb changes to three-dimensional orientation were assessed in the lame forelimb with the IMU.

In the first study, the IMU was found to produce similar, yet not identical, kinematics to the optical system. While the IMU produced highly correlated data in the sagittal plane, the linear and angular profiles in the other planes showed similar trends to the optical system. In the second set of experiments, multiple linear and angular variables of the hoof were altered following induction of lameness, using both kinematic methods. The optical and IMU systems both identified significant changes in sagittal plane (Θ) orientation with lameness. In addition, hoof kinematics were significantly altered in mild lameness at the trot and when no lameness could be visually assessed at the walk. The IMU also detected significant changes in the frontal and transverse planes of rotation following lameness. After peri-neural anesthesia, the IMU detected a significant increase in variance in Θ orientation.

Overall, it was demonstrated that the IMU can be mounted on the hoof to measure both normal kinematics and detect significant orientation changes following both lameness and peri-neural anesthesia. The IMU appeared to be a sensitive device to evaluate hoof kinematics even when lameness is mild or undetectable to the human eye. While its usefulness on clinical lameness has yet to be determined, the IMU should be further investigated for its use in a non-research setting.

ACKNOWLEDGEMENTS

I would like to personally thank my graduate committee, especially Drs. Wayne McIlwraith and Chris Kawcak for providing me an optimal environment to pursue an area of research that requires collaboration with experts outside of the field of veterinary medicine. Thank you for providing me with a number of individuals whom may be future collaborators. I especially thank Dr. Raoul Reiser for spending countless hours in the gait analysis laboratory and teaching me the ins and outs of the optical capture system. Thank you also for loaning your equipment and providing instruction in my soldering project. I also thank Dr. Kevin Haussler for providing a different insight into the scope of my projects and always making me think more critically.

I would like to also thank Dr. Melissa King for her expertise in equine motion analysis and her support when the motion analysis equipment was being finicky. Thank you also for your guidance both professionally and personally.

I would like to thank the staff of the Equine Orthopaedic Research Center and the Equine Sports Medicine Residents for their help with my two projects and during data collection. I especially want to thank Jen Suddreth and Dr. Dora Ferris for being great friends and always being willing to lend a hand. Thanks to Dr. Francisco Olea-Popelka for all his help with the statistical analysis. A special thanks to Dr. Laurie Goodrich for helping me through the last few months with her kind advice.

A special thanks to Dr. Mick Peterson and Dr. Christie Mahaffey for their help with the second IMU project. They spent many hours troubleshooting the IMU, fixing hardware, and writing programs to process the IMU data. I truly appreciate their dedication to this project, especially as there were countless hurdles along the way. Thanks to Dr. Jeff Thomason and Warren Bignell for allowing me to participate in one of their projects and providing me a starting point for working with hoof-mounted strain gauges.

I would like to thank my entire family for providing emotional support throughout all of my post-graduate training. I would like to especially thank my parents for always being there to listen when I need to vent. I want to thank my sister-in-law for giving me advice on how to make it through my PhD. Finally, I give many thanks to all my friends throughout the country who reminded me of the bigger picture. Thanks especially to all my veterinarian friends for always having some interesting clinical consults so I could keep up with my clinical skills. Lastly, thanks to my wonderful boyfriend, Derek, who puts up with my high levels of stress and constant need to be working.

TABLE OF CONTENTS

Chapter One

Inertial Measurement Units (IMUs): A Method to Objectify the Equine Subjective Lameness Examination

Introduction

Musculoskeletal unsoundness has been reported as a leading cause of wastage in athletic horses, with reduced and suboptimal performance reported in horses with mild or subclinical lameness.[1,2] In addition, lameness is reported to be the most common and expensive medical problem in horses.[3]These expenses include loss of purses, loss of training fees, and lost sales fees. In a recent cohort study of 2 and 3 year old racehorses in the UK, approximately 80% of days lost from training were due to lameness.[4] In another study of Dutch sport horses, lameness was the reason for 20% of horse-related career breaks in a group of dressage horses.[5]

Athletic horses are high-performing animals and many are expected to perform at high levels at young ages. When performing at their maximal abilities, some soft tissues of the equine limbs are operating close to overload, which predisposes them to injury.[6]As overload injuries range from mild to catastrophic, it is the early detection of abnormalities when they are still mild and horses show few clinical signs that is the goal of preventing catastrophic injuries. In addition to preventing career-ending injuries, the early detection of lameness may also allow longer athletic careers and potentially a decrease in loss of use of athletic horses. As early injury may present as a subtle to mild lameness, detection of mild lameness is critical, both for animal welfare and public perception. As lameness affects horses in all uses and disciplines, the development of tools that can detect early abnormalities would be beneficial to the overall horse population.

Equine Motion Analysis

Equine motion analysis includes both subjective and objective techniques with the most commonly utilized technique being the subjective lameness examination. As these examinations have been shown to lack high levels of reliability especially during low levels of lameness, supplementary techniques are needed to improve detection of subtle lameness.[7-9]Objective techniques include both kinetic and kinematic analyses, and these are being examined as supplementary methods for the subjective lameness examination.

Subjective Techniques

The simplest and most readily available form of equine motion analysis is the subjective lameness examination. This examination typically involves both a static and dynamic evaluation, with the dynamic evaluation involving examination of the horse at multiple gaits, from several perspectives, on circles and straight lines, and with additional tests, including flexion tests and regional anesthesia. Several ordinal, semi-quantitative scoring systems are described for grading this examination, but one of the most utilized in the United States is the AAEP lameness system, which provides grades from 0 (no lameness observed) to 5 (non-weight-bearing lameness).[10] The inter-observer reliability of this and other similar scoring systems has been shown to be poor for subtle and mild lameness.[7-9] In addition, another investigation demonstrated that observers were more likely to see improvement in lameness if they knew regional anesthesia had been performed.[11] As the subjective lameness examination on its own is not reliable for lameness detection of subtle to mild lameness, supplemental quantitative tools are needed to accurately diagnose these lameness cases. In addition, since assessing the results of regional anesthesia are biased, objective tools to longitudinally assess a lameness work-up are also desirable.

Objective Techniques

Kinetic and kinematic analyses can provide additional quantitative information that can be used for diagnosis in conjunction with the subjective lameness examination. These methods can also provide a mode to monitor lameness progression. There are a variety of techniques that have been utilized to analyze the kinetics and kinematics of equine motion, both in laboratory and clinical environments.

Kinetic Methods

Kinetics is the study of what causes a body to move, which includes forces. The most commonly used method for collection of kinetic data in the horse is the stationary force platform. This instrument measures forces in all three orthogonal directions: vertical, cranial-caudal, and medial-lateral. A single stationary force platform has the disadvantage of only being able to collect one limb strike of a single fore and hind-limb for a useable data trial. Several consecutive force platforms can be set in series to allow the collection of forces for both sets of limbs and several successive strides. As the forward velocity of the horse affects the magnitude of kinetic parameters,[12] velocity must be tightly controlled to collect data for meaningful comparison. Also, tossing of the horse's head can result in alterations in ground reaction forces, so horse cooperation can be critical in collecting adequate data. In addition, because of the small area of the force platform and the necessity to collect multiple strikes at a consistent velocity, data collection with the stationary force platform can be very time consuming. Because of some of the limitations of the stationary force platform, a force measuring treadmill[13] has been developed and can determine vertical forces of multiple consecutive strides. However, this is an expensive, customized piece of equipment that is not widely available to all veterinary practitioners. Thus, collection of kinetic data with both the stationary force platform and force measuring treadmill are only applicable for research/experimental settings.

The dynamometric horse shoe was designed to overcome some of the deficiencies of the force platform: to examine horses in a natural athletic environment and to collect data from multiple consecutive strides. Two dynamometric horse shoes have been designed and validated; one that uses piezoelectric force sensors[14] and the other with rosette strain gauges.[15] Both of these shoes have allowed determination of forces in all three orthogonal planes on horses during normal exercise, but they are substantially more massive than standard shoes. Because of their increased size and mass, these shoes have been hypothesized to alter distal limb kinetics and kinematics, thus impacting their ability to be useful for evaluating both normal and abnormal gait. In addition, these shoes are customized to fit a specific horse, thus making them less widely available.

Pressure plates have also been developed as a cheaper and portable substitute for the stationary force platform. They have an additional advantage of allowing the determination of the distribution of forces, which is not possible using the force platform.[16] While this plate was shown to have good repeatability for the evaluation of symmetry in peak vertical force and impulse of the forelimb of ponies at the walk and trot,[17] peak vertical force and impulse were significantly different compared to a stationary force platform.[18] In addition, the pressure plate is less than 2 m in length, and thus, is unable to be used to collect multiple consecutive strides. The evaluation of several in-series pressure platforms for collection of multiple strides of data has not been performed in the horse, but this could be a potential method of collecting kinetic data more efficiently. In-shoe pressure sensors have also been investigated to examine multiple consecutive strides. However, the precision of the measurements and accuracy of the system compared to the stationary force platform are not promising.[19] As these pressure mats were not manufactured specifically for horses and they lack the durability to hold up to horses, they are likely to require frequent replacement.

There have been methods proposed to calculate kinetic variables using kinematic data: a duty factor calculation[20] and metacarpophalangeal (MCP) joint angle method.[21] The first method (duty factor method) is the simpler of the two, and the peak vertical ground reaction force can be calculated by determining the percentage of time that the limb is in contact with the ground.[20] With the MCP joint angle method, a regression equation can be determined from simultaneous kinetic and kinematic data to determine peak vertical force, using optical kinematic data.[21] The duty factor method requires less equipment, as forces can be readily determined using a horse or hoof-mounted sensor system. The second method requires a calibration step using a force platform or force measuring treadmill, and thus requires laboratory facilities. Nonetheless, neither method has been validated in lame horses, so even if they are accurate for predicting forces in normal horses, they may not be adequate for calculation of forces in lame horses.

Lameness diagnosis using kinetic methods

Kinetic analysis has been shown to be very sensitive for the diagnosis of lameness. Merkens et al.[22] found that mild lameness resulted in a decrease in maximum vertical ground reaction force at the walk in both fore- and hind-limbs. Ishihara et al.[23] demonstrated that peak vertical force and vertical impulse were significantly decreased after experimentally induced lameness (lipopolysaccharide (LPS) injected into the MCP joint) and that significant changes could be detected at subtle levels of lameness (AAEP scale, grades 0.5 and 1 out of 5). As peak vertical force and vertical impulse have been shown to have small inter-horse variability (< 10%) both intra- and inter-day, these parameters appear to be the most useful in cases of subtle lameness.[24]

Kinematic Methods

Kinematic analysis describes the motion of a subject and also encompasses the temporal components of gait. The current gold standard of kinematic analysis is optical kinematics. Most typically infrared cameras are utilized for optical kinematics, and they are best utilized in a research setting where lighting conditions can be controlled. While studies have been performed outdoors, the majority of optical kinematics research has been conducted in a controlled research environment. Three-dimensional (3-D) optical kinematic data can be collected while the horse is moving over-ground or on a treadmill. However, a large number of consecutive strides can be collected on the treadmill, while the number of strides that can be consecutively collected per pass over-ground is limited by the number and arrangement of cameras. While a large capture volume can allow collection of multiple strides over-ground, this decreases the resolution of the markers on the horse making tracking of motion more difficult.[25] A few studies have demonstrated that stride kinematics differ between treadmill and over-ground locomotion,[26, 27] but it is not known how these differences may affect lameness diagnosis or the kinematic parameters that are most useful for lameness diagnosis. Nonetheless, it is not practical to examine and diagnose lame horses in a research environment, including training them to exercise on a treadmill which often takes several training sessions over consecutive days.

The emergence of small and light-weight sensors has set the stage for development of horse-mounted kinematics. As technology has improved, these sensors have become increasingly small, lightweight, more affordable, and telemetric, which contribute to their desirability for use in motion analysis, as they can allow the examination of the horse in a clinical setting. Currently investigated sensors include accelerometers, gyroscopes, global positioning systems (GPS), and combinations of these components. These systems have been reported for use in equine motion analysis as early as the mid-1990's, where two uni-axial accelerometers were mounted over the sternum of both a sound and an experimentally induced lame horse.[28] This body-mounted accelerometric device allowed calculation of stride frequency, stride length, and speed without affecting the movement of the horse.[29] Single- and tri-axial accelerometers have also been mounted on the poll, pelvis, or thorax[30-35] and have allowed left and right symmetry of the horse to be evaluated.

Lameness detection using kinematic methods

A number of investigations using optical methods have examined the kinematic changes that occur with lameness. Buchner et al.[36] found that both stride frequency and stance duration increased after lameness, with the increase in stance duration being observed in both the lame and non-lame limbs. Buchner et al.[37] determined that an induced lameness resulted in less MCP joint hyperextension and distal interphalangeal (DIP) joint flexion during stance in both fore- and hind-limbs. Galisteo et al.[38] found a significant decrease in stride length, stride duration, swing duration, and stride length, and an increase in stance duration in horses with experimentally induced forelimb lameness. However, none of these studies were able to detect a significant difference in variables until at least a moderate degree of lameness was induced. In another evaluation with a similar experimental lameness model, significant differences in maximum fetlock extension, vertical poll excursion, and minimum poll height during right and left stance were detected at the mildest lameness tested.[39] However, the mildest lameness tested by this group of authors was defined as a lameness that was easy to see; no subjective lameness grade was assigned.

Horse velocity has also been investigated for its influence on lameness, and horses with more severe lameness showed greater poll excursion when the velocity was increased.[40] However, horses with subclinical to mild lameness did not show an increase in poll excursion with increasing speed.[40] Peham et al.[41] also examined the effect of mild to moderate forelimb lameness on stride length variability in horses with different sources of clinical lameness. They found that after regional anesthesia, there was more variability in stride length compared to before anesthesia, and concluded that lame horses compensated by reducing inter-stride variability. While optical kinematics is an appropriate method of lameness diagnosis, it is not the most suitable method for supplementing a clinical subjective lameness examination.

Horse-mounted systems are becoming more common in clinical practice for diagnosing lameness. One commercial horse-based system[a] utilizes two single-axis accelerometers on the poll and sacrum to examine head and pelvis symmetry and uses a single-axis gyroscope on the right forelimb to determine phase of stride (stance versus swing).[30] The benefits of this system are its simplicity (single axis sensors), quick set-up time (<3 min), and that it is telemetric.[31] However, since the sensors are only single axis, other movements, such as rotation of the head or pelvis, and non-vertical placement of the axis of a sensor can result in altered accelerations.[30] This system has been shown to be very sensitive in detecting a mild single fore or hind-limb lameness at the trot, however, it has not been shown to be useful for examining horses at the walk or for evaluation of bilateral lameness.[32,33] However, this system has also been shown to detect significant changes in pelvic movement following hind-limb flexion, indicating that it could be a useful tool for supplementing the subjective lameness examination.[42] While this system has shown to be repeatable between consecutive trials,[31] it has not yet been critically evaluated for longitudinal assessment of cases.

Several groups have examined other body-mounted accelerometers for evaluation of lameness. Two uni-axial, sternal mounted accelerometers were found to be sensitive enough to detect subtle lameness.[28] In addition, a single tri-axial accelerometer mounted caudal to the withers was demonstrated to effectively evaluate trunk symmetry and determination of side of lameness.[34,35] Symmetry scores from this system were shown to be more sensitive to changes in forelimb lameness than the subjective AAEP lameness grading scale, indicating that this system may be useful to diagnose and monitor progression of lameness cases.[35]

Inertial Measurement Units

Inertial measurement units (IMUs) are composed of tri-axial rate gyroscopes, accelerometers, magnetometers and a thermostat. These units allow for kinematics to be collected in the local reference frame of the sensor (and the part of the horse where the sensor is attached), and then with the input of the magnetometer, they can be rotated into a global reference frame with true cranial-caudal, medial-lateral, and vertical axes, which are aligned with the earth.

In the scientific literature, the terminology defining the exact components within the IMU is vague, and thus, each report should specifically define the components contained within the unit. A number of terms are used to describe the IMU, including but not limited to inertial sensor, inertial measuring device, and magnetic and inertial measurement unit (MIMU). The term inertial sensor is the most ambiguous of these terms and has been used to describe one or multiple components of the IMU, such as an accelerometer or gyroscope.[31] Occasionally, IMU is used within the scientific literature to describe a combination of accelerometer and gyroscope, without the use of a magnetometer[43] or even as a single accelerometer,[44] instead of a device that contains all the above-mentioned components. One study defined an IMU as the combination of an accelerometer and gyroscope, while a MIMU was defined as the combination of an accelerometer, gyroscope, and magnetometer.[45] Another publication defined the combination of a tri-axial accelerometer, tri-axial gyroscope, and tri-axial magnetic sensor as an integrated IMU.[46] The term IMU will be utilized through the remainder of this document to describe a system composed of accelerometer, gyroscope, magnetometer, and thermostat. Any other variations of this system will be defined.

Accelerations and angular velocities are measured directly with the IMU from the accelerometers and rate gyroscopes, respectively, which can be integrated to determine linear velocities and positions, as well as angular orientation. Since IMUs are attached to the subject, the orientation of the sensor must also be converted from the local sensor reference frame to a global reference frame using a rotation matrix. This can be contained in the proprietary software of the particular unit, or can be custom written in software.[b] This is particularly important when comparing the kinematic data from the IMU to data from an optical kinematic system, in which the output data is already in a global reference frame.

In addition, the gyroscopes are subject to drift, and there is a gradual increase in angular velocity when the individual is either moving or rest. This is especially problematic in long data collection sessions, as drift increases with time leading to errors that increase in magnitude following integration. This results in large errors in orientation. These errors can be minimized by merging the magnetometer, accelerometer, and gyroscope signals as well as the biases from the sensors, which is referred to as a Kalman filter.[47-49] Mazza et al.[50] demonstrated that the use of a Kalman filter with optimization parameters decreased the root mean squared error (RMSEs) in pitch and roll to less than 1^{o} and increased the correlation coefficients to $R > 0.9$ when comparing an IMU to an optical capture system. Contrarily, Brodie et al.[51] found that a commercial Kalman filter showed higher errors than a custom fusion algorithm (11.7^{o} vs. 0.9^{o}) when an IMU was compared to an optical capture system. This custom fusion algorithm estimated orientation using static readings from the accelerometers and magnetometers combined with a continuous reading from the gyroscopes. In addition, Brodie et al.[51,52] found that the error of the IMU determined experimentally was much higher than the manufacturer's claim, when the factory calibration was used. Brodie et al.[51] also determined that the custom algorithm worked best when a motion was bounded by two stationary periods: one before and one after. However, these investigations did not use the same IMU and one investigation used a simple pendulum,[51] while the other examined trunk movement of a person walking.[50] Thus, it is difficult to make direct comparisons amongst the above studies. However, these investigations demonstrate that post-processing of the raw data is important to address gyroscopic drift, and both highlight the need to investigate the accuracy of each IMU, as well as the desired motion that will be studied.

As previously mentioned, gyroscopic drift is impacted by the duration of data collection. Plamondon et al.[53] found that short-duration tasks showed significantly lower errors than longer-duration tasks. These errors likely originated both from gyroscopic drift and magnetic sensor disturbances. However, a more recent study showed that by examining gait based on individual motion cycles, accurate data can be obtained from longer data collection sessions (5 minute trials).[54] This method allows the gyroscope to be reset, thus, eliminating the drift. In addition, temperature, both ambient and from power to the device, can have a significant contribution to drift, leading to additional larger errors in angular orientation post-integration.[47,55] As true IMU's contain a thermostat, the effect of increased temperature can be compensated for internally.

Integration of the three sensor signals within the IMU, via a Kalman filter, also has a positive effect on gyroscopic drift. When only the gyroscopic signal is used to determine orientation, angular orientation drifted by 10-25^{o} after one minute, but the use of a Kalman filter, which blended the input from the accelerometers, gyroscopes, and magnetometers, bringing the orientation down to zero degrees when it was not moving.[47, 55] While both the accelerometer and magnetometer can be used to correct gyroscopic drift, the magnetometer is especially important to correct drift around the vertical axis.[55] When ferromagnetic material is in the vicinity of the IMU during data collection, "magnetic interference compensation" is required in addition to the Kalman filter to eliminate drift.[55] This type of compensation involves decreasing the contribution of the magnetometer signal into the Kalman filter and increasing the input from the accelerometer and gyroscopic signals, which increases the orientation accuracy.[49]

Despite the cautions that exist with IMUs both in data collection and processing of the signal, the ability of the IMU to be used in a non-laboratory environment has spurred interest for a wide range of uses, both human and equine. These uses include assessing rehabilitation from injury, diagnosing abnormal gait (both musculoskeletal and neurologic origin), detecting falls and monitoring daily activity in elderly people, and optimizing performance in athletes.[50, 53, 54, 56-62] The IMU is especially exciting since it allows investigation of both linear and angular components of motion. IMUs have been investigated in humans to evaluate a wide range of motions, including stride characteristics during walking and running,[56,57] joint range of motion (both upper and lower limb),[54, 61, 62] and change in trunk vertical displacement and posture[53, 60]. In the horse, the IMU has been examined as a body-mounted sensor for assessing stride parameters, hind-limb lameness, back movement, and center-of mass movement in the horse.[63-71]

IMU use in human locomotion

As the IMU is still in its infancy in clinical use in human biomechanics, in the literature it is most often compared to the gold standard of kinematics: optical. The most common methods for making statistical comparisons between these two systems include correlation coefficients and root mean squared error (RMSE). While correlation coefficients look for linear trends between systems, the calculation of RMSEs involves examining the difference between the two systems during a collection session or gait cycle. RMSE looks for the two methods to have close to perfect agreement. It is the combination of these two methods that is often performed to validate that the IMU system is accurate for patient-based kinematic analysis.

A number of investigations have examined the linear kinematics of the IMU in humans. An IMU mounted on the lateral aspect of the shank was used to determine walking and running speed of a person on a treadmill.[43,56, 57] These investigators found that the IMU underestimated the velocity at both gaits and found a large range of root mean squared error (RMSEs) values (4% to 19%). One investigator suggested that precise lateral placement of the unit on the shank could result in the underestimation.[56, 57] As the RMSE tended to be larger during longer periods of data collection (90 s), it is likely that gyroscopic drift was a contributing factor to this inaccuracy, and filtering the data or resetting the gyroscope may have improved the accuracy of the data.

As the IMU is becoming increasingly popular as a body mounted system for motion analysis, numerous investigations have been performed comparing the kinematic outputs to the current gold standard of kinematics: optical methods. A number of investigations have examined linear kinematics of both the limbs and the body. One human investigation found that although stride length was comparable, lateral foot placement was significantly different between the IMU and the optical kinematics system, which was postulated to be due to the small range of motion involved in the lateral movement.[58] Even though the values from the optical and IMU systems were significantly different, this study showed high correlations between the systems indicating that while not interchangeable, they may detect similar kinematic changes. In the same study, when comparing an individual with eyes open to eyes closed, an IMU was able to determine significant differences in both stride length and lateral foot placement between the two conditions.[58] Additionally, a shank mounted IMU could accurately detect phase of stride when a person walked over various surfaces.[59] Accurate vertical displacements and accelerations were also found when an IMU was placed over the lumbar spine.[60] From these investigations, it appears that IMUs can be used to measure linear kinematics and that their accuracy largely relies on the proper integration of accelerometer, gyroscopic, and magnetometer signals. These reports also conclude that while the IMU may not always produce equivalent kinematic data as the optical system, it can still discriminate between two conditions (i.e., eyes open and eyes closed).[58] In addition, as optical kinematic methods are prone to errors, such as from skin motion artifacts, any perceived inaccuracy of the IMU could really stem from an inaccuracy within the optical kinematics, not the other way around. As these two methods are not likely to be used interchangeably, it is probably less important that the IMU and optical methods agree perfectly. Thus, as the IMU has been shown to be useful in evaluating gait cycles and stride parameters in humans, thus, should have the same abilities in other species, such as the horse.

In addition to its use in determining linear kinematics, the IMU has also been investigated for the determination of orientation. While other angular kinematic variables can be determined, only angular orientation has been intensely investigated using IMUs. A number of reports have examined the use of the IMU to measure joint range of motion of the lower (ankle, knee, and hip) and the upper limbs (wrist, elbow, and shoulder). There are mixed reports within the literature in the accuracy of the IMU. The IMU has been shown to be most accurate in the sagittal plane, with less accuracy in the transverse and frontal planes.[45, 54, 61, 72, 73] As most motions go through a larger range of orientation change in the sagittal plane, it would be expected that the inaccuracy in the other planes stems from this, as it would be expected that a similar error would be seen in all three rotations. Thus, a 1^{o} error in all three planes would be a larger inaccuracy in the rotation that went through a smaller range of motion.

In addition to measuring joint angles, one investigation examined trunk posture and found that the IMU was more accurate in the sagittal and frontal planes.[53] Contrarily, Zhou et al.[62] and Saber-Sheik et al.[74] found good agreement in all three planes of motion. In a more recent report,[54] the IMU had better agreement with a 3-dimensional (3-D) optical system in the sagittal plane, but fairly good agreement in the coronal and transverse planes. In addition, this investigation found that the IMU could discriminate between healthy individuals and those with osteoarthritis, which is a better indication of its ability to be used clinically.[54]As it is unlikely that an IMU would be used interchangeably with an optical system, having perfect agreement between the two systems should not be the most important criteria for having a clinically useful tool. From these investigations, it is important to determine the accuracy for an IMU in its proposed motion in all three planes of movement, as there may be individual differences between systems and motions. Also, it is important to recognize that errors may result in data in the transverse plane as a result in errors in the magnetometer readings. The use of magnetic compensation during data processing may also decrease the errors in the transverse plane when the magnetic environment is heterogeneous. It is also likely that the differences in accuracy in the three planes arose from the signal processing algorithms. Development of universal filters and fusion algorithms that can be used amongst different IMUs may improve the accuracy of all units.

While the IMU has been widely researched for the evaluation of a wide variety of movements and a large number of tasks, it has been proposed that the amount of error of the IMU is task related, with higher error rates in tasks that have a high frequency of directional changes.[51] Thus, slow motions that are collected over short time frames and those involving movement in one plane are postulated to be more accurate.[51, 52] Less accuracy may be seen during motions with high velocities and changes in direction, as these may result in movement between the sensor and the patient.[48]In addition, it has been documented that the accuracy of a Kalman filter decreases when velocity increases.[75] In addition, as accuracy varies considerably between investigations, it is likely the combination of both filtering and processing the data as well as the hardware that contribute to the errors in the IMU data.

IMU use in the horse

IMUs have been investigated to a limited extent for motion analysis in the horse. One research group has investigated a human designed IMU system[c] mounted on the body of the horse to examine trunk movement at the gallop,[64, 65, 76-78] hind limb lameness,[63, 66] back movement,[70] and evaluation of hind-limb flexion tests.[69] When examining center of mass displacement and orientation at the walk, trot, and canter, the IMU was found to be accurate compared to an optical kinematics system (median errors were < 3.5% of the range of total motion).[76] While this study demonstrated that the IMU can be useful for evaluating motion of the horse's body, this commercial IMU system used does not have a large enough acceleration range (+/- 10G) to be used on the distal limb of the horse. In addition, when examining hind-limb lameness, the IMU showed high sensitivity (100%) and moderate specificity (66%) for discriminating mildly lame (grade 1-2 out of 10) from non-lame horses.[66] Thus, this IMU did not classify a sound horse as lame, but also did not identify all of the lame horses. In the development of a useful clinical tool to objectify the equine lameness examination, we would want an instrument with high specificity, so as not to miss the cases with subtle lameness.

An equine inertial sensor system developed in the United Kingdom[d] has been developed for use on the limbs of horses (metacarpus/metatarsus, and tibia) to monitor distal limb kinematics, such as stride length, stride duration, and speed.[79] While it appears there is some research being performed with this system, the exact components of this system (i.e., accelerometer, gyroscope, etc.) are not defined either on the website or in a peer-reviewed manuscript[79].

While there have been several reports utilizing pelvic-mounted (tuber coxae and tuber sacrale) IMUs for diagnosis of hind-limb lameness[63, 66] and distal metacarpus/metatarsus IMUs for detection of hoof-on and hoof-off,[80] there are no peer-reviewed manuscripts on the use of distal limb mounted IMUs, either on the fore- or hind-limb, for determination of stride characteristics of the hoof. As previous investigations using optical methods have found that lameness can affect the kinematics of the distal limb, the hoof is an ideal place to place an IMU. The IMU has many attributes that make it desirable for use on the distal limb or hoof of a horse. The first is the small size and mass of the IMU. Numerous commercial IMUs are small enough to easily mount on a horse's hoof or distal limb,[ef] either with acrylic or boot attachment. In addition, the majority of these human units are lightweight with a mass under 100 grams. Previous research has reported that placing a 700 gram weighted bell boot at the distal end of the limb (i.e., hoof) can alter the kinematics of the limb,[81] with a greater effect in the hind limb joints than the forelimb. Tactile stimulation, with a 55 gram bracelet, of the pastern and hoof resulted in initial kinematic changes to the forelimbs that were not significantly different from baseline after 300 m.[82] Thus, it would be expected that as long a horse was allowed adequate time for acclimation, the attachment of a small sensor on the hoof would have limited impact on kinematics.

A second attribute of the IMU is its ability to determine accelerations and angular velocities in all three orthogonal planes in a global reference frame. Hoof-mounted accelerometers and gyroscopes have been used to determine stance and swing phases,[30, 31, 32, 83] but they have not been used to examine the motion of the hoof during the stride. When used individually, these components can be used to determine positions and orientations, but they output these variables relative to a local sensor reference frame. The ability of the IMU to produce global reference frame data allows more relevant values of displacement and angular orientation. This can allow for a better interpretation of how the hoof moves three-dimensionally during swing, landing, and break-over relative to the world as opposed to the horse. Lastly, as a distal limb or hoof mounted device, the IMU has the potential to determine certain kinetic variables, such as peak vertical ground reaction force (pVF) by the previously mentioned kinematic methods.[20, 21] This adds additional depth of analysis for the IMU.

There are some attributes of the IMU that are undesirable. The first is the gyroscopic drift that leads to large errors in orientation following integration. However, from the human literature, there are several approaches to dealing with drift by filtering and post-processing, as previously discussed. A second undesirable trait of the IMU is the method of attachment to the distal limb. Attachment of the IMU to the distal limb requires stability so that there is not excess motion between the limb and the sensor. The attachment method also needs to be easy, cost-effective, and non-invasive since the proposed use of this system is for examination of lame horses in their natural athletic environment. Boot attachment is a proposed method that would satisfy all of the above requirements, but its stability (lack of motion between the sensor and the limb) needs to be investigated further. Olsen et al.[80] found that a boot-mounted IMU could be used to accurately detect hoof events, but additional investigations would be needed to determine if that provides sufficient stability to examine other kinematic parameters.

In summary, the IMU has been demonstrated to be a useful tool in the human field of human sports medicine and rehabilitation and can be used as a non-laboratory method of kinematic evaluation. In the last decade, an increasing amount of research has been performed with the IMU in the horse, however, these units have been typically attached to the body, instead of the limbs, of the horse. The many attributes of the IMU make it an exciting method for kinematic and potentially kinetic analysis of the limbs of the horse and may be a useful objective method to supplement the equine subjective lameness examination in clinical cases.

Purpose of Study

As early diagnosis of equine lameness is critical for both animal welfare and for continued use of the horse in athletic endeavors, development of methods for early identification is imperative. This involves development of methods that are not cost prohibitive, are easy to use, and do not affect normal equine locomotion. As IMUs fit these criteria, and they have shown promise in the human field of sports medicine, it is the logical next step to determine their efficacy in equine sports medicine. While, IMUs have been applied to the body of horses and proximal to the fetlock joint, they have not been mounted on the hoof. In addition, there is sparse published data on how hoof kinematics are altered following lameness induction or after peri-neural anesthesia. The purpose of this group of studies is to verify that a hoof-mounted IMU can track normal motion of the hoof and that this device is sensitive enough to detect changes to hoof kinematics once lameness has been induced.

Study Goals

The objective of this group of studies was to first determine the linear and angular kinematics of the hoof at the walk and trot of both sound and lame horses using both IMU and optical methods. The second goal was to determine if the IMU, as mounted on the hoof, would be an appropriate device to detect lameness in the horse, with the long-term goal of using it on horses in their natural athletic environment.

Hypotheses

H1: Linear and angular kinematics of the fore and hind hooves in normal horses at the walk and trot will not be statistically different between IMU and 3-D optical systems.

H2: The linear and angular kinematics of the fore hoof will be significantly altered after induction of lameness and this will be detectable by optical methods at both the walk and the trot.

> H2a: There will be significant intra-limb kinematic changes to both the lame forelimb and to the contra-lateral non-lame forelimb after lameness induction.
>
> H2b: There will be significant inter-limb kinematic changes between the lame and non-lame forelimbs after induction of lameness.

H3: The linear and angular kinematics of the fore hoof will return to baseline (i.e., no significant intra- or inter-limb differences following peri-neural anesthesia) at both the walk and the trot.

H4: The IMU will detect similar intra-limb kinematic changes to the fore hoof as the optical system following induction of lameness and after peri-neural anesthesia at the walk and trot.

Specific Aims

SA1: To validate that the IMU can detect normal motion of the fore- and hind- hooves at the walk and trot.

SA2: To identify the within and between limb changes to hoof motion that occur at the walk and trot at increasing levels of lameness.

SA3: To identify the within and between limb changes in hoof motion following peri-neural anesthesia at the walk and trot.

SA4: To validate a hoof-mounted IMU as a method to detect lameness and evaluate peri-neural anesthesia at the walk and trot.

[a] Lameness Locator, Equinosis LLC; Columbia, MO
[b] MATLab, The MathWorks, Inc; Natick, MA
[c] MTx, XSens North America Inc; Culver City, CA
[d] Pegasus; ETB-Pegasus; Hertfordshire, UK
[e] H3 IMU-HP, Memsense, LLC; Rapid City, SD
[f] 3DM-GX3, LORD Miscrostrain Sensing Systems; Williston, VT

References

1. Gaughan EM. Skeletal origins of exercise intolerance in horses. Vet Clin North Am Equine Pract 1996; 12: 517-535.

2. Parente EJ, Russau AL, Birks EK (2002). Effects of mild forelimb lameness on exercise performance. Equine Vet J Suppl34 2002; 34: 252-256.

3. USDA. National economic cost of equine lameness, colic, and equine protozoal myeloencephalitis in the United States. 2001. Fort Collins, CO, USDA:APHIS:VS, National Health Monitoring System. Information sheet.

4. Dyson PK, Jackson BF, Pfeiffer DU, et al. Days lost from training by two- and three-year-old Thoroughbred horses: A survey of seven UK training yards. Equine Vet J 2008; 40: 650-657.

5. van Oldruitenborgh-Oosterbaan MMS, Genzel W, van Weeren PR. A pilot study on factors influencing the career of Dutch sport horses. Equine Vet J Suppl 38 2010; 42: 28-32.

6. Eliashar E. An evidence-based assessment of the biomechanical effects of the common shoeing and farriery techniques. Vet Clin North Am Equine Pract 2007; 23: 425-442.

7. Keegan KG, Dent EV, Wilson DA, et al. Repeatability of subjective evaluation of lameness in horses. Equine Vet J2010; 42: 92-97.

8 Fuller CJ, Bladon BM, Driver AJ, et al. The intra- and inter-assessor reliability of measurement of functional outcome by lameness scoring in horses. The Vet J 2006;171: 281-286.

9. Hewetson M, Christley RM, Hunt ID, et al. Investigations of the reliability of observational gait analysis for the assessment of lameness in horses. The Vet Rec 2006; 158: 852-858.

10. American Association of Equine Practitioners. Guide for veterinary service and judging of equestrian events. 4th ed. Lexington, Ky: American Association of Equine Practitioners, 1991; 19.

11. Arkell M, Archer RM, Guitian FJ, et al. Evidence of bias affecting the interpretation of the results of local anesthetic nerve blocks when assessing lameness in horses. The Vet Rec 2006; 159: 346-349.

12. McLaughlin RM, Gaughan EM, Roush JK, et al. Effects of subject velocity on ground reaction force measurements and stance times in clinically normal horses at the walk and trot. Am J Vet Res 1996; 57: 7-11.

13. Weishaupt MA, Hogg HP, Wiestner T, et al. Instrumented treadmill for measuring vertical ground reaction forces in horses. Am J Vet Res 2002; 63: 520-527.

14. Chateau H, Robin D, Simonelli T, et al. Design and validation of a dynamometric horseshoe for the measurement of three-dimensional ground reaction force on a moving horse. J Biomech 2009; 42: 336-340.

15. Roland ES, Hull ML, Stover SM. Design and validation of a dynamometric horseshoe for measuring ground reaction loads of horses during racing conditions. J Biomech 2005; 38: 2102-2112.

16. Rogers CW, Back W. The effect of plain, eggbar and 6° –wedge shoes on the distribution of pressure under the hoof of horses at the walk. N Z Vet J 2007; 55: 120-124.

17. Oosterlinck M, Pille F, Back W, et al. Use of a stand-alone pressure plate for the objective evaluation of forelimb symmetry in sound ponies at walk and trot. The Vet J 2010; 183: 305-309.

18. Oosterlinck M, Pille F, Huppes T, et al. Comparison of pressure plate and force plate gait kinetics in sound Warmbloods at walk and trot. The Vet J 2010; 186: 347-351.

19. Perino VV, Kawcak CE, Frisbie DD, et al. The accuracy and precision of an equine in-shoe pressure measurement system as a tool for gait analysis. J Eq Vet Sci 2007; 27: 161-166.

20. Witte TH, Knill K, Wilson AM. Determination of peak vertical ground reaction force from duty factor in the horse (*Equus cabellus*). J Exp Biol 2004; 207: 3639-3648.

21. McGuigan MP, Wilson AM. The effect of gait and digital flexor muscle activation on limb compliance in the forelimb of the horse *Equus caballus*. J Exp Biol 2003; 206: 1325-1336.

22. Merkens HW, Schamhardt HC. Evaluation of equine locomotion during different degrees of experimentally induced lameness I: Lameness model and quantification of ground reaction force patterns of the limbs. Equine Vet J Suppl l6 1988; 20: 99-106.

23. Ishihara A, Bertone AL, Rajala-Schultz PJ. Association between subjective lameness grade and kinetic gait parameters in horses with experimentally induced forelimb lameness. Am J Vet Res 2005; 66: 1805-1815.

24. Lynch JA, Clayton HM, Mullineaux DR. The reliability of force platform data from trotting horses.Eq Comp Exerc Physiol 2005; 2: 129-132.

25. Keegan K. Evidence-based lameness detection and quantification. Vet Clin North Am Equine Pract 2007; 23: 403-423.

26. Barrey E, Galloux P, Valette JP, et al. Stride characteristics of overground versus treadmill locomotion in the saddle horse. Acta Anat 1993; 146: 90-94.

27. Buchner HHF, Savelberg HHCM, Schamhardt HC, et al. Kinematics of treadmill versus overground locomotion in horses. Vet Q 1994; 16 Suppl 2; 87-90.

28. Barrey E, Hermelin M, Vaudelin JL, et al. Utilisation of an accelerometric device in equine gait analysis. Equine Vet J Suppl 17 1994; 26: 7-12.

29. Barrey E, Auvinett B, Courouce A. Gait evaluation of race trotters using an accelerometric device. Equine Vet J Suppl 18 1995; 27: 156-160.

30. Keegan KG, Yonezawa Y, Pai PF, et al. Evaluation of a sensor-based system of motion analysis for detection and quantification of forelimb and hind limb lameness in horses. Am J Vet Res 2004; 65: 665-670.

31. Keegan KG, Kramer J, Yonezawa Y, et al. Assessment of repeatability of a wireless, inertial sensor-based lameness evaluation system for horses. Am J Vet Res 2011; 72: 1156-1163.

32. Keegan KG, MacAllister CG, Wilson DA, et al. Comparison of an inertial sensor system with a stationary force plate for evaluation of horses with bilateral forelimb lameness. Am J Vet Res 2012; 73: 368-374.

33. McCracken MJ, Kramer J, Keegan KG, et al. Comparison of an inertial sensor system of lameness quantification with subjective lameness evaluation. Equine Vet J 2012; 44: 652-656.

34. Thomsen MH, Jensen AT, Sørensen H, et al. Symmetry indices based on accelerometric data in trotting horses. J Biomech 2010; 43: 2608-2612.

35. Thomsen MH, Persson AB, Jensen AT, et al. Agreement between accelerometric symmetry scores and clinical lameness scores during experimentally induced transient distension of the metacarpophalangeal joint in horses. Equine Vet J Suppl 38 2010; 42: 510-515.

36. Buchner HHF, Savelberg HHCM, Schamhardt HC, et al. Temporal stride patterns in horses with experimentally induced fore- or hindlimb lameness. Equine Vet J Suppl 18 1995; 27: 161-165.

37. Buchner HHF, Savelberg HHCM, Schamhardt HC, et al. Limb movement adaptations in horses with experimentally induced fore- or hindlimb lameness. Equine Vet J 1996; 28: 63-70.

38. Galisteo AM, Cano MR, Morales JL, et al. Kinematics in horses at the trot before and after an induced forelimb supporting lameness. Equine Vet J Suppl 23 1997; 29: 97-101.

39. Keegan KG, Wilson DA, Smith BK, et al. Changes in kinematic variables observed during pressure-induced forelimb lameness in adult horses trotting on a treadmill. Am J Vet Res 2000; 61: 612-619.

40. Peham C, Licka T, Mayr A, et al. Individual speed dependency of forelimb lameness in trotting horses. The Vet J 2000; 160: 135-138.

41. Peham C, Licka T, Girtler D, et al. The influence of lameness on equine stride length consistency. The Vet J 2001; 162: 153-157.

42. Marshall JF, Lund DG, Voute LC.Use of a wireless, inertial-sensor-based system to objectively evaluate flexion tests in the horse. Equine Vet J Suppl 43 2012; 44: 8-11.

43. Li Q, Young M, Naing V, et al. Walking speed estimation using a shank-mounted inertial measurement unit. J Biomech 2010; 43: 1640-1643.

44. Tan H, Wilson AM, Lowe J. Measurement of stride parameters using a wearable GPS and inertial measurement unit. J Biomech 2008; 41: 1398-1406.

45. Favre J, Aissaoui R, Jolles BM, et al. Functional calibration procedure for 3D knee joint angle description using inertial sensors. J Biomech 2009; 42: 2330-2335.

46. Sabatini AM. Kalman-filter-based orientation determination using inertial/magnetic sensors: observability analysis and performance evaluation. Sensors 2011; 11: 9182-9206.

47. Sabatini AM. Quaternion-based extended kalman filter for determining orientation by inertial and magnetic sensing. IEEE Trans Biomed Eng 2006; 53: 1346- 1356.

48. Roetenberg D, Slycke PJ, Veltink PH. Ambulatory position and orientation tracking fusing magnetic and inertial sensing. IEEE Trans Biomed Eng 2007; 54: 883- 890.

49. Roetenberg D, Baten CTM, Veltink PH. Estimating body segment orientation by applying inertial and magnetic sensing near ferromagnetic materials. IEEE Trans Neural Syst Rehabil Eng 2007; 15: 469-471.

50. Mazza C, Donati M, McCamley J, et al. An optimized Kalman filter for the estimate of trunk orientation from inertial sensors data during treadmill walking. Gait Posture2012; 35: 138-142.

51. Brodie MA, Walmsley A, Page W. Dynamic accuracy of inertial measurement units during simple pendulum motion. Comput Methods Biomech Biomed Engin 2008; 11: 235-242.

52. Brodie MA, Walmsley A, Page W. The static accuracy and calibration of inertial measurement units for 3D orientation. Comput Methods Biomech Biomed Engin 2008; 11: 641-648.

53. Plamondon A, Delisle A, Larue C, et al. Evaluation of a hybrid system for three-dimensional measurement of trunk posture in motion. Appl Ergon 2007; 38: 697-712.

54. Rouhani H, Favre J, Crevoisier X, et al. Measurement of multi-segment foot joint angles during gait using a wearable system. J Biomech Eng 2012; 134: 061006.

55. Roetenberg D, Luinge HJ, Baten CTM, et al. Compensation of magnetic disturbances improves inertial and magnetic sensing of human body segment orientation. IEEE Trans Neural Syst Rehabil Eng 2005; 13: 395-405.

56. Yang S, Mohr C, Li Q. Ambulatory running speed estimation using inertial sensor. Gait Posture 2011; 34: 462-466.

57. Yang S, Li Q. IMU-based ambulatory walking speed estimation in constrained treadmill and overground walking. Comput Methods Biomech Biomed Engin 2012; 15: 313-322.

58. Schepers HM, van Asseldonk EHF, Baten CTM, et al. Ambulatory estimation of foot placement during walking using inertial sensors. J Biomech 2010; 43: 3138-3143.

59. Kotiadis D, Hermens HJ, Veltink PH. Inertial gait phase detection for control of a drop-foot stimulator: Inertial sensing for gait phase detection. Med Eng Phys 2010; 32: 287-297.

60. Esser P, Dawes H, Collett J, et al. IMU: Inertial sensing of vertical CoM movement. J Biomech 2009; 42: 1578-1581.

61. Favre J, Jolles BM, Aissaoui R, et al. Ambulatory measurement of 3D knee joint angle. J Biomech 2008; 41: 1029-1035.

62. Zhou H, Stone T, Hu H, et al. Use of multiple wearable inertial sensors in upper limb motion tracking. Med Eng Phys 2008; 30: 123-133.

63. Church EE, Walker AM, Wilson AM, et al. Evaluation of discriminant analysis based on dorsoventral symmetry indices to quantify hindlimb lameness during over ground locomotion. Equine Vet J 2009; 41: 304-308.

64. Parsons KJ, Pfau T, Wilson AM. High-speed gallop locomotion in the thoroughbred racehorse. I. The effect of incline on stride parameters. J Exp Biol 2008; 211: 935-944.

65. Parsons KJ, Pfau T, Wilson AM. High-speed gallop locomotion in the Thoroughbred racehorse. II. The effect of incline on centre of mass movement and mechanical energy fluctuation. J Exp Biol 2008; 211: 945-956.

66. Pfau T, Robilliard JJ, Weller R, et al. Assessment of mild hindlimb lameness during over ground locomotion using linear discriminant analysis of inertial sensor data. Equine Vet J 2007; 39: 407-413.

67. Starke SD, Willems E, May SA, et al. Vertical head and trunk movement adaptations of sound horses trotting in a circle on a hard surface. The Vet J 2012; 193: 73-80.

68. Starke SD, Witte TH, May SA, et al. Accuracy and precision of hind limb foot contact timings of horses determined using a pelvis-mounted inertial measurement unit. J Biomech 2012; 45: 1522-1528.

69. Starke SD, Willems E, Head M, et al. Proximal hindlimb flexion in the horse: effect on movement symmetry and implications for defining soundness. Equine Vet J 2012; 44: 657-663.

70. Warner SM, Koch TO, Pfau T. Inertial sensors for assessment of back movement in horses during locomotion over ground. Equine Vet J Suppl 38 2010; 42: 417-424.

71. Walker AM, Wilson AM, Pfau T. Comparison of kinematic symmetry index calculations and the effects of straight and circular trotting. Equine Vet J Suppl 38 2010; 41: 482-487.

72. O'Donovan KJ, Kamnik R, O'Keeffe DT, et al. An inertial and magnetic sensor based technique for joint angle measurement. J Biomech 2007; 40: 2604-2611.

73. Ferrari A, Cutti AG, Garofalo P, et al. First in vivo assessment of "Outwalk": a novel protocol for clinical gait analysis based on inertial and magnetic sensors. Med Biol Eng Comput 2010; 48: 1-15.

74. Saber-Sheikh K, Bryant EC, Glazzard C, et al. Feasibility of using inertial sensors to assess human movement. Man Ther 2010; 15: 122-125.

75. Cooper G, Sheret I, McMillian L, et al. Inertial sensor-based knee flexion/extension angle estimation. J Biomech 2009: 2678-2685.

76. Pfau T, Witte TH, Wilson AM. A method for deriving displacement data during cyclical movement using an inertial sensor. J Exp Biol 2005; 208: 2503-2514.

77. Pfau T, Witte TH, Wilson AM. Centre of mass movement and mechanical energy fluctuation during gallop locomotion in the Thoroughbred racehorse. J Exp Biol 2006; 209: 3742-3757.

78. Pfau T, Ferrari M, Parsons K, et al. A hidden Markov model-based stride segmentation technique applied to equine inertial sensor trunk movement data. J Biomech 2008; 41: 216-220.

79. Walker VA, Walters JM, Griffith L, et al. The effect of collection and extension on tarsal flexion and fetlock extension at trot. Equine Vet J 2012; Sept 4 Epub.

80. Olsen E, Anderson PH, Pfau T. Accuracy and precision of equine gait event detection during walking with limb and trunk mounted inertial sensors. Sensors 2012; 12: 8145-8156.

81. Wickler SJ, Hoyt DF, Clayton HM, et al. Energetic and kinematic consequences of weighting the distal limb. Equine Vet J 2004; 36: 772-777.

82. Clayton HM, White AD, Kaiser LJ, et al. Short-term habituation of equine limb kinematics to tactile stimulation of the coronet. Vet Comp Orthop Traumatol 2008; 21: 211-214.

83. Schamhardt HC, Merkens HW. Objective determination of ground contact of equine limbs at the walk and trot: comparison between ground reaction forces, accelerometer data and kinematics. Equine Vet J Suppl 17 1994; 26: 75-79.

Chapter Two

Validation of an equine inertial measurement unit system in clinically normal horses during walking and trotting[i]

Introduction

Lameness is one of the most common reasons that horses are examined by veterinarians and may account for > $1 billion/y in expenses.[1] Subtle lameness may be difficult to detect, and a lameness examination, as performed by both experienced and inexperienced veterinarians, is subjective with high inter-observer and intra-observer variability.[2,3] One proposed reason for the high amount of variability is the various aspects of gait or body position (ie, head position, foot flight, and limb movement) that are examined by a veterinarian.[4] The most commonly used lameness grading scale in the United States is the American Association of Equine Practitioners scale,[5] which has strict criteria for each grade but also allows for a large amount of variability within each grade.[4] In a recent study,[6] investigators reported that there was better inter-observer agreement with an American Association of Equine Practitioners lameness score > 1.5 (93.1%) than for a score of < 1.5 (61.9%). Thus, because the subjective lameness examination cannot be judged as a true criterion-referenced standard of lameness diagnosis,[6] there is a need for more quantitative motion analysis systems to describe motion and lameness of horses.

---

[i] *Moorman VJ, Reiser RF, McIlwraith CW, Kawcak CE. Validation of an equine inertial measurement unit system in clinically normal horses during walking and trotting. Am J Vet Res 2012; 73: 1160-1170.*

Currently, the most accepted methods for quantitative equine gait analyses are force platforms and 3-D optical kinematics. Both of these systems have variables that are well correlated with lameness, including the kinetic variables peak vertical force and impulse[7] and the kinematic variables extension of the metacarpophalangeal (or metatarsophalangeal) joint (fetlock joint), changes in protraction and retraction of the distal aspects of limbs, temporal changes in stride parameters, and alterations in maximum hoof height.[8,9] However, these systems are best used in research settings because they are available at limited locations, are expensive, require special training for use and interpretation of results, and typically only measure 1 or 2 gait cycles at a time[4]because there is usually a small camera field of view and 1 or 2 consecutive force platforms. Considering that subtle lameness may not be detected at every stride or at every velocity, force platform and 3-D optical kinematics may not be able to evaluate the exact strides at which lameness is apparent.[4]

A force-measuring treadmill has been developed[10]that allows for multiple strides to be evaluated with regard to optical kinematics and vertical forces. Its ability to measure only vertical forces[10] is 1 limitation of this treadmill. However, it also has limited availability, and because it is a custom-made, expensive piece of equipment, its clinical use is unlikely. Additionally, it is often difficult to separate the forces associated with each hoof when the treadmill is used, especially when the detail for detection of subtle lameness is necessary. A force-measuring shoe has been developed that has application for clinical settings,[11] but there is some concern that the weight of the shoe may impact movement of the distal aspect of a limb, which could influence the evaluation of normal gait and lameness.[4] Also, force-measuring shoes currently are machined to fit a particular horse.[12]

Several non-optical motion sensor systems have been developed for use in analysis of equine gaits.[13–16] These motion sensor systems have multiple components, including accelerometers, gyroscopes, magnetometers, and global positioning system data logging systems, and as a group are referred to as inertial sensor (IS) systems. Those composed of an accelerometer, gyroscope, magnetometer, and temperature-correcting thermostat are often referred to as inertial measurement unit(IMU) systems.[15] The most widely used commercially available IS system (Lameness Locator, Equinosis LLC, St Louis, Mo.) uses gyroscopes and accelerometers to identify asymmetric head or pelvic movement to identify a lame limb.[13] Therefore, a hoof-mounted IMU system would provide additional information about alterations in mechanics of the distal aspect of a limb that a body mounted IS system would be unable to provide.

The IMU technology may provide another avenue of equine motion analysis because of the sensor's small size, portability, and ability to measure multiple consecutive strides in field settings. One human IMU system (MT9, Xsens, Enschede, The Netherlands) requires the sensors to be attached to each other by wires, which could be cumbersome if used on the distal aspect of the limbs of horses. This human IMU system has been used to measure equine trunk movement,[15,17] but the sensors can only measure accelerations of ± 10 g, which may not be high enough for the distal aspect of limbs. Investigators in 1 study[15] measured accelerations of ± 5 g when the inertial sensor was mounted on the most dorsal aspect of the shoulders (ie, withers) of a horse traveling at a fast canter. Accelerometers used on the hoof of a horse can typically measure accelerations in the range of ± 9,800 m/s^2.[15,18] Thus, IMU systems designed for use in the study of human locomotion are not adequate for use in examining locomotion of the distal aspect of the limbs and hoof of horses at high speeds. A newly developed equine IMU system differs from other motion analysis systems in that it uses multiple sensors (placed on the head and the distal aspects of up to 4 limbs), which are wireless. In addition, this equine IMU system was developed for potential use on the distal aspects of the limbs of a horse at speeds up to a gallop. This IMU system also differs from other lameness detection systems that use gyroscopes and accelerometers in that the full 3-D kinematics (linear and angular positions, velocities, and accelerations) are accessible for analysis. However, the accuracy of this system has not yet been established by the manufacturer.

A limited number of studies[15,17,19] have been conducted with IMU systems in horses. A validation study[19] of a human IMU system investigating equine trunk movement found that the error of the IMU sensor compared to an optical kinematic system was < 7% of the total range of motion in all 3 orthogonal directions during walking, trotting, and cantering. A larger number of studies have been conducted to determine the accuracy of IMU systems for use in evaluating specific human movements. Several studies[20–22] revealed a high degree of correlation between IMU and optical systems, with most correlations > 0.90. In other studies,[21–23] the root mean squared error (RMSE) has been used to assess the accuracy of IMU systems. Root mean squared errors ranging from 0.7° to 25.6° have been reported for orientation data. In one study[22] conducted to evaluate movement of the upper arm, there was a high overall accuracy of the IMU system with positional RMSEs < 1 cm and orientation RMSEs between 2.5° and 5°. On the basis of these previous comparisons in combination with the knowledge that the acceleration at hoof impact is of higher frequency than that of the assessed human motions, any new IMU system must be validated for use in horses.

Therefore, the objective of the study reported here was to compare the accuracy of an equine IMU system with that of a 3-D optical kinematic system, which is the criterion-referenced standard for motion measurement, and to validate the IMU system by examining equine locomotion of the hooves of the right forelimb and hind limb of non-lame horses during walking and trotting. We hypothesized that the IMU system, rigidly attached to a hoof and to optical markers, would provide data as accurate and precise as those reported by other research groups for a 3-D optical kinematic system.

Materials and Methods

Horses—Five clinically normal Quarter Horses (age, 2 to 3 years) with no obvious lameness while walking or trotting were used for the study. All hooves of each horse were trimmed and balanced before the study began. All horses were acclimated to the Gait Analysis Laboratory where data were collected. All procedures were approved by the Institutional Animal Care and Use Committee of Colorado State University.

IMUs and retro-reflective markers—Each node of the IMU system measured 63 X 63 X 25 mm with a mass of approximately 80 g **(**Figure 2.1**)**. The IMU system was composed of three 3 degree of freedom (DOF) accelerometers, a 3 DOF rate gyroscope, a 3 DOF magnetometer, and a thermostat and sampled at 500 Hz. The 3 accelerometers were used for each orthogonal axis and had operating ranges of ± 1.7 g, ± 18 g, and ± 125 g, which were selected for the highest possible resolution at slow gaits and moderate- and high-impact gaits. Data were collected simultaneously from all accelerometers for all axes. The signal-processing algorithms then selected the accelerometer independently for each axis that provided the most accurate estimate of the acceleration, taking into account their maximum range and sensitivity. The gyroscope range could be programmed for rates of rotation up to ± 10,000°/s.

For each trial, 5 IMU nodes were used (1 on the horse's head over the occipital protrusion at the back of the skull [ie, the poll] and 1 on each limb). The IMU nodes were attached to the lateral hoof wall of all 4 hooves with acrylic glue.[a] Three 1.5-cm-diameter, spherical, retro-reflective markers were placed on top of the IMU nodes located on the hooves of the right limbs of each horse by use of a custom bracket, which created a triad that moved rigidly with the node. The bracket and triad measured 11 X 12.4 X 0.5 cm and were covered by non-reflective white tape. The weight of the bracket and triad was 102.6 g, so the combined node-triad unit weighed approximately 182.6 g. The bracket was attached to the sensor by fabric hook-and-loop fasteners and further stabilized by two 1/8-inch pieces of umbilical tape, which were incorporated into the glue used to attach the sensor to the hoof wall. The markers were located approximately 8 to 10 cm apart on the triad.

Cameras and collection of kinematic data—Eight infrared cameras[b] operating at 200 Hz were used to collect 3-D optical kinematic data. The cameras were placed in a semicircular configuration on the right side of each horse for all trials. Four cameras were placed on tripods near the ground and 4 were placed on elevated overhead positions. Calibration of the optical kinematic system[c] for the trials yielded coordinate resolution to within 2 mm.

Trial design and synchronization—For data collection, all horses were led at a walk and a trot over a rubberized runway covering an asphalt surface measuring 1.2 X 24.8 m with an optical capture volume of 3.7 X 1.3 X 2.4 m. The capture volume was located near the middle of the long axis of the runway, which allowed each horse to be at a constant speed at the location of the capture volume. The capture volume contained 2 force platforms imbedded in the runway; these force platforms were not used for the present study. Horses were led at a walk and a trot at a consistent and comfortable speed for each horse. Each horse dictated its own optimal velocity, and the velocity of each trial was determined by 5 infrared timing gates[d] spaced at intervals of 1.5 m, which were linked to the optical kinematics computer and triggered by a horse immediately before it entered the capture volume.

Five complete strides were collected from the right forelimbs and hind limbs for each horse during walking and trotting. An anomaly detected by the IMU magnetometer in the data of the stride prior to the stride of interest as the horse approached the imbedded force platforms was used to synchronize the 2 systems and ensure that common strides were compared. This anomaly was a consistent, reproducible peak in the magnetic field, with a strength many magnitudes higher than the earth's magnetic field. Because the magnetometers were not used during this phase of the signal processing, the data output from the system was not affected. Typically, only 1 swing phase/runway pass was analyzed, although occasionally data for both a forelimb and hind limb were collected on the same runway pass. The acceleration curves for the Z direction (acceleration in the proximal-distal vertical direction), velocity curves for the X direction (velocity in the cranial-caudal forward direction), and angular orientation curve for Θ (orientation around the hoof medial-lateral axis) were matched between the IMU and optical systems so that the swing phases of the 2 systems were synchronized with regard to time and started and ended at the same times. The beginning of the swing phase examined in the present study included the beginning of hoof rotation (ie, when the heel started to rotate around the toe before leaving the ground). The end of the swing phase was immediately before hoof contact with the ground (the accelerometers within the inertial sensor revealed a ringing artifact when a hoof contacted the ground).

Optical data filtering and reference frames—Optical data were low-pass filtered at 12 Hz with a recursive fourth-order Butterworth filter. To yield linear and angular kinematics consistent with the IMU system, a local optical frame was necessary. The local origin of each triad was determined by creating a virtual point located at the mean of the cranial and caudal markers placing it near the local origin of the IMU node (Figure 2.1). The local optical reference frame was constructed around the local origin with the markers of the triad. The local optical reference frame was aligned with that of the IMU **(**Figure 2.2**)**. The origin of the global optical reference frame was translated to the local origin position at the start of the swing phase with the cranial-caudal axis (x-axis) rotated through the local origin at the end of the swing phase. This kept the z-axis vertical and the y-axis medial-lateral with the horse in motion. The linear position, velocity, and acceleration of the local reference frame origin within the global reference frame were compared with the IMU linear kinematics. Hoof orientation was examined by use of Cardan angles (Θ, Φ, and Ψ), with rotation of the local optical reference frame about the y-axis, followed by rotation around the new x-axis (x'), and lastly rotation around the new z-axis (z'').
This was consistent with the hoof orientations calculated by the equine IMU system.

IMU data processing—The IMU processing began with node synchronization so that all data had a common time base. Because there is little movement when a hoof is on the ground during the stance phase, all values were set to zero. The beginning of the stance phase was detected by identifying a period of high accelerations (hoof impact) followed by low accelerations. The end of the stance phase–beginning of the swing phase was identified by changes in orientation and increased accelerations in the IMUs.[e]

Raw data for the IMU were collected in a local reference frame of the hoof, with x-, y-, and z-axes identical to those of the optical system. Orientation of an IMU node with respect to each horse was determined when the node was not rotating or moving (ie, during the stance phase). Then, by use of measurements from the magnetometers of the earth's magnetic field and from the accelerometers of the earth's gravitational field, orientation of the sensor was established.[e]

Custom software[f] was used to determine linear velocities and positions via single and double integration of the linear acceleration data, respectively. The rate gyroscopes provided angular velocities, which were integrated to provide orientations and differentiated to determine angular accelerations.

All IMU data were collected and processed independently by the IMU manufacturer.[g] Therefore, both parties were not aware of the origin of the data until after comparisons were made. After the IMU data were processed, they were submitted to the authors for synchronization and comparison to the 3-D optical data.

Variables examined—Linear and angular variables were examined in all 3 dimensions. Maximum, minimum, and mean values were extracted for each linear and angular variable **(**Appendix I**)**. In the Z direction (proximal-distal), the position-versus-time curve had 2 peaks, so 2 maxima were extracted for this variable.

Statistical analysis—Linear and angular positions, velocities, and accelerations were compared between systems. The maximum, minimum, and mean values were extracted and compared by use of commercial software[h] via a paired *t* test or Wilcoxon signed rank tests and via Pearson correlation coefficients, with significance set at values of $P< 0.05$. All horses, gaits, and hooves were pooled for statistical analysis (total of 70 trials). To determine the appropriate paired test of difference, tests of normality were performed on the differences of the 2 systems; histograms and normal plots were also graphed from these differences. A paired *t* test was performed when data appeared to be normally distributed, and the Wilcoxon signed rank test was used for non-normally distributed data.

Root mean squared errors were calculated for each hoof of each horse at each gait across the entire swing phase to evaluate the overall error between the 2 systems. Because the 3-D optical kinematics system recorded data at 200 Hz and the inertial sensor recorded data at 500 Hz, the 2 systems were compared at a common frequency of 100 Hz. Mean RMSE and SD was calculated for the 5 horses for each gait and hoof (eg, forelimb hoof during trotting). The mean RMSE was compared with the range of values collected for each swing phase. A mean range was then calculated for the 5 horses for each gait and hoof. The RMSE was then calculated as a percentage of the range. Finally, time-normalized and mean curves were created and overlaid for the 2 systems to visually explore the profiles of each variable.

Results

Twenty-five strides, including both stance and swing phases, were collected for each hoof at each gait. The mean velocity of all trials for all horses during trotting was 2.75 m/s, with a range of 2.4 to 3.2 m/s. The mean velocity of all trials for all horses during walking was 1.3 m/s, with a range of 1.1 to 1.5 m/s. Individual horses typically moved at a consistent speed throughout the trials for each gait; the velocities of all trials were within 10% of the individual mean for each gait, and 53/70 (75%) were within 5% of the mean.

Because data for the stance phase were set to zero for IMU processing, only swing phase data were analyzed. Fifteen trials for the right forelimb hoof during trotting, 14 trials for the right hind limb hoof during trotting, 22 trials for the right forelimb hoof during walking, and 19 trials for the right hind limb hoof during walking yielded common data sets that were complete for both linear and angular kinematics from both systems.

Overall, results for the linear and angular variables determined by the IMU correlated well with results for the 3-D optical kinematic system **(**Table 2.1**)**. In the cranial-caudal (X) direction, 6 of 9 extracted values were highly correlated (r> 0.8) and 2 of 9 were moderately correlated (r>0.5). The minimum position, which was close to zero for both systems (the translated origin), was the only variable that was weakly correlated (r< 0.25). Six of 9 extracted x-axis values were significantly different between the 2 systems, as determined via the paired test of differences. Only 3 extracted values (mean position, minimum acceleration, and mean acceleration) were not significantly different between the 2 systems.

In the Y direction (medial-lateral), 7 of 9 extracted values were highly correlated and the remaining 2 were moderately correlated. Five of 9 y-axis values were significantly different between the 2 systems. The 4 extracted values that were not significantly different between the 2 systems were maximum, minimum, and mean position and mean acceleration.

In the Z direction (proximal-distal), 4 of 10 extracted values were highly correlated, 3 were moderately correlated, 2 were mildly correlated($r>0.25$), and 1 (ie, minimum position) was weakly correlated. Five of the 10 values were significantly different between the 2 systems. The 5 values that were not significantly different between the 2 systems were minimum position, second maximum position, maximum and minimum velocities, and minimum acceleration. Similar to results for the minimum position of the X direction, the minimum position of the Z direction was close to zero for both systems, although in the Z direction, it could occur at the beginning or end of the swing phase.

For the angular variables, Θ (ie, rotation around the medial-lateral axis) appeared to have the highest correlation between the 2 systems. Four of 9 extracted values were highly correlated, 4 of 9 were moderately correlated, and 1 of 9 was mildly correlated. Six of 9 values were significantly different between the 2 systems. The 3 values that were not significantly different between the 2 systems were minimum angular orientation, mean angular velocity, and mean angular acceleration.

For Φ, 1 of 9 values was highly correlated, 3 were moderately correlated, and 5 were mildly correlated. Seven of 9 values were significantly different between the 2 systems. The 2 values that were not significantly different between the 2 systems were minimum angular orientation and mean angular acceleration.

For ψ, 3 of 9 values were highly correlated, 4 were moderately correlated, and 2 were mildly correlated. Seven values were significantly different between the 2 systems. Only 2 values (ie, maximum angular orientation and mean velocity) were not significantly different between the 2 systems.

Root mean squared errors, as a percentage of the mean of the range for each variable, were similar between gaits **(**Table 2.2**)**. Linear displacement in the cranial-caudal direction and Θ (ie, rotation around the medial-lateral axis) appeared to have the least error (1.1% to 2.9% and 2.6% to 3.5%, respectively). The RMSE percentages for position and acceleration in the Y-direction (medial-lateral) typically were higher than those for both the X direction (cranial-caudal) and Z direction (proximal-distal). The range of RMSE percentages for position, velocity, and acceleration in the X direction were 1.1% to 2.9%, 3.8% to 6.1%, and 7.2% to 11.8%, respectively. The range of RMSE percentages for position, velocity, and acceleration in the Y direction were 12.4% to 19.2%, 9.4% to 18.7%, and 20.7% to 27.0%, respectively. The range of RMSE percentages for position, velocity, and acceleration in the Z direction were 10.1% to

17.7%, 8.4% to 11.4%, and 12.5% to 20.2%, respectively. For the angular variables, the RMSE percentages were higher for Φ and Ψ than for Θ. The range of RMSE percentages for position, velocity, and acceleration of Θwere 2.6% to 3.5%, 4.3% to 6.7%, and 9.5% to 22.3%, respectively. The range of RMSE percentages for position, velocity, and acceleration of Φ were 16.16% to 46.06%, 15.16% to 23.58%, and 22.61% to 28.95%, respectively. The range of RMSE percentages for position, velocity, and acceleration of Ψwere 17.2% to 31.7%, 19.5% to 22.5%, and 22.6% to 33.3%, respectively.

The appearance of the time-normalized and mean overlay plots was extremely similar between the 2 systems, both gaits, and both limbs **(**Figures 2.3– 2.8**)**. For the linear variables, positional and velocity data in all 3 directions had similar patterns. The accelerations in all 3 directions had a similar appearance, but the IMU curves contained more fluctuations and higher frequencies. In addition, the IMU curves had larger magnitude peaks and troughs for accelerations in the Y and Z directions in the hoof of the right forelimb during trotting (Figure 2.5, B and C).

For the orientation variables for the IMU system, Θ and Ψ were fairly similar in shape compared to the optical system, whereas Φ typically had higher values. For angular velocity, Θ had similar patterns between the two systems. Angular velocities for the IMU system for Φ and Ψ typically had higher magnitude peaks near the beginning of the swing phase at both gaits. For all 3 angular accelerations, there were similarities in appearance of the curves, but there were more fluctuations in the IMU compared to the optical curves (Figure 2.8, B and C).

Discussion

In the present study, we compared a novel equine IMU system with a commercially available 3-D optical system. The objective of the study was to determine whether the equine IMU system would provide similar data to that of the criterion-referenced standard of kinematics via the commercially available 3-D optical system. The swing phase was examined because during IMU processing, data in the stance phase were set to zero. In addition, there is a larger range of excursion in the linear and angular variables examined during the swing phase. Clinically, the stance phase, especially initial hoof impact and planting of the hoof, is more important in the pathogenesis of injury than is the swing phase.[18]The ringing artifact from the accelerometer in the IMU system at the end of the swing phase precluded the ability to examine hoof impact and planting of the hoof. The source of the ringing artifact is unclear and has not been previously observed by the manufacturer.[e] It is speculated that this ringing may be caused by a combination of factors, including rigid attachment of the IMU node to the hoof (compared with a boot attachment method), a relatively hard surface (compared with dirt), and the additional mass of the marker triad. Additional research to evaluate surface and attachment method would need to be performed to determine the source of the ringing. Even though hoof impact and planting of the hoof could not be examined, break-over at the end of the stance phase could be evaluated, as indicated in the present study, and this may be an additional phase of the stride important for evaluation. Considering that the IMU system has a high frequency event at toe-off, which was not evident in data for the optical system, the IMU system may be preferable to the optical system to examine this phase of the stride.

Temporal components of the stride and duty factor (i.e., percentage of the stride when the limb is weightbearing) of each limb are variables that could be measured by the IMU system and could be important in lameness evaluation. Because the swing phase comparisons were closely matched on the basis of time, these components were not statistically evaluated between the 2 systems. From cursory examination of the data, the swing phase times appeared to be extremely similar between the 2 systems.

In general, the IMU system was correlated fairly well with the 3-D optical kinematic system, as indicated by the high number of moderate to high correlations (Table 2.1). There were 25 of 55 (45%) extracted values with high correlations ($r > 0.8$) and 18 of 55 (33%) values with moderate correlations ($r > 0.5$). As expected, several variables were not highly correlated. These variables included minimums in the X and Z direction, which were clustered around zero and were not expected to be correlated. The IMU and 3-D optical systems did not always provide exactly the same values for the linear and angular variables examined, which was indicated by the paired tests of differences and RMSEs. However, the overall shape of each variable versus percentage time curve was extremely similar.

The same handler assisted for all horses, trials, and gaits. This handler allowed each horse to move at a comfortable speed chosen by each horse. This approach was used to mimic a clinical setting. In addition, because all comparisons between the IMU and optical systems were made on the basis of individual trial and later the mean was calculated for each horse and gait, differences in individual trial velocities did not hinder comparison between the 2 systems. Also, in determining correlations, it is useful to have a range of data, which was accomplished by combining walking and trotting data and enhanced by the small amount of variability in gait velocity.

A few studies in humans have used the Pearson correlation coefficients for comparison of IMU to 3-D optical systems. A study[21] on human vertebral column posture in the X and Y directions revealed correlations of > 0.77 for thoracic movements and > 0.97 for lumbar movements. Another study[22] in which upper limb movements in humans were evaluated revealed correlations > 0.96 for linear position in the X, Y, and Z directions and > 0.94 for orientation. A third study[20] conducted to evaluate the stride, step, and stance duration in humans during running at various velocities revealed correlations > 0.76, with the majority (10/12 variables) of correlations > 0.90. Overall, these studies, in which several IMU units were compared with optical systems, revealed higher correlations in both linear positional and angular orientation values than were determined for the equine IMU system used in the present study. Overall, the equine IMU system used in the present study only had 10 of 55 (18%) values of $r > 0.90$, and when examining linear positions and angular orientations, there were only 3 of 19 variables with $r > 0.90$ (Table 2.1). A small number of the variables examined would not be expected to have high correlations because they are expected to cluster around zero. From this correlation data, it is not clear whether the equine IMU system at this stage of development would perform adequately for use in clinical cases.

The IMU system collected linear data with accelerations, and these variables were integrated to calculate velocities and positions, whereas the 3-D optical system began with positional data and differentiated these variables to calculate velocities and accelerations.

Because of this difference in calculation of variables, examining linear positions and accelerations allowed the evaluation of both ends of the calculation process. The RMSEs for both position and acceleration in the X direction (cranial-caudal) direction were smaller than for the Y and Z directions, and overall, the RMSE percentages for position were slightly to moderately better than the RMSE percentages for acceleration. Given that the IMU system starts with linear acceleration, it is likely that some of the errors in the acceleration values originated from the 3-D optical system. Because the calculation of acceleration involves 2 differentiations from the initial positional data, any errors to determine velocities are compounded in the calculation of acceleration. Also, the 2 systems differ in frequency content, which may also lead to the differences in acceleration. Because the 3-D optical system collected data at a lower frequency (200 Hz) and was then low-pass filtered, this system yielded a smoother profile and lower magnitude maximum and minimum velocities and accelerations (Figures 2.4 and 2.5). Although this may reduce the accuracy of the linear acceleration data within the optical system, it does provide for a more stable output. The higher frequency content of the IMU system, although more sensitive to high-frequency fluctuations, may make it more difficult to use acceleration data clinically. However, further evaluation of the higher frequency IMU system for both detection and quantification of lameness, whether clinical or experimentally induced, is warranted.

The angular variables were calculated from linear positions in the 3-D optical system and integrated and differentiated from angular velocities in the IMU system. Analysis of the graphs revealed that Φ and Ψ have the same general shape, but there was high variability leading to higher RMSE percentages for the Φ and Ψ variables, compared with the variability for the Θ

variables. It is also expected that Φ and Ψ would have higher error than Θbecause the order of calculation of these 3 variables starts with Θ rotation, then Φ, and finally Ψ. Any errors for Θ would also be added to errors in Φ, and both of those errors would be compounded in Ψ. In the human IMU literature, higher error rates have been reported in both Φ and Ψ than in Θ.[24]

In general, the variables that performed best in the RMSE evaluations were those that had larger ranges (specifically the position for the X direction and Θ, generally in the sagittal plane). This is a similar finding to that in a report[22] of a human IMU system in which there was less accuracy in movements with small ranges of motion (< 2^o or < 0.5 cm). When comparing mean RMSEs among variables with the same limb and gait, there were few consistent results. However, when the mean RMSE was converted into a percentage of its range, the variables with larger range had lower errors. It is possible that if a larger range of motion was performed for the Y, Z, Φ, and Ψ variables, the performance of these variables would improve.

A large range of RMSEs for both position and orientation have been reported for a variety of movements in humans[20-23]as well as movement of the trunk in horses.[19]Analysis of data for the study reported here indicated positional RMSEs within 5 cm in all 3 orthogonal directions, with larger RMSEs in the X direction where there is a larger range of motion (Table 2). Most RMSEs in the Y and Z directions were < 1 cm. These Y and Z values corresponded fairly well (positional errors < 1cm) with those in a previous report.[22]In another study,[19] investigators reported errors as a percentage of the range, with positional values of< 6.5% during walking and < 4.3% during trotting for all 3 directions. In general, RMSE positional values in the present study were higher (< 18.6% during walking and < 19.3% during trotting). Investigators in that study[19]also found a trend in that the Y direction had higher RMSEs than did the X or Z directions, which is similar to results of the present study. For orientation data, investigators in another study[23]founda large variability in RMSEs (depending on movement), with mean RMSEs ranging from 0.7° to 25.6°. In the present study, we found similar but higher results, with orientation RMSEs ranging from 2.6° to 46.06°.

The ultimate clinical goal of a motion-sensing system, such as an IMU system, would be accurate detection and evaluation of lameness. Asymmetry between the lame and non-lame limbs in vertical displacement of lameness during the swing phase has been reported in a small number of horses.[25] Thus, accuracy in the proximal-distal (Z) direction is necessary to appreciate those asymmetries. This equine IMU system performs moderately well in the Z direction (moderate to high correlations, but moderately high RMSEs). Further comparison of this IMU system to the optical system would be needed to determine whether the IMU system provides sufficient accuracy in the Z direction. In addition, comparing the vertical displacements measured by the IMU system in a lame versus a non-lame limb may provide additional information about the ability of this system to identify asymmetry.

In addition, accelerations of the hoof in the X and Z direction have been measured previously for use in evaluation of ground surfaces because the accelerations at hoof impact may be important in the development of injury.[26] In the present study, acceleration in the X and Z directions had moderate to high correlations and had similar appearance in the percentage-versus-time graphs (Figure 2.8) but had RMSEs (percentage of range) that were fairly high (7.2% to 11.8% and 12.5% to 20.2%, for X and Z, respectively). However, considering that there was a ringing artifact of unknown origin for the accelerometers at hoof impact, it is unclear whether this equine IMU system is adequate for use in examination of the impact phase of the stride. Given that hoof impact is an important phase of the stride for evaluation, the lack of ability of this equine IMU system to evaluate this phase of the stride would severely hinder its clinical usefulness. Determination of the source and elimination of the ringing artifact would be necessary to determine whether the IMU system would be useful in the examination of hoof impact.

Measurement of 3-D rotations of joints has been reported in clinically normal horses and may also be important in evaluating lameness.[27] Thus, if IMU systems are to be used, it is important that they provide accurate measurement of dynamic orientation. The equine IMU system examined in the present study appeared to provide adequate accuracy for the Θ rotation but may not be adequate in the Φ and Ψ rotations (larger RMSEs and lower correlations). The limited accuracy in measurement of orientation in all 3 rotations may reduce the clinical usefulness of this equine IMU system; however, this hypothesis would need to be tested in horses with experimentally induced lameness.

Overall, the IMU system attached rigidly to a hoof provided similar data with patterns similar to those for the criterion-referenced standard 3-D optical system during the swing phase of walking and trotting horses. Further studies would need to be performed to examine faster gaits (canter and gallop). Although the 2 systems did not provide identical data, overall, there was moderate to high correlation between most variables determined by the 2 systems during the swing phase of the stride. Considering that there was more error between the 2 systems when the variable went through a small range of motion, it would be important to compare these 2 systems during the stance phase of the stride when the hoof has small ranges of motion. In addition, if the IMU nodes are attached by a non-rigid method to a hoof, such as with elastic bandage material or a boot, there may be different results because of motion of the node relative to the hoof. It would be important to examine attachment methods other than acrylic glue because a quick and easy method of IMU node attachment would be desirable for clinical use of this system. Additionally, because there was a ringing artifact during a key phase of the stride (hoof impact), further investigation of the source of the artifact would be necessary before this IMU system could be recommended for clinical use. Marketing point of this product would undoubtedly include clinical use for lameness detection; thus, it would be necessary to determine the diagnostic utility of this IMU system for various degrees of lameness in horses with experimentally induced lameness or clinical cases.

---

[a] Superfast glue, Vettec Hoof Care Products, Oxnard, Calif.
[b] Volant by Peak, Performance Technologies Inc, Centennial, Colo.
[c] Vicon-Motus 9.2, Vicon Motion Systems Inc, Centennial, Colo.
[d] MEK 92-PAD photoelectric control Mekontrol Inc, Northboro, Mass.
[e] Davies M, EquuSys Inc, Sudbury, Mass: Personal communication, 2011.
[f] MATLAB, Mathworks, Natick, Mass.
[g] Equusense Ultra, EquuSys Inc, Sudbury, Mass.
[h] SAS, version 9.2, SAS Institute Inc, Cary, NC.

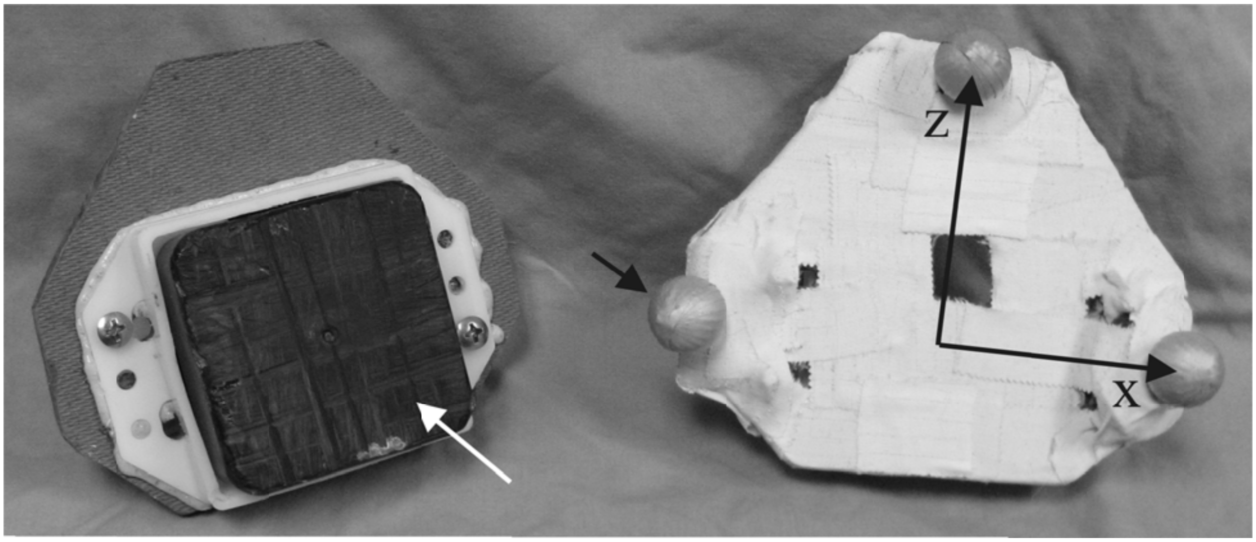

Figure 2.1—Photograph of medial (left) and lateral (right) views of an IMU with a triad of retro-reflective markers (arrowhead) attached by use of a custom bracket. The IMU node (white arrow) is exposed. Grooves have been made in the medial aspect of the IMU casing to increase the surface area for attachment of the IMU to a hoof wall. Notice on the lateral view the local optical reference frame with the origin for the z- and x-axes between the cranial and caudal markers. The marker triad measures 11 x 12.4 x 0.5 cm.

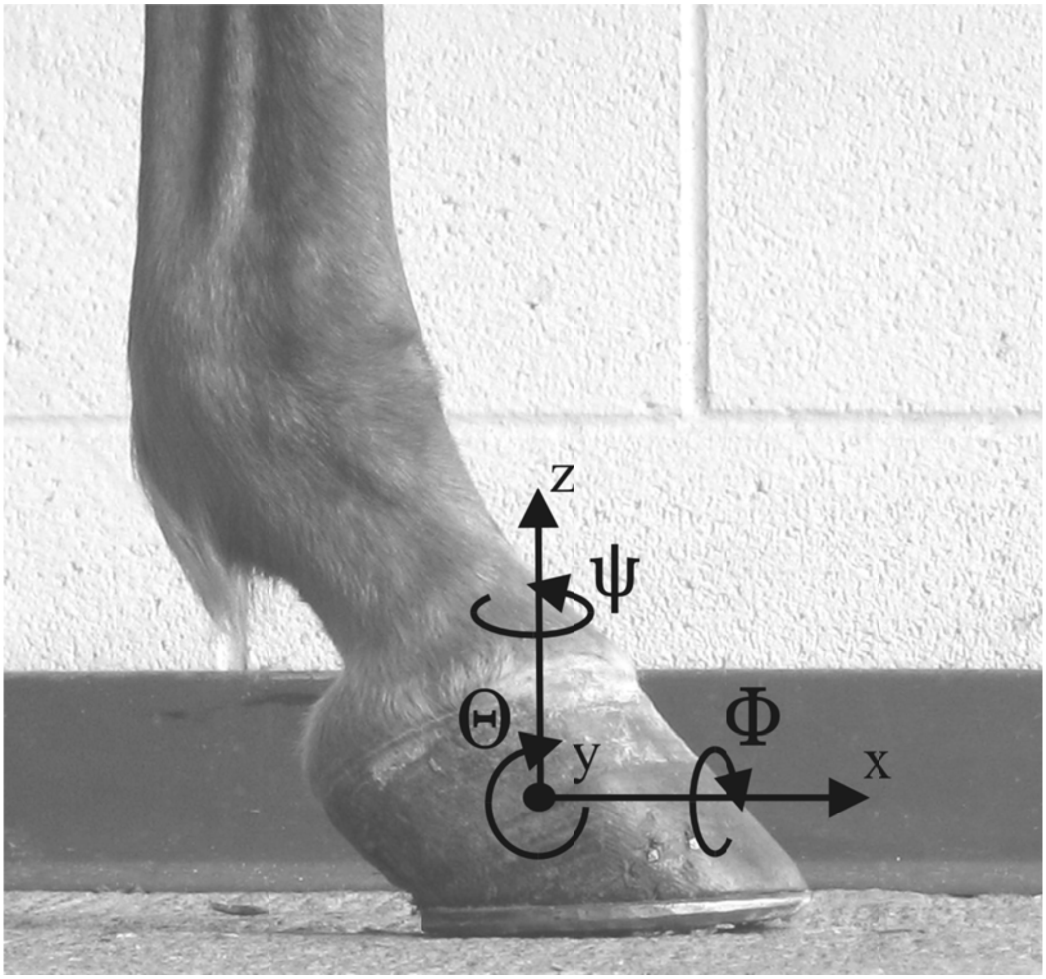

Figure 2.2—Schematic of the local 3-D orientations of axes overlaying an equine hoof. The cranial-caudal axis (x-axis) is positive in the cranial direction, the medial-lateral axis (y-axis) is positive medially, and the proximal-distal axis (z-axis) is positive in a proximal vertical direction when the hoof is flat on the ground. Rotation around the y-axis (Θ),x-axis(Φ) and z-axis(Ψ) are indicated. Rotation in all axes is positive in the counter-clockwise direction (right hand rule).

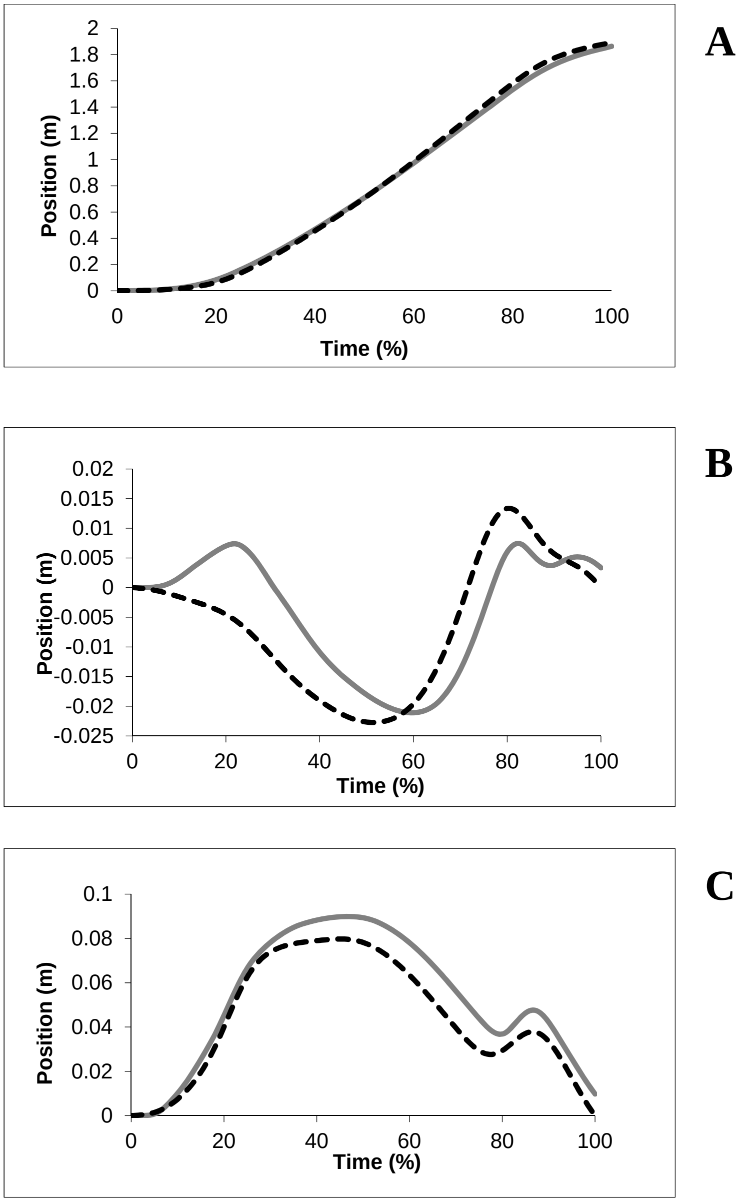

Figure 2.3—Time-normalized curves of mean values determined by use of an IMU system (solid line) and a 3-D optical system (dashed line) for the position in the X direction (cranial-caudal; A), Y direction (medial-lateral; B), and Z direction (proximal-distal; C) of the right forelimb hoof of 5 horses during trotting. Time is presented as the percentage of swing phase. Notice that the scale on the y-axis differs among panels.

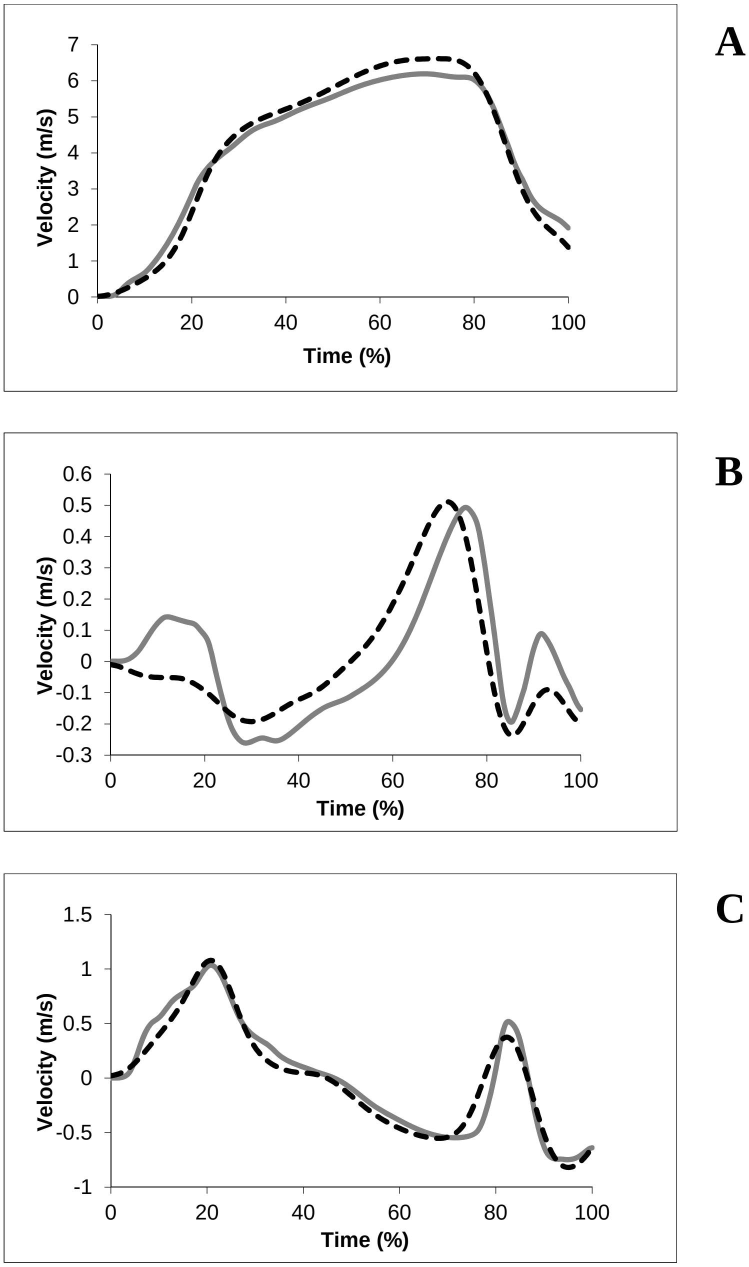

Figure 2.4—Time-normalized curves of mean values determined by use of an IMU system (solid line) and a 3-D optical system (dashed line) for the velocity in the X direction (cranial-caudal; A), Y direction (medial-lateral; B), and Z direction (proximal-distal; C) of the right forelimb hoof of 5 horses during trotting.
See Figure 2.3 for remainder of key.

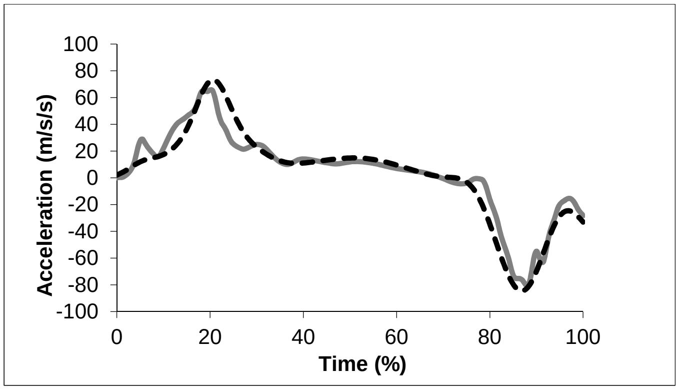

A

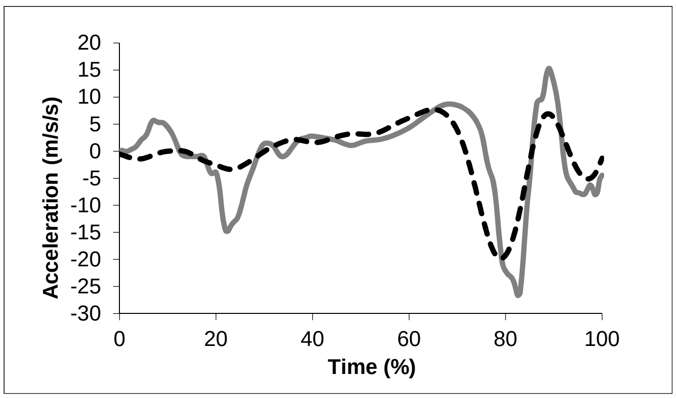

B

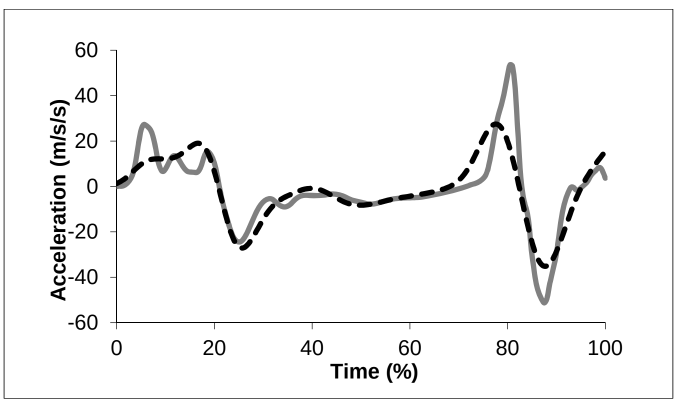

C

Figure 2.5—Time-normalized curves of mean values determined by use of an IMU system (solid line) and a 3-D optical system (dashed line) for the acceleration in the X direction (cranial-caudal; A), Y direction (medial-lateral; B), and Z direction (proximal-distal; C) of the right forelimb hoof of 5 horses during trotting.
See Figure 2.3 for remainder of key.

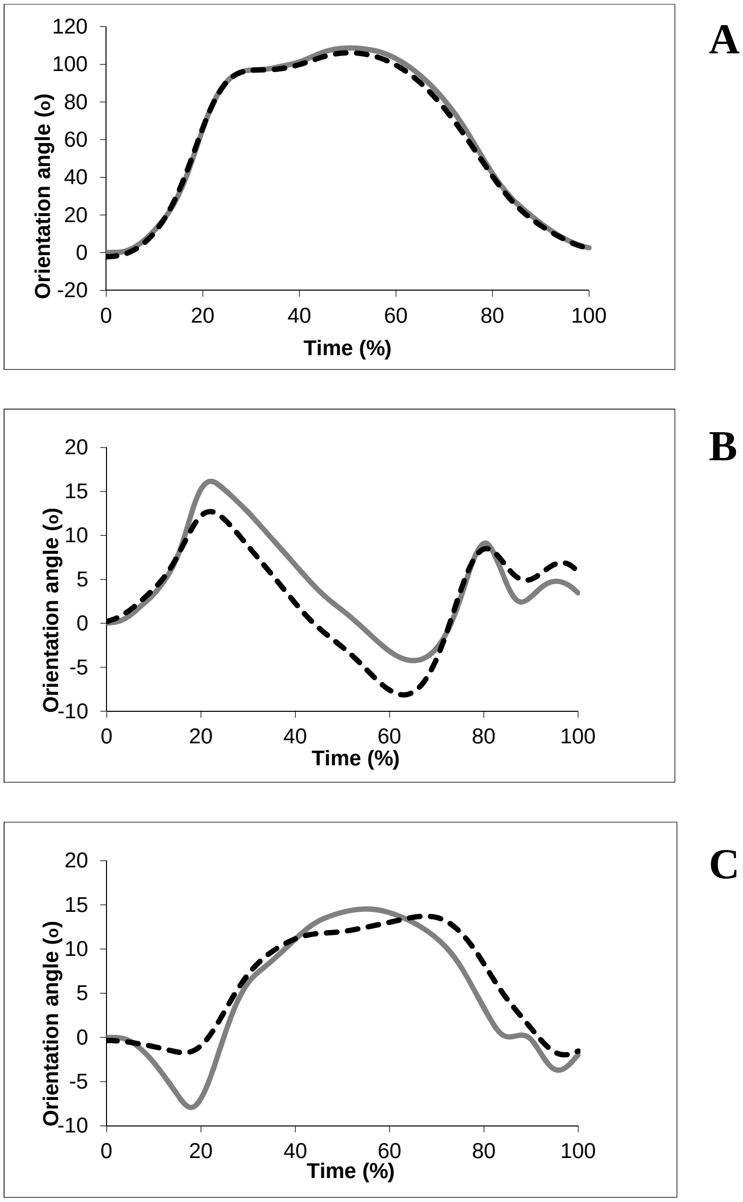

Figure 2.6—Time-normalized curves of mean values determined by use of an IMU system (solid line) and a 3-D optical system (dashed line) for angular orientation forΘ (rotation around the y-axis; A), Φ (rotation around the x'-axis; B), and Ψ (rotation around the z"-axis; C) of the right forelimb hoof of 5 horses during trotting.
See Figure 2.3 for remainder of key.

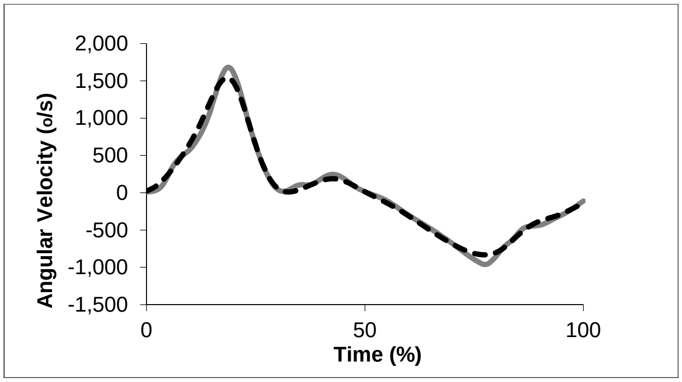

A

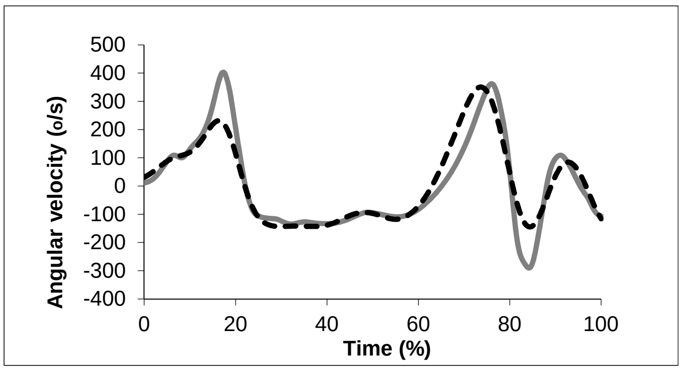

B

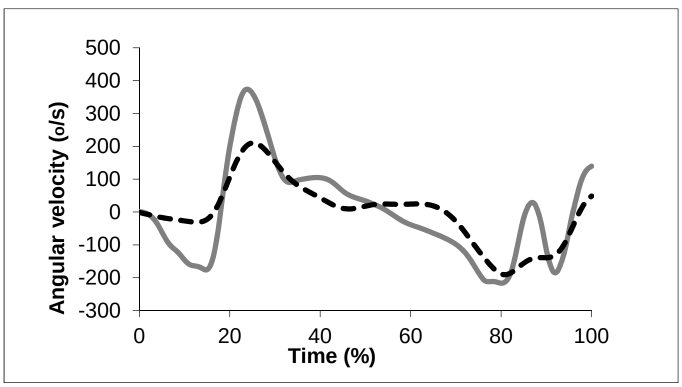

C

Figure 2.7—Time-normalized curves of mean values determined by use of an IMU system (solid line) and a 3-D optical system (dashed line) for angular velocity for Θ (rotation around the y-axis; A), Φ (rotation around the x’-axis; B), and Ψ (rotation around the z”-axis; C) of the right forelimb hoof of 5 horses during trotting.
See Figure 2.3 for remainder of key.

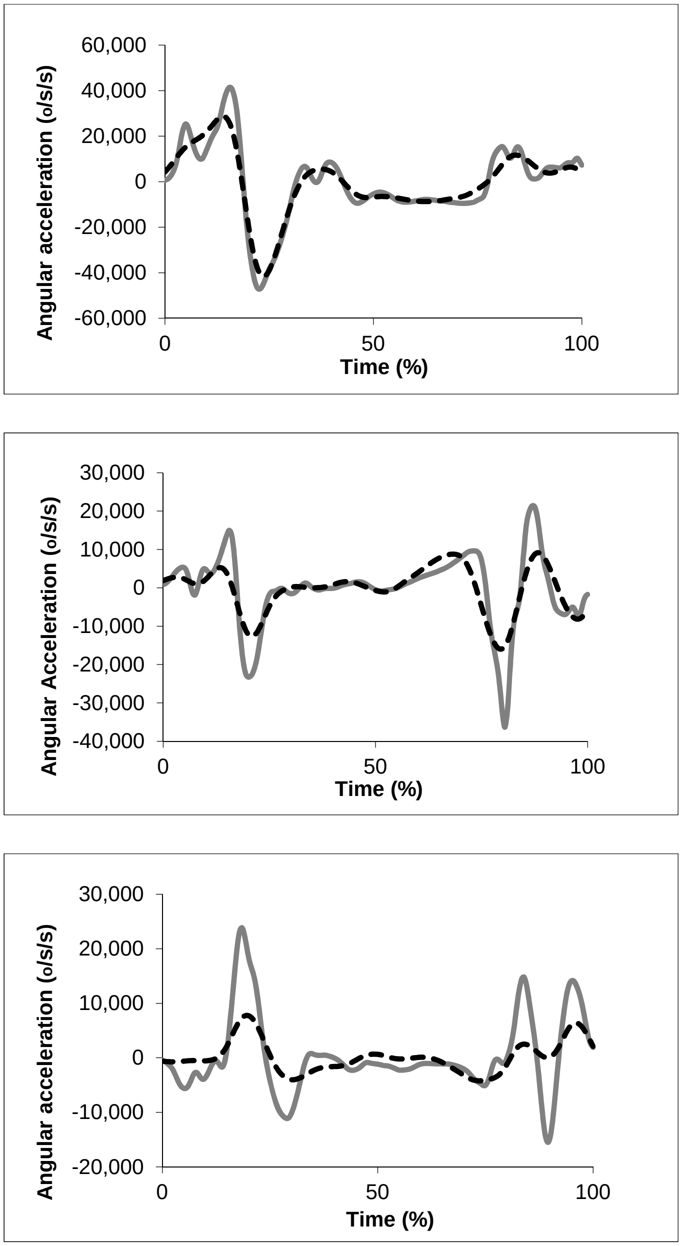

A

B

C

Figure 2.8—Time-normalized curves of mean values determined by use of an IMU system (solid line) and a 3-D optical system (dashed line) for angular acceleration for Θ (rotation around the y-axis; A), Φ (rotation around the x’-axis; B), and Ψ (rotation around the z”-axis; C) of the right forelimb hoof of 5 horses during trotting.
See Figure 2.3 for remainder of key.

Table 2.1—Pearson correlation coefficients with their associated *P* values and results for paired test of differences (*t* test or Wilcoxon signed rank test) for the X direction (cranial-caudal), Y direction (medial-lateral), and Z direction (proximal-distal) between the 3-D optical kinematics and IMU systems in horses during walking and trotting. Correlations were considered high ($r>0.8$), moderate ($r>0.5$ to ≤ 0.8), or mild ($r>0.25$ to ≤ 0.5). *Values differed significantly ($P<0.05$) between the 2 kinematic systems.†A paired *t* test was performed.

		X direction			Y direction			Z direction		
Variable	**Value**	***r***	***P* value**	***P* value for *t* test or Wilcoxon signed rank test***	***r***	***P* value**	***P* value for *t* test or Wilcoxon signed rank test***	***r***	***P* value**	***P* value for *t* test or Wilcoxon signed rank test***
Linear Position	Maximum 1	0.93	< 0.001	< 0.001†	0.83	< 0.001	0.247†	0.88	< 0.001	< 0.001
	Maximum 2	NA	NA	NA	NA	NA	NA	0.51	< 0.001	0.255
	Minimum	0.12	0.321	< 0.001	0.84	< 0.001	0.218†	0.08	0.492	0.107
	Average	0.93	< 0.001	0.896	0.78	< 0.001	0.825†	0.63	< 0.001	0.014†
Linear Velocity	Maximum	0.96	< 0.001	< 0.001	0.91	< 0.001	0.005†	0.87	< 0.001	0.938
	Minimum	–0.56	< 0.001	< 0.001†	0.87	< 0.001	< 0.001†	0.85	< 0.001	0.413†
	Average	0.96	< 0.001	0.003	–0.87	< 0.001	0.036†	–0.33	0.005	< 0.001†
Linear Acceleration	Maximum	0.89	< 0.001	< 0.001	0.64	< 0.001	< 0.001	0.76	< 0.001	< 0.001
	Minimum	0.94	< 0.001	0.296†	0.91	< 0.001	< 0.001	0.83	< 0.001	0.922†
	Average	0.67	< 0.001	0.979	0.90	< 0.001	0.938†	0.48	< 0.001	0.001†

Table 2.1---Continued

		X direction			Y direction			Z direction		
Variable	**Value**	***r***	***P* value**	***P* value for *t* test or Wilcoxon signed rank test***	***r***	***P* value**	***P* value for *t* test or Wilcoxon signed rank test***	***r***	***P* value**	***P* value for *t* test or Wilcoxon signed rank test***
Angular Orientation	Maximum	0.88	< 0.001	< 0.001†	0.31	0.008	< 0.001†	0.85	< 0.001	0.450†
	Minimum	0.46	< 0.001	0.601†	0.69	< 0.001	0.052†	0.42	< 0.001	< 0.001†
	Average	0.91	< 0.001	0.0169†	0.45	< 0.001	< 0.001†	0.72	< 0.001	0.002†
Angular Velocity	Maximum	0.97	< 0.001	< 0.001†	0.41	< 0.001	< 0.001†	0.82	< 0.001	< 0.001
	Minimum	0.91	< 0.001	< 0.001	0.77	< 0.001	< 0.001	0.72	< 0.001	< 0.001†
	Average	0.58	< 0.001	0.219†	0.40	< 0.001	< 0.001†	0.49	< 0.001	0.314†
Angular Acceleration	Maximum	0.66	< 0.001	< 0.001	0.70	< 0.001	< 0.001	0.77	< 0.001	< 0.001
	Minimum	0.76	< 0.001	< 0.001	0.80	< 0.001	< 0.001	0.83	< 0.001	< 0.001
	Average	0.71	< 0.001	0.054†	0.50	< 0.001	0.315†	0.67	< 0.001	< 0.001†

Table 2.2—Mean ± SD RMSE, mean range, and RMSE as a percentage of the mean range for each gait and hoof for the X direction (cranial-caudal), Y direction (medial-lateral), and Z direction (proximal-distal) during the swing phase at the walk and trot.

		X direction			**Y direction**			**Z direction**		
Variable	**Speed and limb**	**RMSE mean ± SD**	**Range of mean**	**RMSE as % of range**	**RMSE mean ± SD**	**Range of mean**	**RMSE as % of range**	**RMSE mean ± SD**	**Range of mean**	**RMSE as % of range**
Position (m)	Trotting and forelimb	0.029 ± 0.015	1.88	1.57	0.009 ± 0.005	0.04	19.23	0.008 ± 0.006	0.08	10.13
	Trotting and hind limb	0.025 ± 0.015	1.89	1.33	0.012 ± 0.007	0.10	12.42	0.012 ± 0.010	0.07	17.70
	Walking and forelimb	0.044 ± 0.039	1.53	2.89	0.009 ± 0.007	0.05	18.57	0.006 ± 0.003	0.05	10.40
	Walking and hind limb	0.016 ± 0.009	1.53	1.06	0.007 ± 0.003	0.04	16.69	0.008 ± 0.005	0.06	12.91
Velocity (m/s)	Trotting and fore limb	0.410 ± 0.194	6.71	6.11	0.193 ± 0.062	1.03	18.72	0.211 ± 0.088	2.11	9.96
	Trotting and hind limb	0.256 ± 0.070	6.45	3.97	0.169 ± 0.075	1.80	9.39	0.200 ± 0.123	1.97	10.14
	Walking and forelimb	0.259 ± 0.109	4.37	5.94	0.122 ± 0.073	0.76	16.03	0.093 ± 0.037	1.11	8.38
	Walking and hind limb	0.190 ± 0.093	4.94	3.84	0.110 ± 0.037	0.77	14.29	0.115 ± 0.060	1.01	11.41
Acceleration (m/s^2)	Trotting and forelimb	17.44 ± 8.97	197.59	8.83	12.74 ± 5.39	47.25	26.96	20.55 ± 8.68	101.95	20.16
	Trotting and hind limb	11.80 ± 3.53	100.14	11.79	8.04 ± 2.13	38.86	20.69	9.38 ± 3.16	74.83	12.54
	Walking and forelimb	7.11 ± 1.74	99.11	7.18	3.94 ± 2.08	18.68	21.09	4.49 ± 1.64	32.89	13.67
	Walking and hind limb	5.85 ± 2.32	78.44	7.46	4.03 ± 1.41	18.97	21.25	4.30 ± 1.93	26.65	16.14

Table 2.2--- Continued

		X direction			Y direction			Z direction		
Variable	**Speed and limb**	**RMSE mean ± SD**	**Range of mean**	**RMSE as % of range**	**RMSE mean ± SD**	**Range of mean**	**RMSE as % of range**	**RMSE mean ± SD**	**Range of mean**	**RMSE as % of range**
Angular orientation (°)	Trotting and forelimb	2.92 ± 1.28	108.98	2.68	3.79 ± 1.43	22.94	16.51	3.36 ± 1.21	19.54	17.22
	Trotting and hind limb	2.52 ± 1.25	96.72	2.60	3.44 ± 2.21	21.30	16.16	5.20 ± 2.48	21.19	24.55
	Walking and forelimb	3.42 ± 1.78	98.75	3.46	5.77 ± 3.08	13.90	41.49	4.01 ± 2.34	17.44	23.03
	Walking and hind limb	2.80 ± 1.90	88.75	3.16	5.03 ± 2.48	10.92	46.06	4.77 ± 2.23	15.05	31.74
Angular velocity (^{o}/s)	Trotting and forelimb	121.80 ± 43.40	2,531	4.81	121.20 ± 30.84	799.40	15.16	129.70 ± 51.22	609.63	21.28
	Trotting and hind limb	136.80 ± 62.89	2,046	6.68	97.18 ± 70.71	580.57	16.74	112.27 ± 51.03	512.38	21.91
	Walking and forelimb	83.31 ± 39.21	1,921	4.34	96.90 ± 49.15	410.87	23.58	85.23 ± 47.82	437.23	19.49
	Walking and hind limb	74.10 ± 47.81	1,560	4.75	97.24 ± 56.81	420.19	23.14	82.26 ± 40.87	365.53	22.51
Angular acceleration ($^{o}/s^{2}$)	Trotting and forelimb	13,297 ± 4,975	77,451	17.17	13,150 ± 4,039	54,020	24.34	11,383 ± 3,419	34,172	33.31
	Trotting and hind limb	15,403 ± 8,142	69,169	22.27	8,097 ± 5,824	27,964	28.95	7,606 ± 3,445	28,364	26.82
	Walking and forelimb	6,142 ± 2,602	64,652	9.50	5,479 ± 2,437	21,843	25.08	4,836 ± 2,699	21,383	22.62
	Walking and hind limb	5,295 ± 3,028	50,820	10.42	5,657 ± 3,735	25,017	22.61	4,052 ± 2,423	17,853	22.70

References

1. USDA. National economic cost of equine lameness, colic, and equine protozoal myeloencephalitis in the United States.Information sheet. Fort Collins, Colo: USDA APHIS Veterinary Services National Health Monitoring System, 2001.

2. Fuller CJ, Bladon BM, Driver AJ, et al. The intra- and inter-assessor reliability of measurement of functional outcome by lameness scoring in horses. Vet J 2006;171:281–286.

3. Hewetson M, Christley RM, Hunt ID, et al. Investigations of the reliability of observational gait analysis for the assessment of lameness in horses. Vet Rec 2006;158:852–857.

4. Keegan KG. Evidence-based lameness detection and quantification. Vet Clin North Am Equine Pract 2007;23:403–423.

5. American Association of Equine Practitioners. Guide for veterinary service and judging of equestrian events. 4th ed. Lexington, Ky: American Association of Equine Practitioners, 1991;19.

6. Keegan KG, Dent EV, Wilson DA, et al. Repeatability of subjective evaluation of lameness in horses. Equine Vet J 2010;42:92–97.

7. Ishihara A, Bertone AL, Rajala-Schultz. Association between subjective lameness grade and kinetic gait parameters in horses with experimentally induced forelimb lameness. Am J Vet Res 2005; 1805–1815.

8. Buchner HHF, Savelberg HHCM, Schamhardt HC, et al. Limb movement adaptations in horses with experimentally induced fore- or hindlimb lameness. Equine Vet J 1996;28:63–70.

9. Keegan KG, Wilson DA, Smith BK, et al. Changes in kinematic variables observed during pressure-induced forelimb lameness in adult horses trotting on a treadmill. Am J Vet Res 2000;61:612–619.

10. Weishaupt MA, Hogg HP, Wiestner T, et al. Instrumented treadmill for measuring vertical ground reaction forces in horses. Am J Vet Res 2002;63:520–527.

11. Robin D, Chateau H, Pacquet L, et al. Use of a 3D dynamometric horseshoe to assess the effects of an all-weather waxed track and a crushed sand track at high speed trot: preliminary study. Equine Vet J 2009;41:253–256.

12. Chateau H, Robin D, Simonelli T, et al. Design and validation of a dynamometric horseshoe for the measurement of three-dimensional ground reaction force on a moving horse. J Biomech 2009;42:336–340.

13. Keegan KG, Yonezawa Y, Pai PF, et al. Evaluation of a sensor-based system of motion analysis for detection and quantification of forelimb and hind limb lameness in horses. Am J Vet Res 2004;65:665–670.

14. Parsons KJ, Pfau T, Wilson AM. High-speed gallop locomotion in the thoroughbred racehorse. I. The effect of incline on stride parameters. J Exp Biol 2008;211:935–944.

15. Pfau T, Robilliard JJ, Weller R, et al. Assessment of mild hindlimb lameness during over ground locomotion using linear discriminant analysis of inertial sensor data. Equine Vet J 2007;39:407–413.

16. Witte TH, Hirst CV, Wilson AM. Effect of speed on stride parameters in racehorses at gallop in field conditions. J Exp Biol 2006;209:4389–4397.

17. Pfau T, Ferrari M, Parsons K, et al. A hidden Markov model-based stride segmentation technique applied to equine inertial sensor trunk movement data. J Biomech 2008;41:216–220.

18. Thomason JJ, Peterson ML. Biomechanical and mechanical investigations of the hoof-track interface in racing horses. Vet Clin North Am Equine Pract 2008;24:53–77.

19. Pfau T, Witte TH, Wilson AM. A method for deriving displacement data during cyclical movement using an inertial sensor. J Exp Biol 2005;208:2503–2514.

20. Lee JB, Mellifont RB, Burkett BJ. The use of a single inertial sensor to identify stride, step, and stance durations of running gait. J Sci Med Sport 2010;13:270–273.

21. Wong WY, Wong MS. Trunk posture monitoring with inertial sensors. Eur Spine J 2008;17:743–753.

22. Zhou H, Stone T, Hu H, et al. Use of multiple wearable inertial sensors in upper limb motion tracking. Med Eng Phys 2008;30:123–133.

23. Godwin A, Agnew M, Stevenson J. Accuracy of inertial motion sensors in static, quasistatic, and complex dynamic motion. J Biomech Eng 2009;131:114501-1 - 114501-5.

24. O'Donovan KJ, Kamnick R, O'Keeffe DT, et al. An inertial and magnetic sensor based technique for joint angle measurement. J Biomech 2007;40:2604–2611.

25. Pourcelot P, Audigie F, Degueurce C, et al. Kinematic symmetry index: a method for quantifying the horse locomotion symmetry using kinematic data. Vet Res 1997;28:525–538.

26. Setterbo JJ, Garcia TC, Campbell IP, et al. Hoof accelerations and ground reaction forces of Thoroughbred racehorses measured on dirt, synthetic, and turf track surfaces. Am J Vet Res 2009;70:1220–1229.

27. Clayton HM, Sha DH, Stick JA, et al. 3D kinematics of the interphalangeal joints in the forelimb of walking and trotting horses. Vet Comp Orthop Traumatol 2007;20:1–7.

Chapter Three

The effect of equine forelimb lameness on hoof kinematics at the trot[ii]

Introduction

Lameness accounts for up to $1 billion in losses to the equine industry every year[1] and has been one of the most important medical issues faced by horse owners.[2] Mild and subclinical lameness has been reported to have a detrimental effect in horses, resulting in reduced and suboptimal performance.[3, 4] While the detection of mild lameness is especially important in competition horses where suboptimal performance is unacceptable, it is also important for other populations as all would benefit from early detection of injury.

The subjective lameness examination is the most common diagnostic tool used for detection and monitoring lameness.[5] Even though the common scoring systems used for these evaluations have specific criteria, there is much variability within a grade, making longitudinal assessment of an animal challenging when only slight improvement is noted.[6] Several studies have demonstrated that subjective scoring systems are not reliable enough for clinical use, especially when the lameness is mild.[6-9] In addition, observer bias has been reported when assessing improvement in lameness after peri-neural anesthesia.[6] Thus, more accurate, objective tools are needed to supplement the subjective lameness examination for the detection and tracking of mild lameness, as well as to assess improvement from peri-neural anesthesia.

[ii] *Moorman VJ, Reiser RF, Peterson ML, McIlwraith CW, Kawcak CE. The effect of equine forelimb lameness on hoof kinematics at the trot. Am J Vet Res 2013: Accepted.*

Objective methods of lameness evaluation using kinetics and kinematics have been widely investigated to determine their efficacy in cases of mild lameness. Stationary force platform analysis is a sensitive kinetic tool for the detection of lameness, with peak vertical force and vertical impulse as parameters at the trot that are significantly altered in cases of mild lameness (< 1.5 out of 5).[10] Unfortunately, stationary force platform analyses are limited by availability, expense, time for collection/analysis, and necessary expertise for the use of the equipment. Alterations in distal limb kinematics, such as stride length, step length, hoof height, and sagittal plane joint angles have been investigated using optical methods following induction of lameness.[11-13] While alterations to these parameters have been documented at both the walk and the trot, the trot appears to be the more useful gait to detect kinematic changes.[11] As optical kinematics suffer from many of the limitations of stationary force platform analyses, other kinematic horse-based motion analysis systems are currently being investigated to objectively characterize lameness, both in research and clinical practice. These horse-based systems utilize multiple micro electromechanical components, such as accelerometers, gyroscopes (combined to produce an IMU), and GPS tracking devices and have wireless and/or telemetric components for data transmission.[14-16] One inertial sensor system has been shown to be very sensitive for detection of mild single forelimb or hind-limb lameness at the trot by examining movement of the head or pelvis,[5] but its use has not been reported at the walk and its use for longitudinal assessment of lameness has not been determined.[17] As sensors are becoming increasingly small and lightweight, they should be able to be placed on the distal limb of the horse without inducing large alterations in motion. In addition, the hoof is a suitable place for mounting a small sensor, since a sensor can be rigidly attached to the hoof, removing motion artifacts. As kinematics of the limb are known to change with a single limb lameness, measuring hoof kinematics may be another method to diagnose and monitor lameness. While hoof displacement or position has been investigated, there are no reports describing other linear and angular changes to the lame and contra-lateral non-lame hoof after induction of lameness, which may be ideally suited for measurement with an IMU. As it is likely that these other kinematic changes occur in both the lame and non-lame hooves, both intra- and inter-limb comparisons may also prove useful in identification of mild lameness.

As optical methods are the current gold-standard for determination of kinematics, our objective was to identify changes in kinematic variables when a weight-bearing lameness was induced in a single forelimb at the trot, as well as when the lameness was blocked with peri-neural anesthesia. These variables could then be further investigated using a hoof-mounted kinematics system, which could be used on horses in a clinical setting. We hypothesized that after induction of lameness, there would be significant differences in sagittal plane kinematics from the fore hooves both intra- and inter-limb at the trot, and that these differences could be detected in the mildest grade of lameness. We also hypothesized that following peri-neural anesthesia of the medial and lateral palmar nerves, these kinematic changes would not be significantly different from baseline.

Materials and Methods

Horses - Six normal quarter horses, with no perceptible lameness at the walk or trot (grade 0 out of 5, using a modified AAEP Lameness Scale[18]) were used for the study. These six horses were used for a companion study, for which, the data were collected during the same session.[19] The horses were age 2-9 years, with mass 364 +/-19kg (mean +/- standard deviation) and wither height 1.46 +/-0.03m. All horses had their feet trimmed and balanced, were shod with a normal steel keg shoe (mass 324.8 +/- 23.5g) on the left front hoof, and a similar shoe on the right front hoof with a nut welded to the inner web of the medial and lateral branches of the shoe between the third and fourth nail hole (mass 333.7 +/- 25.6g) (Figure 3.1A). The nuts on the right hoof were welded to the shoe so that they were flush with the solar aspect of the shoe and did not contact the horse's sole during weight-bearing (Figure 3.1B). This shoe design was similar to that described by Merkens et al.[20] The median weight of the two screws added to the right shoe (lame limb) was 7.8 g (6.8g to 10.6g, depending on length). Prior to initiation of the study, all horses were acclimated to the Gait Analysis Laboratory where data were collected. All procedures were approved by the Institutional Animal Care and Use Committee.

Lameness Induction - Each horse had lameness induced in the right front hoof. A 6mm diameter threaded screw, either blunt or with a 2mm diameter tapered distal end (Figure 3.1A), was inserted into the medial and lateral nuts in the shoe on the right front hoof. Screws ranged from 11 mm to 17 mm in length. Blunted screws were used to induce all lameness grades in the first two horses, and to induce the mildest lameness (grade 1 out of 5) in the remaining four horses. The tapered screws were used to induce more severe lameness (grades 2 and 3 out of 5) in the last four horses. The screw was fully inserted into the nut, and the head of the screw was in contact with the ground when the horse was weight-bearing. If the screw did not cause the desired degree of lameness, it was exchanged for a longer or shorter screw, as needed. The screw length which induced each grade of lameness was recorded for each horse.

Lameness Trials - Following the collection of baseline data (no induced lameness), each horse had lameness grades 1-3 out of 5 using a five-point scale modified from the AAEP Lameness Scale,[18] starting with the mildest and proceeding to the most severe. Briefly, grade 1 was described as intermittently lame at the trot, grade 2 was mildly but consistently lame at the trot, and grade 3 was moderately and consistently lame at the trot. None of the lameness grades examined resulted in visible lameness at the walk. Horses were allowed to rest for several minutes between lameness conditions to limit the effect of fatigue. After induction of the grade 3 lameness, 3 mL of 2% mepivacaine was injected subcutaneously around the medial and lateral palmar nerves. After 10 minutes, if the horse did not show sufficient visual improvement in lameness (> 80%) or skin desensitization, a second 1.5 mL of 2% mepivacaine was injected subcutaneously around the medial and lateral palmar nerves. The horse was then re-assessed after another 5 minutes.

Retro-reflective Markers - An aluminum base plate (8.8 cm long x 1.9 cm high x 0.3 cm wide, mass 14.2 g) was adhered to each front hoof with hoof acrylic.[a] An additional piece of aluminum (7-9 cm long x 1.5 cm high x 0.1 cm wide, mass 3.4 g) was attached with screws to the base plate and conformed to the dorsal aspect of the hoof to provide additional support and additional surface area for the adhesive. A marker triad composed of three 2.0 cm diameter, spherical, retro-reflective markers was attached to the base plate with two 4 mm screws, creating a triad that moved rigidly with the hoof (Figure 3.2). The marker triad measured 15cm tall by 13cm wide by 0.1cm thick with a mass of 37.6 g and was composed of an aluminum frame stiffened with a uni-axial carbon sandwich structure with a balsa core (4.6 cm x 2.8 cm x 0.6

cm). The stiffeners were placed behind each of the three retro-reflective markers, for added stability with the markers rigidly by machine screws. The markers were 10-11 cm apart.

An IMU[b] (5.1 cm x 3.8 cm x 1.6 cm, 58.6 g) was attached to the marker triad of the right front hoof, and a custom, machined piece of metal (3.6 cm x 3.1 cm x 1.2 cm, 75.7 g), was attached to the triad on the left front hoof. The total mass of the right marker triad with IMU was 113.8 g and the mass of the left marker triad was 130.9 g. The difference between the two triads was made up by the mass of the IMU cable. The cable from the IMU was loosely attached to the horse's limb with a wrap of elastic bandage[c] around the distal metacarpus and distal antebrachium and was attached to a handheld computer, mounted on a surcingle around the horse. Strain gauges were glued on the hooves of both forelimbs, which had cables integrated into the elastic bandages and terminated at a data collection source also mounted on the surcingle (9.5 kg). The data collected from the IMU and the strain gauges were a subset of this study and will be presented elsewhere.

Trial set-up and synchronization - Data were collected in the Gait Analysis Laboratory; all horses were first walked and then trotted over a rubberized runway (9.3 mm thickness), covering an asphalt surface, measuring 1.2 m wide by 24.8 m long with an optical capture volume of 3.7 m in length, 1.3 m wide, and 2.4 m high. Only the trot data will be presented here; the walk data is contained within a companion manuscript.[19] The capture volume was located near the middle of the length of the runway, allowing the horse to achieve a constant velocity while within the capture volume. Each horse was trotted at a consistent and comfortable speed for that individual. Each horse dictated its own optimal velocity, and the velocity of each trial was measured by the use of five infrared timing gates[d] spaced 1.5 m apart, linked to the optical kinematics computer and triggered by the horse as it traveled through the capture volume.

At least four acceptable trials were collected from each horse at the trot for the right and left forelimbs. An acceptable trial was defined as one where the horse traveled straight and at a consistent velocity through the capture volume. Not all trials contained a full stance and swing for both forelimbs, so up to eight acceptable trials were collected to ensure that there were four trials per limb. In addition, during the baseline trot trials, an average velocity was calculated for each horse at each gait. Throughout the remainder of the trials, only trials where the horse was traveling within 10% of its average initial velocity were included for analysis.

Camera Set-up - Eight infrared cameras[e] operating at 200 Hz were used to collect the 3-D optical kinematic data. Four cameras were placed on either side of the horse and were suspended from overhead beams. Calibration of the optical kinematic system[f] for the over-ground trials yielded coordinate resolution to within 1.2mm.

Kinematic Data - Optical coordinate data were low-pass filtered at 15 Hz with a recursive 4th-order Butterworth filter. A virtual marker was created between the cranial and caudal markers of the hoof triad, and this was used as a local origin to track the motion of the hoof.

The linear movement of the hoof was tracked in the sagittal plane: cranial-caudal (X) and proximal-distal (Z). Hoof events were determined by evaluation of the X and Z acceleration profile of the stride (Appendix II). Briefly, hoof contact was the last peak in the Z acceleration curve before a period of smaller accelerations. Heel-off was defined as the first peak in the Z acceleration after the period of minimal accelerations. Toe-off was defined as the second peak in Z acceleration, which also corresponded to an inflection point in the X acceleration curve. The above mentioned events were used to divide the stride into total stance (hoof contact to toe-off), break-over (heel-off to toe-off), total swing (toe-off to hoof contact), initial swing (toe-off to initial 25% of swing), and terminal swing (75% of swing to hoof contact).

The origin of the coordinate system was set at toe-off, so translations of the hoof at all other events were relative to the virtual marker location at toe-off. To ensure the coordinate system was aligned with horse travel, the x-axis was aligned with the virtual marker at the second hoof contact. X and Z axes were then positive cranially and proximally, respectively. Heel-down hoof orientation within the sagittal plane about the medial-lateral Y axis was positive, while toe-down orientation was negative. As the marker triad was not perfectly parallel to the ground, the orientation of the hoof during the middle of stance (when the cannon bone was perpendicular to the ground – as determined by visual assessment of the optical data), was used to adjust the sagittal orientation of the hoof such that 0° of the hoof was level to the ground.

Temporal parameters, as well as maxima, minima, and averages were determined for each variable during break-over, total swing, initial 25% of swing, and terminal 25% of swing. Instantaneous positions, velocities, accelerations, and sagittal plane orientation were determined at hoof contact, heel-off, and toe-off. Total range of motion of the hoof during break-over, total swing, initial 25%, and terminal 25% of swing was also determined.

Statistical Analysis - A commercial program[g] was utilized for statistical analysis. Data were examined for normality, and if normality was not met, they were log transformed. A repeated measures mixed model ANOVA was performed with each parameter of interest as the outcome variable. Comparisons were made within each limb (lame and non-lame) and between limbs at each treatment. Within limb comparisons used the baseline trot as the control compared to each treatment (lameness grades 1-3 and after peri-neural anesthesia). Between limb comparisons were made for each treatment condition (baseline, lameness grades 1-3, and after per-neural anesthesia). Any variables that were significantly different between limbs at baseline were not further compared after lameness induction or after blocking. Lameness grade and limb (lame versus sound) were fixed effects with horse velocity included as a confounding variable, and horse was included as a random effect. Significance was set at $P < 0.05$.

Results

Lameness was successfully induced in all horses. Blunt screws were used to induce lameness in the first two horses. In one of these horses, only lameness grades 1 and 2 could be induced because of a decreased sensitivity of the horse to the longest screws available at that time. In addition, the longest blunt screws used with the initial two horses tended to push the shoe away from the hoof, instead of threading into the sole. For the subsequent four horses, longer screws with tapered ends were used, which more readily induced the desired lameness. Thus, data for baseline, grade 1, and grade 2 lameness were collected from all six horses, and for grade 3 and after blocking, data were only collected from five horses. Within 24 hours after lameness induction, there was no perceptible lameness in any horse at the trot.

Lame limb - Significant intra-limb changes to hoof kinematics were observed in the lame limb at all grades of lameness and following peri-neural anesthesia (after block) as compared to baseline trot. These intra-limb changes were present during both stance (hoof contact and break-over) (Table 3.1) and swing (terminal 25% of swing and total swing) (Table 3.2). Significant intra-limb kinematic changes were apparent at the most mild lameness (grade 1) during stance (Table 3.1).

Non-lame Limb - Significant intra-limb changes to hoof kinematics were observed in the non-lame limb at all grades of lameness and following peri-neural anesthesia (after block) as compared to baseline trot. These intra-limb changes were present during both stance (hoof contact and break-over) (Table 3.1) and swing (initial 25% of swing, terminal 25% of swing, and total swing) (Table 3.2). Significant intra-limb kinematic changes were apparent at the most mild lameness (grade 1) during both stance and swing (Tables 3.1 and 3.2).

Between limbs - Thirty-four out of ninety-four (36.2%) kinematic variables were significantly different inter-limb at baseline trot. During hoof contact and all subsets of stride, there were 14 out of 36 (38.9%) cranial-caudal (X) variables, 17 out of 35 (48.6%) vertical (Z) variables, 2 out of 17 (11.8%) sagittal plane orientation variables, and 1 out of 6 (16.7%) temporal variables.

Significant inter-limb changes to hoof kinematics were observed at all grades of lameness and following peri-neural anesthesia (after block) as compared to baseline trot. These inter-limb changes were present during both stance (hoof contact and break-over) (Table 3.1) and swing (initial 25% of swing, terminal 25% of swing, and total swing) (Table 3.2). Significant inter-limb kinematic changes were absent at baseline but apparent at the most mild lameness (grade 1) in variables during both stance and swing (Tables 3.1 and 3.2).

The full trot kinematic data set is contained within Appendix IV.

Discussion

Our first hypothesis of this study was well supported by the data; multiple kinematic variables were significantly altered after lameness was induced in a single forelimb. We were able to identify both stance phase and swing phase variables that were significantly altered at the most mild grade of lameness. Multiple comparisons were not made to determine if a variable was altered depending on the lameness grade, as the initial hypothesis was not to distinguish between the different grades of lameness. However, as was expected, there were an increased number of altered kinematic variables as lameness increased in severity.

There were significant changes to several variables during the stance phase of the trot, which were present at the mildest lameness (grade 1). At the beginning of stance, the lame limb had a significantly greater caudal acceleration at hoof contact compared to both itself at baseline trot and to the non-lame limb at all three lameness conditions and appeared to be returning towards normal after peri-neural anesthesia (Table 3.1). This change in cranial-caudal acceleration may indicate that the horse is slowing the lame limb more than the contra-lateral limb before maximum weight-bearing, which occurs towards the middle of stance. In sound horses, the time to peak vertical ground reaction force in the forelimb at the trot has been reported to be at approximately 44% of stance over-ground[21] and 47% of stance on a treadmill.[22]With induction of subtle lameness, the time to peak vertical force in the lame limb was not significantly different compared to the sound limb.[23]

In the contra-lateral limb, there was a statistically significant change in hoof orientation at hoof contact, with the non-lame limb having a more positive orientation angle compared to both itself at baseline and to the lame limb at the same lameness grade (Table 3.1). This effect occurred at both mild and increasing lameness grades, and indicates that the non-lame hoof is landing slightly heel-first. During break-over, the lame limb appeared to be more rapidly unloaded. This is supported by a decrease in break-over duration, an increase in maximum and average cranial (X) acceleration, a smaller minimum orientation angle, and a smaller range of motion in the lame limb (Table 3.1). The smaller minimum orientation represents the hoof at toe-off, adding further support to the finding of a smaller range of motion of the lame hoof during break-over. A significant inter-limb difference in maximum cranial acceleration, minimum orientation, and range of motion were demonstrated in the mildest lameness (grade 1), indicating that these may be sensitive variables for mild lameness.

Stance duration has been a kinematic variable that has been proposed to increase with lameness in both lame and non-lame limbs. [23, 24] Galisteo et al also found that the stance phase increased in the lame diagonal compared to the non-lame diagonal pair.[12]We did not find a significant increase in stance duration to either limb, which is supported by Ishihara et al.[10]

It has been previously suggested that swing phase kinematics are minimally affected with a weight-bearing lameness.[24] However, we identified several kinematic variables that were altered during the swing phase. Overall, the duration of swing was significantly longer in the lame limb versus the non-lame limb during mild lameness (grades 1 and 2), and was approaching significance at grade 3 lameness (P = 0.083) (Table 3.2). This result differs from several previous reports, where the swing (suspension) duration was found to decrease in lameness.[12, 24] However, this effect was only seen after a more severe lameness was induced (lameness was slightly visible at the walk). Even the most severe lameness induced in the current study did not demonstrate visible lameness at the walk.

Several swing phase variables were found to be significantly altered at the mildest lameness grade. During the initial 25% of swing, the range of motion of the lame limb was significantly greater than the non-lame limb. As the lame limb went through a smaller range of motion during break-over, it is possible that this extra rotation was a compensatory change. During the terminal 25% of swing, non-lame limb had a greater maximum cranial (X) and vertical (Z) velocity and a smaller minimum cranial acceleration. The alterations to the cranial variables indicate that the non-lame limb began the terminal swing phase more quickly and thus required more caudal acceleration to slow the hoof for impact. As the total swing phase was longer for the lame limb, it would be expected that the lame limb might move slower through swing and thus have smaller accelerations, which is supported by these data. The maximal vertical velocity likely occurs as the hoof is undergoing a final rotation to prepare for landing. As the non-lame hoof appeared to have more of a flat to heel-first landing, the vertical velocity of the hoof is likely attributing to this rotation. As the lame hoof had a more toe-down orientation, it would require less proximal velocity to rotate the hoof into a final position for landing.

The lame hoof appeared to have a higher maximum vertical position during swing compared to the non-lame hoof, which was appreciated as a significant difference during the terminal 25% of swing at lameness grade 2, and during entire swing at lameness grade 3. Although not statistically significant, there also seemed to be a trend for the maximum vertical position of the lame limb to be more proximal during total swing compared to the non-lame limb during more mild lameness (grades 1 and 2). These findings are different from what has been previously reported, where the non-lame limb had a significantly greater vertical position than the lame limb[11]. As we were determining the position of the hoof by multiple markers, most likely it is the rotation of the hoof that makes it appear to be located more proximally; since the hoof is in a more toe-down orientation, the hoof would appear to have a more proximal position.

Some of the data supported the second hypothesis: that the kinematic changes induced in both the lame and non-lame limbs would return to baseline after performing peri-neural anesthesia. Following peri-neural anesthesia, there was not a significant intra- or inter-limb difference in orientation at hoof contact. This was also true for maximum cranial velocity during the terminal 25% of swing. However, there were multiple variables that did not return to baseline after peri-neural anesthesia, such as cranial acceleration at hoof contact, range of motion of the hoof during break-over, and hoof orientation during the initial 25% of swing. As peri-neural anesthesia alters the neural pathways in the limb, it would be expected that the lame limb, as well as the contra-lateral limb, might not show completely normal kinematics following this procedure. Thus, the data were not able to completely support our second hypothesis, as not all kinematic variables returned to baseline.

There were a number of inter-limb kinematic variables that were statistically different at baseline trot. Due to the inherent asymmetry of these variables, inter-limb significance was not compared when lameness was induced or after peri-neural anesthesia. This inter-limb asymmetry could stem from lameness that we could not visually detect. Ishihara et al and McCracken et al found that the stationary force platform and an inertial sensor system, respectively, could detect lameness before it could be seen by the human eye.[5, 10]It is possible that the optical kinematics system used in this study also had that potential. Looking at a larger number of horses would be necessary to verify this. Another possibility is the laterality or handedness of the horses. It has been previously recognized that many horses show a preference towards one limb during either motion or grazing, and this laterality begins at a young age.[25,26] Wilson et al also found that limb segment asymmetries exist in horses, which are likely related to inter-limb hoof conformation differences.[27] These intra-horse conformational asymmetries could contribute to differences in distal limb kinematics. The measurement of hoof and limb segments was outside the scope of this study. Since there were a number of variables from this study that were symmetrical at baseline, we chose to use those variables for inter-limb comparisons during lameness. The inter-limb asymmetry that we identified in this study also supports the use a combination of intra- and inter-limb kinematic comparisons for lameness determination.

The lameness model used in this study induced a consistent lameness that was rapidly reversible. While sole pressure induced lameness is not the cause of the majority of clinical lameness cases, the kinematic changes that occur with this model are thought to be similar to lameness from other sources.[11] This method of lameness induction has been a well-accepted model for weight-bearing lameness and for the analysis of both kinetic and kinematic methods of lameness detection.[5, 12-14, 20] We modified the model in order to consistently induce all three grades of lameness by tapering the distal ends of the screw. Data from the first two horses were collected using blunt ended screws. While lameness was effectively induced in one of the horses, only lameness grades 1 and 2 could be induced in the other horse. As the objective of the project was to determine kinematic parameters of the hoof that were useful for diagnosis of mild lameness, it was more important to have data on all six horses at the lower grades of lameness, so we do not think this is a major deficiency in this investigation.

As it has been previously documented that the horizontal velocity of the horse affects distal limb kinematics,[28] we ensured that each horse had a consistent velocity during data collection. At baseline, each horse was allowed to trot at a velocity comfortable for that individual and then a range of acceptable velocities were calculated for the remainder of the trials. This mimics clinical lameness examinations, as horses are routinely examined in hand at a speed dictated by the individual. Peham et al previously reported that at an optimum speed, a horse has a smaller variation in motion, thus producing more meaningful results of kinematic analysis.[29] When examining vertical head excursion, Peham et al also found that in mild lameness, there is no increase in asymmetry of head motion when speed is increased.[30] Thus, lameness can be adequately detected with the horse moving at a comfortable speed instead of using one predetermined speed for all horses.

Previous kinematic studies have examined the equine stride by dividing it into stance and swing phases.[12, 13] However, these studies did not examine the stride in smaller subsections. We were able to further divide the stride into smaller components by identifying specific hoof events using the X and Z acceleration curves. This technique has not been previously described. We expected that there could be subtle kinematic changes that would occur during sub-sections of the stride that would be overlooked if swing or stance was evaluated as a whole. Significant changes to several kinematic variables were identified during these sub-sections, such as an increase in the maximum vertical velocity of the non-lame hoof during the terminal 25% of swing and orientation changes during hoof contact, break-over, and the initial 25% of swing.

Linear and angular kinematic data were also evaluated for the hoof events of hoof contact, heel-off, and toe-off, as well as for sub-sections of the stride (break-over, total swing, initial swing, and terminal swing). The kinematic variables determined at heel-off and toe-off were reflected in break-over and initial swing; however, the kinematics at hoof contact were not as well represented during terminal swing. This was especially true for sagittal plane orientation, as the maximum sagittal plane orientation during terminal swing often occurs right before hoof contact, as the hoof undergoes a final counter-clockwise rotation. Thus, the instantaneous hoof contact kinematic data were included in addition to the kinematic data from the sub-sections of stride.

From this study, we identified several sagittal plane kinematic variables that may be useful for lameness diagnosis in a single forelimb with a mild (grade 1) weight-bearing lameness at the trot. These included both intra- and inter-limb kinematic changes after introduction of lameness. As we were able to detect these significant changes during mild lameness at the trot, it would also be beneficial to determine if similar kinematic changes can be detected at the walk for the same grades of lameness. Optimally, kinematics should be collected from both forelimbs, as we were able to detect significant inter-limb asymmetries following lameness, which were not always significantly different intra-limb. In addition, we found that some hoof kinematics returned to baseline following peri-neural anesthesia, and thus could be utilized to objectively assess the effect of blocking at the trot. As this study was performed using a small number of horses, further work needs to be performed on a larger number of horses with clinical lameness to validate that these parameters can be clinically useful. Future investigation will be performed using a hoof-mounted system, an IMU, to examine its sensitivity to detect mild lameness. Such a system would allow an alternate approach to diagnosing and monitoring lameness in a clinical setting. In addition, a hoof mounted system may be more sensitive to detecting changes outside of the sagittal plane, which may also be altered with lameness.

[a] Equi-Thane SuperFast, Vettec; Oxnard, CA
[b] H3-IMU, MemSense; Rapid City, SD
[c] Vetrap, 3M; St. Paul, MN
[d] MEK 92-PAD photoelectric control, Mekontrol Inc, Northboro, MA
[e] Volant by Peak, Performance Technologies Inc, Centennial, CO
[f] Vicon-Motus 9.2, Vicon Motion Systems Inc, Centennial, CO
[g] STATA 11, StataCorp LP; College Station, TX

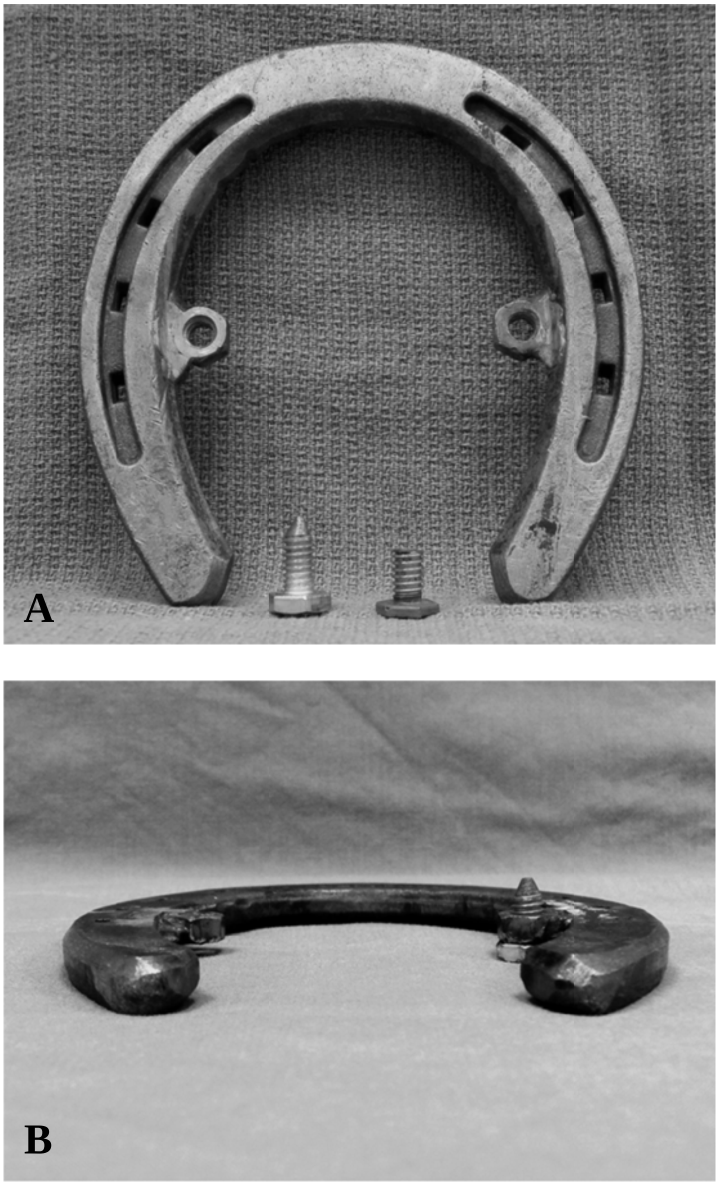

Figure 3.1 – Photographs of a modified steel keg shoe for induction of lameness. (A) A nut was welded to the inner edge of the medial and lateral web of the shoe between the third and fourth nail holes for insertion of two 6 mm diameter screws either with a blunt or tapered end. (B) The nut was set flush to the solar side of the shoe and the head of the screw was flush with the ground.

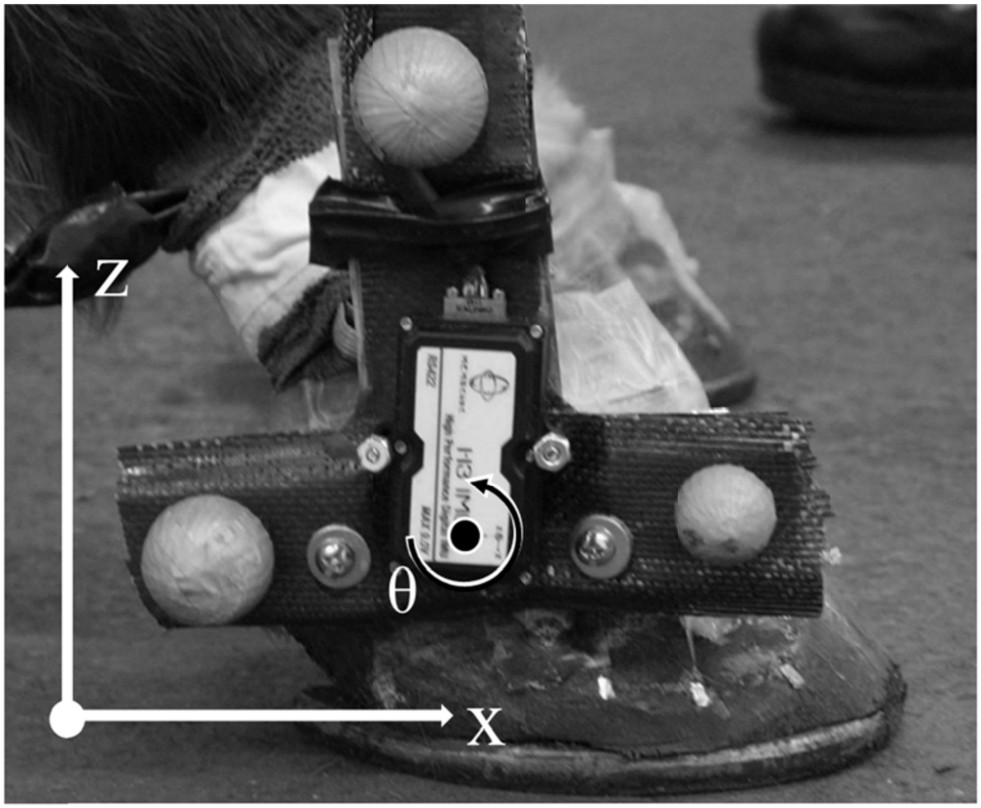

Figure 3.2 – Photograph of the retro-reflective marker triad that was attached to the horse's right fore hoof. The triad was placed laterally on the hoof and the most proximal aspect did not touch the metacarpophalangeal joint. An IMU is attached to the triad in the center of the marker triad. Superimposed are the global origin, virtual hoof marker, and rotation reference of the hoof. The cranial-caudal (x) axis positive cranially, the vertical (z) axis positive proximally, and the sagittal plane rotation (θ) is positive with a counter-clockwise rotation, i.e., heel-down is positive.

Table 3.1 - Intra- and inter-limb means and standard deviations of specific kinematic parameters during stance at the trot
* indicates a significant inter-limb difference at a specific lameness grade at the trot (P < 0.05). † indicates a significant intra-limb difference between a specific lameness grade and baseline (P < 0.05).

			Baseline		Grade 1		Grade 2		Grade 3		After Block	
Hoof Contact:			mean	st dev	mean	st dev	mean	st dev	mean	st dev	mean	st dev
X acceleration (m/s^2)		L	-40.35	10.07	-45.11*†	15.10	-45.81*†	12.10	-46.68*†	9.76	-42.93*†	10.97
		NL	-38.21	10.22	-41.07*	13.91	-41.83*†	12.23	-38.57*	13.39	-38.87*†	11.86
Orientation (^{o})		L	-1.4	2.4	-1.3*	2.6	-1.2*	2.8	-0.4*	2.4	-0.5	2.6
		NL	-0.8	3.0	0.2*†	2.2	0.1*†	2.6	0.2*†	2.7	-0.9	2.3
Break-over:												
Duration (s)		L	0.055	0.011	0.054	0.009	0.053†	0.009	0.053	0.009	0.052†	0.006
		NL	0.054	0.009	0.054	0.009	0.054	0.009	0.052	0.008	0.054	0.009
X acceleration (m/s^2)	Max	L	45.78	12.71	48.73*†	12.91	49.11*†	16.06	51.77*	13.99	48.78*	11.33
		NL	44.48	14.26	47.84*	15.09	44.80*	13.59	42.91*	11.63	44.40*	13.45
	Avg	L	27.68*	6.51	28.82*	6.02	28.41*†	7.47	28.60*†	6.19	27.55*	4.42
		NL	24.84*	6.65	26.20*	6.55	25.26*†	6.55	25.14*†	5.38	23.47*†	4.44
Orientation (^{o})	Min	L	-45.7	6.0	-44.8*	5.2	-44.0*	3.7	-43.3*	3.8	-43.6*	5.5
		NL	-47.0	7.6	-48.6*†	6.9	-47.9*	5.8	-47.1*	5.0	-49.3*	5.4
Range of motion (^{o})		L	42.1	5.5	41.4*	5.1	40.1*†	3.5	39.8*†	3.8	39.6*†	5.4
		NL	43.1	7.4	44.7*†	6.8	44.0*	5.8	43.0*	4.9	44.8*	5.1

Table 3.2 - Intra- and inter-limb means and standard deviations of specific kinematic parameters during swing at the trot. *See Table 3.1 for remainder of the key*

			Baseline		Grade 1		Grade 2		Grade 3		After Block	
Initial Swing:			mean	st dev	mean	st dev	mean	st dev	mean	st dev	mean	st dev
Orientation (°)	Max	L	-45.0	6.4	-44.8*	5.3	-44.2*	3.8	-44.3*	5.9	-43.8*	4.5
		NL	-47.2	7.3	-49.2*	6.9	-46.8*	5.8	-47.2*	4.8	-48.6*	5.4
	Min	L	-108.6	5.7	-110.0*	4.5	-110.0	5.1	-109.9*	5.2	-110.0*	4.1
		NL	-109.4	4.9	-111.2*†	4.8	-110.6†	5.9	-111.4*	3.8	-112.1*†	5.2
	Avg	L	-92.6	5.2	-93.4*	3.5	-93.1*	3.9	-93.3*	4.7	-93.1*	3.5
		NL	-93.8	4.9	-95.7*†	4.3	-94.5*	4.6	-95.2*	3.4	-95.8*	3.9
Range of motion (°)		L	63.6	8.4	65.2*	8.0	65.7*	7.3	65.6	7.5	66.1*	6.2
		NL	62.3	7.8	62.0*	8.4	63.8*	8.4	64.3	5.8	63.5*	7.5
Terminal Swing:												
X velocity (m/s)	Max	L	6.44	0.45	6.57*	0.54	6.55*	0.31	6.51*	0.30	6.41	0.38
		NL	6.54	0.46	6.80*†	0.63	6.78*†	0.35	6.63*†	0.28	6.55	0.57
X acceleration (m/s^2)	Min	L	-112.15	19.94	-111.77*	18.60	-111.20*	18.75	-108.43*†	21.06	-107.88*†	18.83
		NL	-115.65	21.33	-117.05*	21.28	-117.81*	18.52	-115.52*	17.56	-120.98*	21.79
Z position (m)	Max	L	0.05	0.01	0.05	0.01	0.05*	0.01	0.05	0.01	0.05*	0.01
		NL	0.05	0.01	0.05	0.01	0.04*†	0.01	0.05	0.01	0.04*†	0.01
Z velocity (m/s)	Max	L	0.36	0.42	0.35*	0.33	0.39	0.38	0.32*	0.33	0.48*	0.35
		NL	0.41	0.34	0.45*	0.35	0.48	0.34	0.46*	0.34	0.54*	0.27
Total Swing:												
Duration (s)		L	0.38	0.02	0.38*	0.01	0.39*	0.02	0.39	0.02	0.39	0.02
		NL	0.38	0.02	0.38*	0.02	0.38*	0.02	0.37	0.02	0.39	0.02
X position (m)	Avg	L	0.97	0.08	0.98	0.07	1.00*	0.10	0.99	0.10	0.97	0.07
		NL	0.97	0.10	1.00	0.09	0.97*	0.08	0.96	0.08	0.96	0.07
Z position (m)	Max	L	0.11	0.02	0.11	0.02	0.11	0.02	0.11*	0.02	0.11*	0.02
		NL	0.11	0.02	0.10	0.01	0.10	0.02	0.10*	0.02	0.09*	0.02
Z acceleration (m/s^2)	Min	L	-64.87	20.02	-64.34	22.43	-62.27*	19.10	-59.88*	17.75	-72.14	28.07
		NL	-68.44	19.21	-68.60	27.22	-76.09*	26.39	-70.49*	16.10	-64.82	15.50

References

1. USDA. National animal health monitoring system equine study. Part I: baseline reference of 1998 equine health and management. Fort Collins, CO: USDA, APHIS, Veterinary Services. 1998.

2. Kaneene JB, Ross WA, Miller RA. The Michigan equine monitoring system. II. Frequencies and impact of selected health problems. Prev Vet Med 1997;29:277-292.

3. Gaughan EM. Skeletal origins of exercise intolerance in horses. Vet Clin North Am Equine Pract 1996;12:517-535.

4. Parente EJ, Russau AL, Birks EK. Effects of mild forelimb lameness on exercise performance. Equine Vet J Suppl 34 2002;34:252-256.

5. McCracken MJ, Krammer J, Keegan KG, et al. Comparison of an inertial sensor system of lameness quantification with subjective lameness evaluation. Equine Vet J 2012;44:652-656.

6. Arkell M, Archer RM, Guitian FJ, et al. Evidence of bias affecting the interpretation of the results of local anesthetic nerve blocks when assessing lameness in horses. Vet Rec 2006;159:346-349.

7. Fuller CJ, Bladon BM, Driver AJ, et al. The intra- and inter-assessor reliability of measurement of functional outcome by lameness scoring in horses. The Vet J 2006;171:281-286.

8. Hewetson M, Christley RM, Hunt ID, et al. Investigations of the reliability of observational gait analysis for the assessment of lameness in horses. Vet Rec 2006;158:852-858.

9. Keegan KG, Dent EV, Wilson DA, et al. Repeatability of subjective evaluation of lameness in horses. Equine Vet J 2010;42:92-97.

10. Ishihara A, Bertone AL, Rajala-Schultz PJ. Association between subjective lameness grade and kinetic gait parameters in horses with experimentally induced forelimb lameness. Am J Vet Res 2005;66:1805-1815.

11. Buchner HHF, Savelberg HHCM, Schamhardt HC, et al. Limb movement adaptations in horses with experimentally induced fore- or hindlimb lameness. Equine Vet J 1996;28:63-70.

12. Galisteo AM, Cano MR, Morales JL, et al. Kinematics in horses at the trot before and after an induced forelimb supporting lameness. Equine Vet J Suppl 23 1997;29:97-101.

13. Keegan KG, Wilson DA, Smith BK, et al. Changes in kinematic variables observed during pressure-induced forelimb lameness in adult horses trotting on a treadmill. Am J Vet Res 2000;61:612-619.

14. Keegan KG, Yonezawa Y, Pai PF, et al. Evaluation of a sensor-based system of motion analysis for detection and quantification of forelimb and hind limb lameness in horses. Am J Vet Res 2004;65:665-670.

15. Pfau T, Robilliard JJ, Weller R, et al. Assessment of mild hindlimb lameness during over ground locomotion using linear discriminant analysis of inertial sensor data. Equine Vet J 2007;39:407-413.

16. Moorman VJ, Reiser RF, McIlwraith CW, et al. Validation of an equine inertial measurement unit system in clinically normal horses during walking and trotting. Am J Vet Res 2012;73:1160-1170.

17. Keegan KG, Kramer J, Yonezawa Y, et al. Assessment of repeatability of a wireless, inertial sensor-based lameness evaluation system for horses. Am J Vet Res 2011;72:1156-1163.

18. American Association of Equine Practitioners. Guide for veterinary service and judging of equestrian events. 4th ed. Lexington, KY: American Association of Equine Practitioners, 1991;19.

19. Moorman VJ, Reiser RF, Peterson ML, et al. The effect of equine forelimb lameness on hoof kinematics at the walk. Am J Vet Res 2013; **In Press**.

20. Merkens HW, Schamhardt HC. Evaluation of equine locomotion during different degrees of experimentally induced lameness I: Lameness model and quantification of ground reaction patterns of the limbs. Equine Vet J Suppl 6 1988;20:99-106.

21. Merkens HW, Schamhardt HC, Van Osch GJ, et al. Ground reaction force patterns of Dutch Warmblood horses at normal trot. Equine Vet J 1993;25:134-137.

22. Weishaupt MA, Wiestner T, Hogg HP, et al. Vertical ground reaction force-time histories of sound Warmblood horses trotting on a treadmill. The Vet J 2004;168:304-311.

23. Weishaupt MA, Wiestner T, Hogg HP, et al. Compensatory load redistribution of horses with induced weight-bearing forelimb lameness trotting on a treadmill. The Vet J 2006;171:135-146.

24. Buchner HHF, Savelberg HHCM, Schamhardt HC, et al. Temporal stride parameters in horses with experimentally induced fore- or hindlimb lameness. Equine Vet J Suppl 18 1995;27:161-165.

25. Murphy J, Sutherland A, Arkins S Idiosyncratic motor laterality in the horse. Appl Anim Behave Sci 2005;91:297-310.

26. Van Heel MCV, Kroekenstoel AM, Van Dierendonck MC, et al. Uneven feet in a foal may develop as a consequence of lateral grazing behavior induced by conformational traits. Equine Vet J 2006;38:646-651.

27. Wilson GH, McDonald K, O'Connell MJ. Skeletal forelimb measurements and hoof spread in relation to asymmetry in the bilateral forelimb of horses. Equine Vet J 2009;41:238-241.

28. Clayton HM. Comparison of the stride kinematics of the collected, working, medium and extended trot in horses. Equine Vet J 1994;26:230-234.

29. Peham C, Licka T, Mayr A, et al. Speed dependency of motion pattern consistency. J of Biomech 1998;31:769-772.

30. Peham C, Licka T, Mayr A, et al. Individual speed dependency of forelimb lameness in trotting horses. The Vet J 2000;160:135-138.

Chapter Four:

The effect of equine forelimb lameness on hoof kinematics at the walk[iii]

Introduction

Lameness accounts for up to $1 billion in losses to the equine industry every year[1] and has been one of the most important medical issues faced by horse owners.[2] Mild and subclinical lameness has been reported to have a detrimental effect in horses, resulting in reduced and suboptimal performance,[3, 4] and as less severe lameness may be a precursor to a severe or catastrophic musculoskeletal injury, early diagnosis is especially important for animal welfare. In addition, when reassessing a horse following treatment and rehabilitation from injury, sensitive methods are needed to determine when the animal can safely return to more strenuous exercise without risking re-injury.

The subjective lameness examination is the most common diagnostic tool used for detection and monitoring lameness, and horses are commonly assessed both at the walk and the trot during evaluation and when assigning a lameness grade. However, these subjective scoring systems are not clinically reliable, especially when lameness is mild.[6-9] In addition, assessing improvement in lameness following peri-neural anesthesia has been shown to have inherent bias.[6] Thus, more accurate, objective tools are needed to supplement the subjective lameness examination for the detection and tracking of mild lameness, as well as to assess improvement

---

[iii] *Moorman VJ, Reiser RF, Peterson ML, McIlwraith CW, Kawcak CE. The effect of equine forelimb lameness on hoof kinematics at the walk. Am J Vet Res 2013: Accepted.*

from peri-neural anesthesia. As horses with mild to moderate lameness do not have perceptible lameness at the walk,[5] they are often not examined extensively at that gait during the subjective lameness examination. However, if the walk could be used to effectively evaluate for lameness, it would aid in the examination of horses especially in situations where observing the animal at a faster gait might be detrimental.

Objective methods of lameness evaluation utilizing kinetics and kinematics have been widely investigated to determine their efficacy at both the walk and trot. Stationary force platform kinetics and horse-based and optical kinematics have been shown to be as sensitive or more sensitive as the human eye for diagnosing mild lameness at the trot.[10-12] There are fewer reports of altered kinetics and kinematics when there is mild or no visible lameness at the walk. Merkens et al demonstrated that horses with mild lameness at the trot with no visual abnormalities at the walk had significant kinetic alterations.[13] Buchner et al demonstrated that optical kinematics were altered when mild to moderate lameness was induced in the forelimb at the walk.[14] As kinematic changes have been documented in both the lame and non-lame forelimb hooves at the trot,[12] identification of both intra- and inter-limb differences may also prove beneficial in identification of lameness at the walk.

The objective of this study was to examine the effects of lameness on intra- and inter-limb kinematics of the forelimb hooves at the walk. As optical methods are the current gold-standard for determination of kinematics, our objective was to identify distal limb kinematic changes at the walk when a weight-bearing lameness, only perceptible at the trot, was induced in a single forelimb. In addition, we wanted to identify the specific kinematic variables that are significantly altered with lameness during pre-defined phases of the stride, as well as when the lameness is blocked with peri-neural anesthesia. We hypothesized that after induction of lameness, there would be significant intra- and inter-limb differences in kinematic variables from the fore hooves, and that these differences could be detected at the walk. We also hypothesized that following peri-neural anesthesia of the medial and lateral palmar nerves, these kinematic changes would not be significantly different from baseline.

Materials and Methods

Horses- Six normal quarter horses, with no perceptible lameness at the walk or trot (grade 0 out of 5 using a modified AAEP Lameness Scale[5]) were used for the study. These six horses were used concurrently for a companion study, of which data were collected during the same session.[12]The horses were age 2-9 years, with mass 364 +/-19 kg (mean +/- standard deviation) and wither height 1.46 +/-0.03 m. All horses had their feet trimmed and balanced and were shod as previously described.[12] Prior to initiation of the study, all horses were acclimated to the Gait Analysis Laboratory where data were collected. All procedures were approved by the Institutional Animal Care and Use Committee.

Lameness Induction - Lameness was induced as previously described.[12] In brief a 6mm diameter, threaded screw, either with a blunt or tapered distal end, was inserted into the medial and lateral nuts in the shoe on the right front hoof. Screws ranged from 11 mm to 17 mm in length. Blunted screws were used to induce all lameness grades in the first two horses, and to induce the mildest lameness (grade 1 out of 5) in the remaining four horses. The tapered screws were used to induce more severe lameness (grades 2 and 3 out of 5) in the last four horses. The screw was fully inserted into the nut, and the head of the screw was in contact with the ground when the horse was weight-bearing.

Lameness Trials - Following the collection of baseline data (no induced lameness), each horse had lameness grades 1- 3 out of 5 using a five-point modified AAEP Lameness Scale,[5] starting with the mildest and proceeding to the most severe. Briefly, grade 1 was described as intermittently lame at the trot, grade 2 was mildly but consistently lame at the trot, and grade 3 was moderately and consistently lame at the trot. None of the lameness grades examined resulted in visible lameness at the walk. Horses were allowed to rest for several minutes between lameness conditions to limit the effect of fatigue. After induction of the grade 3 lameness, 3mL of 2% mepivacaine was injected subcutaneously around the medial and lateral palmar nerves. After 10 minutes, if the horse did not show sufficient visual improvement in lameness (> 80%) or skin desensitization, a second 1.5 mL of 2% mepivacaine was injected subcutaneously around the medial and lateral palmar nerves. The horse was then re-assessed after another 5 minutes.

Retro-reflective Markers - A marker triad, measuring 15 cm tall by 13 cm wide by 0.1 cm thick with a mass of 37.6 g, was rigidly attached by an aluminum base plate with hoof acrylic[a] to each fore hoof as previously described.[12] The triad was composed of an aluminum frame stiffened with a uni-axial carbon sandwich structure with a balsa core (4.6 cm x 2.8 cm x 0.6 cm). The stiffeners were placed behind each of the three retro-reflective markers, for added stability with the markers rigidly attached with machine screws.

As previously described,[12] an IMU[b] was attached to the marker triad of the right front hoof, and a machined piece of metal was attached to the triad on the left front hoof. The total mass of the right marker triad with IMU was 113.8g and the mass of the left marker triad was 130.9 g. The difference between the two triads was made up by the mass of the IMU cable. Strain gauges were glued on the hooves of both forelimbs, which had cables integrated into the elastic bandages and terminated at a data collection source also mounted on the surcingle (9.5 kg). The data collected from the IMU and the strain gauges were a subset of this study and will be presented elsewhere (Chapter 5).

Trial set-up and synchronization - Data were collected first at the walk and then at the trot in the Gait Analysis Laboratory as previously described.[12] Trot data are presented in a companion manuscript.[12] Briefly, each horse was walked at a consistent and comfortable speed for that individual, and the velocity of each trial was measured by the use of five infrared timing gates[c] spaced 1.5m apart, linked to the optical kinematics computer and triggered by the horse as it traveled through the capture volume.

Four to five acceptable trials were collected from each horse at the walk for the right and left forelimbs. An acceptable trial was defined as one where the horse traveled straight and at a consistent velocity through the capture volume. In addition, during the baseline walk trials, an average velocity was calculated for each horse. Throughout the remainder of the trials, only trials where the horse was traveling within 10% of its average initial velocity were included for analysis.

Camera Set-up - Eight infrared cameras[d] operating at 200 Hz were used to collect the optical kinematic data. Four cameras were placed on either side of the horse and were suspended from overhead beams. Calibration of the optical kinematic system[e] for the over-ground trials yielded coordinate resolution to within 1.2 mm.

Kinematic Data - Optical coordinate data were low-pass filtered at 15 Hz with a recursive 4th-order Butterworth filter. A virtual marker was created between the cranial and caudal markers of the hoof triad, and this was used as a local origin to track the motion of the hoof.

The linear movement of the hoof was tracked in the sagittal plane: cranial-caudal (X) and proximal-distal (Z). The hoof events of hoof contact, heel-off, and toe-off were determined by evaluation of the X and Z acceleration profile of the stride as previously described.[12] The above mentioned events were used to divide the stride into total stance (hoof contact to toe-off), break-over (heel-off to toe-off), total swing (toe-off to hoof contact), initial swing (toe-off to initial 25% of swing), and terminal swing (75% of swing to hoof contact).

The origin of the coordinate system was set at toe-off, so translations of the hoof at all other events were relative to the virtual marker location at toe-off. To ensure the coordinate system was aligned with horse travel, the x-axis was aligned with the virtual marker at the second hoof contact. X and Z axes were then positive cranially and proximally, respectively. Heel-down hoof orientation within the sagittal plane about the medial-lateral Y axis was positive, while toe-down orientation was negative. As the marker triad was not perfectly parallel to the ground, the orientation of the hoof during the middle of stance (when the cannon bone was perpendicular to the ground – as determined by visual assessment of the optical data), was used to adjust the sagittal orientation of the hoof such that 0° of the hoof was level to the ground.

Temporal parameters, maxima, minima, and averages were determined for each variable during break-over, total swing, initial 25% of swing, and terminal 25% of swing. Instantaneous positions, velocities, accelerations, and sagittal plane orientation were determined at hoof contact, heel-off, and toe-off. Total range of motion of the hoof during break-over, total swing, initial 25%, and terminal 25% of swing was also determined.

Statistical Analysis - A commercial program[f] was utilized for statistical analysis. Data were examined for normality, and if normality was not met, they were log transformed. A repeated measures mixed model ANOVA was performed with each parameter of interest as the outcome variable. Comparisons were made within each limb (lame and non-lame) and between limbs at each lameness condition. Intra-limb comparisons used the baseline walk as the control for each treatment (lameness grades 1 – 3 and after peri-neural anesthesia). Inter-limb comparisons were made for each treatment condition (baseline, lameness grades 1-3, and after peri-neural anesthesia). When there were significant inter-limb differences at baseline, no further inter-limb comparisons were assessed after lameness induction or peri-neural anesthesia. Lameness grade and limb (lame versus sound) were fixed effects with horse velocity included as a confounding variable, and horse was included as a random effect. Significance was set at $P < 0.05$.

Results

Lameness was successfully induced in all horses; the lameness induced was only visually apparent to the human eye at the trot. The lameness model was modified as previously described[12] to induce all three grades of lameness. Within 24 hours after removal of the shoe, there was no perceptible lameness in any horse at the trot.

Lame limb - Significant intra-limb changes to hoof kinematics were observed in the lame limb at all grades of lameness and following peri-neural anesthesia (after block) as compared to baseline walk. These intra-limb changes were present during both stance (hoof contact and break-over) (Table 4.1) and swing (initial 25% of swing, terminal 25% of swing and total swing) (Table 4.2). Significant intra-limb kinematic changes were apparent at the most mild lameness (grade 1) during both stance and swing (Tables 4.1 and 4.2).

Non-lame Limb - A significant intra-limb change to hoof kinematics was only observed in the non-lame limb at the most severe lameness (grade 3) as compared to baseline walk. This intra-limb change was a significant increase in orientation at hoof contact (Table 4.1). No significant intra-limb changes were observed during break-over or any sub-section of swing.

Between limbs - Thirty-eight out of ninety-four (40.4%) kinematic variables were significantly different inter-limb at baseline walk. During hoof contact and all subsets of stride, there were 12 out of 36 (33.3%) cranial-caudal (X) variables, 20 out of 35 (57.1%) vertical (Z) variables, 5 out of 17 (29.4%) sagittal plane orientation variables, and 1 out of 6 (16.7%) temporal variables.

Significant inter-limb changes to hoof kinematics were observed at all grades of lameness and following peri-neural anesthesia (after block) as compared to baseline walk. These inter-limb changes were present during both stance (hoof contact and break-over) (Table 4.1) and swing (initial 25% of swing, terminal 25% of swing and total swing) (Table 4.2). Significant inter-limb kinematic changes were only apparent at the most mild lameness (grade 1) during stance (Table 4.1).

The complete kinematic set at the walk is contained within Appendix V.

Discussion

The data supported our first hypothesis that we could detect significant kinematic changes at the walk in the lame forelimb when there was no perceptible lameness at the walk. We found that even at very mild lameness (grade 1) where the lameness was not visible to the naked eye at the walk, we could detect intra-limb kinematic changes to the lame limb, including a longer break-over duration, a longer stance duration, an increased maximum cranial (X) acceleration at break-over, and an increased swing length. The break-over duration was significantly longer in the lame limb at the mildest lameness (grade 1) while a significant increase in stance duration of the lame limb did not occur until more severe lameness (grade 3). The stance duration in the non-lame limb also appeared to increase at more severe lameness (grade 3), but this change was not significantly different from baseline. Stance duration has been reported to be prolonged after induction of weight-bearing lameness in both the lame and non-lame forelimbs at the trot as a mechanism to maintain the vertical impulse while allowing for a decreased peak vertical force.[15, 16] Our data supported this finding and demonstrated that this prolongation of stance duration also occurred at the walk. We did find a significant increase to break-over duration at mild lameness, indicating a slower unloading of the lame limb, which could function to maintain the vertical impulse. The authors are unaware of other studies that have examined break-over at the walk. This finding was opposite to what was identified in Moorman et al, where the break-over duration was significantly shorter at the trot after lameness was induced.[12]This may indicate that there are different mechanisms, depending on gait, which result in differences in break-over duration.

A variable that was significantly altered with lameness at both the walk and trot[12] was maximum cranial acceleration during break-over. This variable was significantly increased in the lame limb compared to baseline at the walk; however, the effect was significant at mild lameness (grade 1) at the trot compared to the walk, where it only became significant at grade 2 lameness. In addition, after peri-neural anesthesia, the maximum cranial acceleration of the lame limb at the trot had returned to baseline, while it was still significantly different from baseline at the walk.

The swing length (maximum X position) of the lame hoof increased at the walk after induction of lameness during the two most mild lameness conditions (grades 1 and 2) but returned to baseline after more severe lameness (grade 3). In previous reports, the swing length has been reported to be shortened at the trot, but this effect was seen at a more severe lameness, when lameness was visually present at the walk.[17] We noticed significant differences to swing length at a less severe lameness condition, and this may explain why there was an elongation instead of a shortening of swing length. This indicates that stride length, like break-over duration, may be differentially expressed depending on the severity of the lameness or gait examined.

A significant increase in hoof orientation occurred in the non-lame limb at hoof contact, indicating that it landed with a more heel-down orientation. This intra-limb change was not significant at the walk until a more severe lameness (grade 3) was induced. However, this change was also an inter-limb change, which was significant at more mild lameness (grade 2). Both the intra- and inter-limb changes to orientation at hoof contact were also seen at the trot[12] but were also significantly different at mild lameness (grade 1). In addition, this orientation change after peri-neural anesthesia returned to baseline at the trot, which did not occur at the walk.

Some of the data also supported the second hypothesis that kinematic changes induced by lameness would return to baseline following peri-neural anesthesia. Break-over duration, swing length, and maximum cranial (X) position during swing of the lame limb returned to baseline following peri-neural anesthesia. In addition, there was no longer a significant inter-limb difference in the average orientation of the hoof during the terminal 25% of swing following peri-neural anesthesia. However, the orientation of the lame hoof at hoof contact was significantly greater than baseline following peri-neural anesthesia. This change in sagittal plane orientation in the lame hoof could be a useful kinematic tool to determine if a horse was adequately blocked following peri-neural anesthesia.

The lameness model used in this study induced a consistent, rapidly reversible, weight-bearing lameness that resulted in visible lameness to the human eye at the trot but not the walk. While sole-pressure induced lameness is not the source of lameness in the majority of clinical cases, the kinematic changes that occur with this model are thought to be similar to lameness from other sources.[14] This method of lameness induction has been a well-accepted model for weight-bearing lameness and for the analysis of objective methods of lameness detection at the walk and the trot.[11-13,17-19] However, the majority of these reports have not investigated the kinematic alterations at the walk. In addition, the kinematic alterations that have been documented at the walk have only been identified when the horse is visually lame at the walk.[14]

From this study, we identified several kinematic variables that may be useful for lameness diagnosis at the walk in a single forelimb with a weight-bearing lameness. Both intra-limb changes to the lame limb and inter-limb kinematic changes may be useful for evaluating lameness. Since sagittal plane orientation at hoof contact and maximum cranial acceleration during break-over were altered during both the walk and the trot, these variables are likely more significant and should be further assessed to determine their utility in clinical cases, as other variables were not significantly altered at both gaits. In addition since this study was performed on a small number of horses, examining a larger number of horses with forelimb lameness would be warranted to determine which parameters are most clinically useful. In addition, as several hoof kinematic variables returned to baseline following peri-neural anesthesia, these could be useful to objectively assess the effect of peri-neural anesthesia at the walk. This could potentially improve our assessment of regional anesthesia if examining the horse at the trot might be detrimental. As horse mounted kinematic systems are becoming more popular for clinical use and there is a trend for smaller and lighter-weight sensors, utilizing a hoof-based sensor system would be an appropriate method to evaluate lameness. Thus, these specific kinematic changes should be re-assessed using a hoof-based kinematic system, such as an IMU. In addition, this technology may allow evaluation of motion in the frontal and transverse planes, as lameness and blocking may also induce changes outside the sagittal plane.

[a] Equi-Thane SuperFast, Vettec; Oxnard, CA
[b] H3-IMU, MemSense; Rapid City, SD
[c] MEK 92-PAD photoelectric control, MekontrolInc, Northboro, MA
[d] Volant by Peak, Performance Technologies Inc, Centennial, CO
[e] Vicon-Motus 9.2, Vicon Motion Systems Inc, Centennial, CO
[f] STATA 11, StataCorp LP; College Station, TX

Table 4.1 - Intra- and inter-limb means and standard deviations of specific kinematic parameters during stance at the walk
* indicates a significant inter-limb difference at a specific lameness grade at the walk. † indicates a significant intra-limb difference between a specific lameness grade and baseline walk ($P < 0.05$).

			Baseline		Grade 1		Grade 2		Grade 3		After Block	
Hoof Contact:			mean	st dev	mean	st dev	mean	st dev	mean	st dev	mean	st dev
Orientation (^{o})		L	0.7	3.2	0.6	2.9	0.6*	2.5	0.4*	2.0	1.5†	2.8
		NL	1.2	2.7	0.8	2.7	1.4*	2.4	1.8*†	2.7	1.2	3.0
Break-over:												
Stance duration (s)		L	0.81	0.05	0.79	0.07	0.80	0.07	0.83†	0.07	0.84†	0.05
		NL	0.82	0.05	0.79	0.07	0.81	0.06	0.84	0.07	0.84	0.05
Break-over duration (s)		L	0.09*	0.01	0.09†	0.02	0.10†	0.01	0.09†	0.01	0.09	0.01
		NL	0.10*	0.01	0.09	0.02	0.09	0.02	0.09	0.02	0.09	0.01
X position (m)	Min	L	-0.05	0.01	-0.05*	0.01	-0.05*	0.01	-0.04*	0.01	-0.04*	0.01
		NL	-0.04	0.01	-0.04*	0.01	-0.04*	0.01	-0.04*†	0.01	-0.04*†	0.01
	Avg	L	-0.03	0.01	-0.03*	0.01	-0.03*	0.01	-0.03*	0.01	-0.03*†	0.01
		NL	-0.03	0.01	-0.03*	0.01	-0.03*	0.01	-0.03*	0.01	-0.03*†	0.01
X acceleration (m/s^2)	Max	L	39.16*	5.24	41.08*	6.26	42.56*†	7.09	41.63*	6.41	44.05*†	7.11
		NL	37.29*	8.41	37.89*	7.82	38.88*	7.45	38.06*	6.45	38.11*	6.89
Z velocity (m/s)	Max	L	0.70*	0.14	0.71*	0.17	0.73*	0.17	0.77*	0.10	0.80*†	0.10
		NL	0.63*	0.16	0.62*	0.17	0.66*	0.14	0.62*	0.15	0.65*	0.14

Table 4.2 - Intra- and inter-limb means and standard deviations of specific kinematic parameters during swing at the walk. *See Table 4.1 for remainder of the key*

			Baseline		Grade 1		Grade 2		Grade 3		After Block	
Initial Swing:			mean	st dev	mean	st dev	mean	st dev	mean	st dev	mean	st dev
Z velocity (m/s)	Max	L	0.82	0.13	0.82	0.18	0.86*	0.18	0.88*	0.12	0.93*†	0.11
		NL	0.75	0.17	0.78	0.14	0.76*	0.12	0.76*	0.15	0.77*	0.14
Terminal Swing:												
X position (m)	Max	L	1.54	0.09	1.58	0.08	1.58†	0.08	1.55	0.08	1.54	0.11
		NL	1.56	0.10	1.58	0.09	1.58	0.09	1.57	0.09	1.56	0.12
	Avg	L	1.46	0.09	1.49†	0.08	1.49	0.07	1.46	0.06	1.44	0.09
		NL	1.48	0.09	1.50	0.07	1.49	0.08	1.48	0.08	1.48	0.10
Orientation (°)	Max	L	1.8	3.4	1.3	3.4	1.4*	3.1	0.9*	2.2	2.5	2.9
		NL	2.7	4.4	2.6	4.6	2.9*	3.7	2.8*	3.8	2.1	4.0
	Avg	L	-14.8	3.6	-15.3	4.1	-16.0*	4.0	-15.4	3.7	-16.1	4.1
		NL	-13.1	3.9	-13.1	4.6	-13.6*	3.9	-14.2	5.3	-15.5	5.0
Total Swing:												
X position (m)	Max	L	1.54	0.09	1.56†	0.08	1.58†	0.08	1.55	0.08	1.54	0.11
		NL	1.55	0.10	1.57	0.09	1.57	0.09	1.55	0.09	1.53	0.11
	Avg	L	0.80	0.05	0.82†	0.05	0.82†	0.04	0.80	0.03	0.80	0.05
		NL	0.81	0.06	0.82	0.04	0.82	0.04	0.81	0.04	0.80	0.05
Z velocity (m/s)	Max	L	0.82	0.13	0.84	0.17	0.86*	0.18	0.90*	0.17	0.96*†	0.15
		NL	0.79	0.19	0.78	0.13	0.76*	0.12	0.77*	0.15	0.77*	0.13
Orientation (°)	Max	L	2.0	3.6	1.4	3.5	1.4	3.1	0.9*	2.2	2.5	2.9
		NL	2.0	3.9	1.8	4.6	2.1	3.6	2.8*	3.5	1.6	3.9
	Avg	L	-64.7	3.4	-64.8	3.2	-66.5*†	3.3	-64.9	2.4	-66.1†	3.3
		NL	-64.6	4.0	-65.0	3.9	-64.6*	2.6	-64.0	3.3	-65.4	2.8

References

1. USDA. National animal health monitoring system equine study. Part I: baseline reference of 1998 equine health and management. Fort Collins, CO: USDA, APHIS, Veterinary Services;1998.

2. Kaneene JB, Ross WA, Miller RA. The Michigan equine monitoring system. II. Frequencies and impact of selected health problems. Prev Vet Med 1997;29:277-292.

3. Gaughan EM. Skeletal origins of exercise intolerance in horses. Vet Clin North Am Equine Pract 1996;12:517-535.

4. Parente EJ, Russau AL, Birks EK. Effects of mild forelimb lameness on exercise performance. Equine Vet J Suppl 34 2002;34:252-256.

5. American Association of Equine Practitioners. Guide for veterinary service and judging of equestrian events. 4th ed. Lexington, Ky: American Association of Equine Practitioners, 1991;19.

6. Arkell M, Archer RM, Guitian FJ, et al. Evidence of bias affecting the interpretation of the results of local anesthetic nerve blocks when assessing lameness in horses. Vet Rec 2006;159:346-349.

7. Fuller CJ, Bladon BM, Driver AJ, et al. The intra- and inter-assessor reliability of measurement of functional outcome by lameness scoring in horses. The Vet J 2006;171:281-286.

8. Hewetson M, Christley RM, Hunt ID, et al. Investigations of the reliability of observational gait analysis for the assessment of lameness in horses. Vet Rec 2006;158:852-858.

9. Keegan KG, Dent EV, Wilson DA, et al. Repeatability of subjective evaluation of lameness in horses. Equine Vet J 2010;42:92-97.

10. Ishihara A, Bertone AL, Rajala-Schultz PJ. Association between subjective lameness grade and kinetic gait parameters in horses with experimentally induced forelimb lameness. Am J Vet Res 2005;66:1805-1815.

11. McCracken MJ, Krammer J, Keegan KG, et al. Comparison of an inertial sensor system of lameness quantification with subjective lameness evaluation. Equine Vet J 2012;44:652-656.

12. Moorman VJ, Reiser RF, Peterson ML, et al. The effect of equine forelimb lameness on hoof kinematics at the trot. Am J Vet Res 2013; **In Press**.

13. Merkens HW, Schamhardt HC. Evaluation of equine locomotion during different degrees of experimentally induced lameness I: Lameness model and quantification of ground reaction patterns of the limbs. Equine Vet J Suppl 6 1988;20:99-106.

14. Buchner HHF, Savelberg HHCM, Schamhardt HC, et al. Limb movement adaptations in horses with experimentally induced fore- or hindlimb lameness. Equine Vet J 1996;28:63-70.

15. Buchner HHF, Savelberg HHCM, Schamhardt HC, et al. Temporal stride parameters in horses with experimentally induced fore- or hindlimb lameness. Equine Vet J Suppl 18 1995;27:161-165.

16. Weishaupt MA, Wiestner T, Hogg HP, et al. Compensatory load redistribution of horses with induced weight-bearing forelimb lameness trotting on a treadmill. The Vet J 2006;171:135-146.

17. Galisteo AM, Cano MR, Morales JL, et al. Kinematics in horses at the trot before and after an induced forelimb supporting lameness. Equine Vet J Suppl 23 1997;29:97-101.

18. Keegan KG, Wilson DA, Smith BK, et al. Changes in kinematic variables observed during pressure-induced forelimb lameness in adult horses trotting on a treadmill. Am J Vet Res 2000;61:612-619.

19. Keegan KG, Yonezawa Y, Pai PF, et al. Evaluation of a sensor-based system of motion analysis for detection and quantification of forelimb and hind limb lameness in horses. Am J Vet Res 2004;65:665-670.

Chapter Five

Use of an inertial measurement unit to assess the effect of forelimb lameness in the horse on three-dimensional hoof orientation at the walk and trot

Introduction

Lameness is one of the largest medical issues to both owners and the equine industry.[1,2] In addition, mild and subclinical lameness can result in reduced and suboptimal performance.[3,4] While the detection of mild lameness is especially important in competition horses where suboptimal performance is unacceptable, it is also important for other equine populations as all would benefit from early detection of injury. As mild lameness may indicate the start of a serious injury or the presence of an existing injury, early identification is critical to prevent exacerbation. Thus, mild lameness is also an issue of animal welfare.

The subjective lameness examination is the most common diagnostic tool used for detection and monitoring lameness.[5] Even though the common scoring systems used for these evaluations have specific criteria, there is much variability within a grade, making longitudinal assessment of an animal challenging when only slight improvement is noted.[6] Several studies have demonstrated that subjective scoring systems are not reliable enough for clinical use, especially when the lameness is mild.[6-9]In addition, observer bias has been reported when assessing improvement in lameness following peri-neural anesthesia.[6] Thus, more accurate, objective tools are needed to supplement the subjective lameness examination for the detection and tracking of mild lameness, as well as to assess improvement from peri-neural anesthesia.

Several objective methods of lameness evaluation using kinetics and kinematics have proven to be effective in detecting mild lameness. Peak vertical force and vertical impulse, as measured by a stationary force platform, have been shown to be significantly altered with mild lameness (< 1.5 out of 5).[10] Unfortunately, stationary force platform analyses are limited by availability, expense, time for collection/analysis, and necessary expertise for the use of the equipment, as well as their limitation of only being able to capture a single hoof strike per pass. Significant changes to distal limb kinematics following induction of lameness have been documented at mild to moderate degrees of lameness at both the walk and trot using optical methods.[11-15] Optical kinematics suffer from many of the limitations of stationary force platform analyses. In addition, skin movement artifact is documented for the distal limb, and while there are corrections for 2-D analysis,[16] there are not reported skin correction algorithms for 3-D analyses of the distal limb.[17] Previous work in normal horses demonstrated that the equine distal interphalangeal joint undergoes on average 3 – 6^{o} of frontal and transverse rotation compared to 46-47^{o} of sagittal rotation at the walk and trot.[17] As the accurate assessment of 3-D orientations of the equine distal limb involves placement of bone fixed markers, using alternative, non-invasive methods to measure these rotations should be assessed.

Because of the inadequacies of stationary force platform and optical kinematics, other kinematic horse-based motion analysis systems are currently being investigated to objectively characterize lameness, both in research and clinical practice. These horse-based systems utilize multiple micro electromechanical components, such as accelerometers, gyroscopes, and GPS tracking devices and have wireless and/or telemetric components for data transmission.[5, 18-22] Multiple horse-mounted systems have been shown to be very sensitive for detection of mild single forelimb or hind-limb lameness at the trot by examining movement of the head or pelvis.[5, 19] One inertial sensor system has been shown to be sensitive enough to objectify hind-limb flexion tests.[21] However, this same system was found to be deficient in detecting bilateral forelimb lameness.[22] Thus, identifying hoof associated kinematic changes that result from lameness may be another method to objectify lameness.

As sensors are becoming increasingly small and lightweight, they can be placed on the distal limb of the horse without inducing large alterations in motion. In addition, the hoof is a suitable place for mounting a small sensor, as it can be rigidly attached, removing motion artifacts. These hoof-mounted sensors can be utilized to collect data on multiple hoof strikes and can be used in many environments, making them desirable for clinical use. In previous human studies, the IMU showed good agreement with an optical system in the examination of 3-D kinematics.[23] In addition, previous IMU data from the equine hoof demonstrated that while sagittal plane data had higher correlations to an optical system, the IMU also produced swing phase data with a similar appearance in the frontal and transverse planes of motion.[20] Thus, a hoof-mounted IMU should be able to detect of abnormal kinematics in all three rotations in a less invasive manner than a 3-D optical system.

Recently, optical methods detected significant changes in sagittal plane kinematics of the hoof at the walk and trot with lameness.[14,15] In addition, 3D orientations of the metacarpophalangeal joint have been shown to be significantly altered when medial to lateral imbalance was induced.[24] Since 3-D orientations have been shown to significantly change by altering hoof balance, it is also likely that lameness may significantly change the 3-D orientation of the hoof during motion. Thus, a hoof-mounted IMU should be able both identify both previously detected sagittal changes, as well as non-sagittal changes to the hoof with lameness.

As the 3-D orientation of the hoof has not been extensively studied, our objective was to determine how these orientations are altered with lameness. A second objective was to determine if the same changes to sagittal plane rotation (Θ), which were detected using optical methods[14, 15] could also be identified with an IMU when a weight-bearing lameness was induced in a single forelimb at the walk and trot. We hypothesized that after induction of lameness, there would be significant intra-limb differences in all three planes of rotation in the lame forelimb hoof at both the walk and trot. We also hypothesized that the changes in Θ that were detected using the optical system would also be significantly different following lameness with the IMU system. We further hypothesized that the differences in orientation could be detected in the mildest grade of lameness at both the walk and trot. Additionally, we hypothesized that following peri-neural anesthesia of the medial and lateral palmar nerves, the kinematic changes would not be significantly different from baseline.

Materials and Methods

Horses **-** Six normal quarter horses, with no perceptible lameness at the walk or trot (grade 0 out of 5, using a modified AAEP Lameness Scale[25]) were used for the study. These same six horses had been used for another subset of this study, which has been presented elsewhere.[14, 15] Data for all three studies were collected simultaneously. The horses were age 2-9 years, with mass 364 +/-19 kg (mean +/- standard deviation) and wither height 1.46 +/-0.03 m. All horses had their feet trimmed and balanced, were shod with a normal steel keg shoe (mass 324.8 +/- 23.5 g) on the left front hoof, and a similar shoe on the right front hoof with a nut welded to the inner web of the medial and lateral branches of the shoe between the third and fourth nail hole (mass 333.7 +/- 25.6 g). The nuts on the right hoof were welded to the shoe so that they were flush with the solar aspect of the shoe and did not contact the horse's sole during weight-bearing. This shoe has been previously described[14, 15]. The median weight of the two screws added to the right shoe (lame limb) was 7.8 g (6.8 g to 10.6 g, depending on length). Prior to initiation of the study, all horses were acclimated to the Gait Analysis Laboratory where data were collected. All procedures were approved by the Institutional Animal Care and Use Committee of Colorado State University.

Lameness Induction - Each horse had lameness induced in the right front hoof by inserting a 6 mm diameter threaded screw, either blunt or with a 2 mm diameter tapered distal end, into the medial and lateral nuts in the shoe. Screws ranged from 11 mm to 17 mm in length. Blunted screws were used to induce all lameness grades in the first two horses, and to induce the mildest lameness (grade 1 out of 5) in the remaining four horses. The tapered screws were used to induce more severe lameness (grades 2 and 3 out of 5) in the last four horses. The screw was fully inserted into the nut, and the head of the screw was in contact with the ground when the horse was weight-bearing. If the screw did not cause the desired degree of lameness, it was exchanged for a longer or shorter screw, as needed. The screw length which induced each grade of lameness was recorded for each horse.

Lameness Trials - Following the collection of baseline data (no induced lameness), each horse had induction of three grades of lameness, grades 1 - 3 out of 5 using a modified AAEP Lameness Scale,[25] starting with the mildest and proceeding to the most severe. Briefly, grade 1 was described as intermittently lame at the trot, grade 2 was mildly but consistently lame at the trot, and grade 3 was moderately and consistently lame at the trot. None of the lameness grades examined resulted in visible lameness at the walk. Walk data was collected prior to trot data for each lameness condition. Horses were allowed to rest for several minutes between lameness conditions to limit the effect of fatigue. After collection of the grade 3 lameness trials, 3 mL of 2% mepivacaine was injected subcutaneously around the medial and lateral palmar nerves. After 10 minutes, if the horse did not show sufficient visual improvement in lameness (> 80%) or skin desensitization, a second 1.5 mL of 2% mepivacaine was injected subcutaneously around the medial and lateral palmar nerves. The horse was then re-assessed after another 5 minutes.

Horse Instrumentation - The IMU[a] (5.1 cm x 3.8 cm x 1.6 cm, 58.6 g) was composed of a tri-axial gyroscope (+/- 1200^{o}/s), tri-axial accelerometer (+/- 200 G), tri-axial magnetometer (+/- 1.9 Gauss), and a thermostat (0 – 70^{o}C), sampled at 800 Hz. Data were sampled real-time and were stored on a hand-held computer mounted on the horse until the end of the data collection session. The IMU was attached to a marker triad on the right front hoof, and a custom, machined piece of metal (3.6 cm x 3.1 cm x 1.2 cm, 75.7 g) was attached to the triad on the left front hoof (Figure 5.1). The application of the marker triad to the hoof has been previously described.[14] The total mass of the right marker triad with IMU was 113.8 g as well as the mass of the cable and associated fixation, while the mass of the left marker triad was 130.9 g. The cable from the IMU was loosely attached to the horse's limb with a wrap of elastic bandage[b] around the distal metacarpus and distal antebrachium and was attached to a laptop computer, mounted on a surcingle around the horse. Strain gauges were glued on the hooves of both forelimbs, which had cables integrated into the elastic bandages and terminated at a data collection source also mounted on the surcingle (9.5 kg). The data collected from the strain gauges were a subset of this study and will be presented elsewhere.

***Trial set-up and synchronization* -** Data were collected in the Gait Analysis Laboratory; all horses were walked and trotted over a rubberized runway (9.3 mm thickness), covering an asphalt surface, measuring 1.2 m wide by 24.8 m long. A stationary force platform was located in the middle of the length of the runway, and the velocity of each trial was measured by the use of five infrared timing gates[c] spaced 1.5 m apart, which were located along the length of the force platform. This area of the runway is referred to as the capture volume. While in the capture volume, the horse had achieved a constant velocity. During the baseline trials, an average velocity was calculated for each horse at each gait. Five to nine acceptable trials were collected from each horse at the walk and the trot for the right forelimb. An acceptable trial was defined as one where the horse traveled straight and at a consistent velocity that was within 10% of its average initial velocity.

***Data Processing* -** Data from the IMU were transferred from the hand-held computer to another computer for processing and analysis. The orientation angles in all three planes were determined using scripts[d] from a computer program[e] developed by the manufacturer,[a] which were modified for use with the 200 g accelerometers in the IMU unit. The data processing script calculated three angle rotations through a series of time steps using rotation matrices calculated from the accelerometer and magnetometer data from the IMU. Pre-smoothing of the sensor data was performed with a 5-point moving average within the script.

As mounted on the marker triad on the right fore hoof, positive was directed caudally in the cranial-caudal (y) axis, medially in the medial-lateral (z) axis, and distally in the vertical (x) axis (Figure 5.2). Rotation around each axis followed the right-hand rule. Rotation around the cranial-caudal (y) axis (abduction/adduction) is further referred as Phi (Φ), with a positive rotation defined as abduction. Rotation around the medial-lateral (z) axis (flexion-extension) is Theta (Θ), with a positive rotation defined as toe-down. Rotation around the vertical (x) axis (internal/external rotation) is Psi (Ψ), with a positive rotation defined as external rotation.

The output of the magnetometer in the cranial-caudal (Y) direction was also used to locate the force platform. As the horse moved into the capture volume and over the metal force platform, the magnetometer reading increased in magnitude. Orientation and accelerometer data in all three axes from three strides around the vicinity of the force platform were extracted from the entire trial data set. These data were imported into a commercial kinematics system[f] for further processing.

Orientation angles and linear accelerations were low-pass filtered at 15 Hz with a recursive 4^{th}-order Butterworth filter. The events of hoof contact, heel-off, and toe-off were determined by evaluation of the X and Z acceleration profile of the stride, as reported previously[14]. These gait events were used to divide the stride into segments: stance (hoof contact to toe-off), break-over (heel-off to toe-off), total swing (toe-off to hoof contact), initial swing (toe-off to initial 25% of swing), and terminal swing (75% of swing to hoof contact). As there was an offset in the data for each angular orientation during stance resulting from how the IMU was mounted on the hoof, the orientation in each of the three planes during the middle half of stance was subtracted from all variables within that particular stride.

Temporal parameters, as well as maxima, minima, and averages were determined for each variable during break-over, total swing, initial 25% of swing, and terminal 25% of swing. Instantaneous sagittal plane orientations in all three planes were determined at hoof contact, heel-off, and toe-off. Total range of motion of the hoof during break-over, total swing, initial 25%, and terminal 25% of swing was also determined. For each trial, an average of each variable was determined for the three strides.

Statistical Analysis - A commercial program[g] was utilized for statistical analysis. Data were examined for normality by examining normality plots, and if values were non-parametric, they were $\log_e$ transformed. Data sets with negative values were rank ordered. A repeated-measures mixed model ANOVA was performed with each parameter of interest as the outcome variable. Intra-limb comparisons were made using baseline walk or trot as the control compared to each treatment (lameness grades 1 – 3 and following peri-neural anesthesia (block)). Lameness grade was a fixed effect with horse velocity included as a confounding variable, and horse was included as a random effect. Significance was set at $P < 0.05$. Considering the relatively small sample size of the data set, a trend towards significance was set at $P < 0.10$.

As the standard deviations of the peri-neural (block) condition appeared larger than the other conditions, homogeneity of variance was tested with Levene's test (if data appeared normal) or Brown-Forsythe test (if data was non-parametric). If the test of homogeneity was significant ($P < 0.05$), individual comparisons were made between each condition (baseline or lameness) and peri-neural (block) condition. Homogeneity of variance was tested for all three orientations.

Results

Lameness was successfully induced in all horses. Blunt screws were used to induce lameness in the first two horses. In one of these horses, the IMU stopped communicating with the data logger following the baseline trials, so no lameness or blocking data were collected from that horse. Data was also not logged in the last horse at the trot for baseline or the most severe (grade 3 out of 5) lameness. At the trot, baseline, grade 1, grade 2, and blocked condition data were collected from five horses, and grade 3 data were collected from four horses. At the walk, baseline data were collected from six horses, and all lameness and blocked condition data were collected from five horses. Within 24 hours after lameness induction, there was no perceptible lameness in any horse at the trot.

Trot **-** Significant intra-limb changes to all three angular orientations were detected following induction of lameness (Table 5.1) during both stance and swing phases of stride, as well as individual hoof events (Table 5.2) at the trot. Significant changes to the angular orientation of the hoof were also detected at the most mild degree of lameness (grade 1) during break-over, total swing, and initial swing. Significant changes to Ψ and Φ were more commonly detected at the mildest degree of lameness, as compared to Θ. Following peri-neural anesthesia, several variables were returning towards baseline at the trot, including variables during break-over (Ψ minimum, Φ average, Θ maximum and average, and Ψ and Θ range of motion), swing (Φ minimum), initial swing (Φ minimum), and toe-off (Θ). At the walk, Θ orientation at toe-off returned to baseline following peri-neural anesthesia.

Following peri-neural anesthesia (block), the standard deviations in the Θ angular orientation were significantly larger compared to baseline and lameness conditions at the trot (Table 5.3). This effect was seen during both stance and swing phases, as well as during individual hoof events. In total, twelve out of nineteen Θ variables showed heterogeneity of variance. In eight of those twelve variables, there was a significant difference in standard deviation in the baseline and all lameness groups from the blocked condition. In the Φ and Ψ angular orientations, there were six of thirty-eight variables with heterogeneity of variance, but only one showed a larger standard deviation for the peri-neural (block) condition (Tables 5.4 and 5.5).

Walk **-** Significant intra-limb changes to all three angular orientations were detected following induction of lameness (Table 5.6) during both stance and swing phases of stride, as well as individual hoof events (Table 5.7) at the walk. Significant changes to the angular orientation Φ of the hoof were also detected at the most mild degree of lameness (grade 1) during break-over, and during the stride events of hoof contact and heel-off. Ψ showed a trend ($P < 0.10$) towards statistical significance during break-over in the mildest lameness at the walk. Only Θ at toe-off returned to baseline following peri-neural anesthesia; the remainder of the significant orientation variables were still significantly different from baseline walk.

Similar to the trot, the standard deviations in the Θ angular orientation were found to be larger following peri-neural anesthesia compared to baseline and lameness conditions at the walk (Table 5.8). This effect was seen during both stance and swing phases. Twelve out of nineteen Θ variables had significantly larger standard deviations in the blocked condition versus baseline and lameness conditions. In the Φ and Ψ angular orientations, there were five of thirty-eight variables with heterogeneity of variance, but only one showed a larger standard deviation for the peri-neural (block) condition (Tables 5.9 and 5.10).

Discussion

From this current study, we have documented significant changes to 3-D orientations of the hoof using an IMU after induction of an experimental, weight-bearing lameness. As an IMU was mounted on the lame limb, only intra-limb changes were evaluated. Significant changes to sagittal plane orientation (Θ) during both stance and swing phases of the hoof were demonstrated following lameness. These changes to the sagittal plane orientation of the hoof have previously been described at the trot and walk using optical methods, which were collected simultaneously on the same set of horses as presented here.[14, 15] When comparing the optical to IMU, the Θ data showed similar trends; however, the IMU method was able to detect a statistical significance intra-limb in the lame forelimb more commonly. During both the trot and walk, it was more common for the Θ orientation changes detected using the optical system to be inter-limb, with the majority of intra-limb changes present in the non-lame limb. While kinematics were not collected with the IMU on the non-lame limb, similar results would be expected. As a larger number of strides were examined using the IMU (three strides per trial), this may have improved the ability to see a statistical intra-limb difference. While sagittal plane linear and angular kinematics of the distal limbs have been shown to be altered with lameness[11-15], there has not been investigation of 3-D changes to the orientation of the hoof with lameness. Several studies have examined the 3-D distal limb orientations in normal horses and the changes to these kinematics when the hoof is imbalanced medial-lateral and cranial-caudal.[24,26, 27] We found significant changes to abduction/adduction (Φ) and internal/external rotation (Ψ) orientations at the walk and trot followed induction of lameness. This included a greater external rotation (Ψ) of the hoof during both break-over and toe off, which was seen at the mildest lameness (grade 1). In addition during break-over, the hoof on average was more abducted than baseline, which again was found to be significant at the mildest lameness (grade 1). During the initial 25% of swing, lameness resulted in an increased range of motion in both Ψ and Φ. These changes to the range of motion stem from an increased internal rotation (Ψ) and adduction (Φ) during initial swing, which may be compensatory changes for the external rotation and abduction of the hoof during break-over.

Following peri-neural anesthesia (block), several variables in all three planes of rotation were returned to baseline at the trot. At the walk, only Θ orientation at toe-off returned to baseline following peri-neural anesthesia. As lameness was only visualized at the trot, and blocking resulted in a significant reduction of lameness, it would be expected that a larger number of variables would return to normal at the trot. At the walk, lameness was not visually detectable, so it would be expected that blocking would result in both a smaller number of significant variables with lameness, as well as fewer variables returning to baseline following peri-neural anesthesia. Thus, the assessment of peri-neural anesthesia using 3-D orientations on a single lame forelimb may be more easily assessed at the trot.

Also following peri-neural anesthesia, there was a significant increase in standard deviation in the Θ orientation (Tables 5.3 and 5.8). This phenomenon was not seen as consistently in the Φ and Ψ angular orientations (Tables 5.4, 5.5, 5.9, 5.10). It has been previously reported that the range of motion of the distal interphalangeal joint in the sagittal plane (Θ) is much greater compared to abduction/adduction and internal/external rotation,[17] so it would be logical that Θ standard deviations would be greater compared to the other two rotations. In addition, the effect of peri-neural anesthesia on proprioception may have a greater effect on flexion/extension, as ligaments provide support to the distal limb in the frontal and transverse planes. Previously, Peham et al[28] found that horses showed greater variability in stride length following blocking, and concluded that lame horses showed less variance than sound horses. However, these authors only examined horses with naturally occurring lameness before and after regional anesthesia; they did not include any sound horses. Thus, their conclusions are most relevant for lame versus blocked horses. In the current study, we found that both normal horses (baseline) and lame horses showed less variability in the sagittal plane compared to blocked horses. Thus, an increase in sagittal plane variability may be a good indicator of a successful block or to test if a horse has been blocked prior to examination, such as in a pre-purchase evaluation.

The range of motion of the hoof for Φ and Ψ did appear larger than were expected, compared to previously reported data.[19] However, the ranges for Θ were very similar to this previous data. This discrepancy may have originated from higher frequencies in the IMU data presented here resulting from differences in sampling rate and filtering, which may impact the maximum and minimum values. This discrepancy may also originate from extra-sagittal motion of the marker triad/IMU independent of the hoof, which could explain the larger Φ orientation (rotation around the cranial-caudal (y) axis. While the triad was rigidly attached to the hoof, it is not likely that this created a large amount of motion. It is also not as likely that the triad would rotate around the vertical (z) axis, so the increased range of motion in Ψ would likely occur from another source. Sensory impact from the wires connecting the IMU to the data logging device may have affected the motion of the horse's forelimb, resulting in altered rotations. Previous work has shown that tactile stimulation at the level of the pastern has short-term effects on sagittal plane kinematics of the forelimb.[29] However, the horses wore the system for an extended period of time before and during the course of the data collection, suggesting that any tactile stimulation would have subsided during data collection. The authors are unaware of any investigations looking at the effects of tactile stimulation on extra-sagittal plane movements at the level of the hoof.

While it has been previously demonstrated that an IMU can be highly accurate in all three rotations,[23] it has also been shown that processing methods can affect the accuracy of the IMU.[30] With additional data processing, the three-axis gyroscope in the IMU used in this study has the potential to provide improved resolution to the angles currently calculated from the proprietary data processing routine. This has the potential for improved resolution of the IMU orientations. Efforts to improve upon the IMU manufacturer's code are ongoing. In addition, it is warranted to calibrate the orientations in a laboratory setting with pre-determined rotations to ensure that the IMU is appropriately detecting changes in orientation. The increased ranges in abduction/adduction (Φ) and internal/external rotation (Ψ) would indicate that further calibration is required.

In summary, the IMU was able to detect significant intra-limb orientation changes in all three planes of motion following the induction lameness at both the walk and trot, with the majority of significant changes during mild lameness in Ψ and Φ orientations. The Θ kinematic changes detected by the IMU were similar to what was detected using optical kinematics; however, the IMU appeared to be slightly more sensitive in detecting intra-limb changes compared to the optical system. Following peri-neural anesthesia, the IMU was able to detect a return to baseline for several orientation variables, mainly in the trot data. In addition, the IMU identified a significant increase in the standard deviations in Θ orientation, which may be a useful indicator of assessing regional anesthesia. Thus, the IMU as mounted on the hoof differentiated between sound, an experimentally induced single forelimb lameness, and following peri-neural anesthesia at both the trot and the walk. In the future, it would be worthwhile to determine the usefulness of the IMU in detecting inter-limb differences following lameness, as well as investigating the IMU for its usefulness in bilateral forelimb lameness. In addition, further work should be done with the IMU to evaluate the influence of other local anesthetic blocks on the variance of Θ. In addition, examining the IMU in non-laboratory settings and on other footings would be beneficial as the goal is to use it on clinical cases.

---

[a] HP200-1200F0400R, H3-IMU, MemSense; Rapid City, SD
[b] Vetrap, 3M; St. Paul, MN
[c] MEK 92-PAD photoelectric control, Mekontrol Inc, Northboro, MA
[d] Konvalin, C. 2008. Technical Document: Calculating Heading, Elevation and Bank Angle. MemSense, http://memsense.com/docs/MTD-0801_1_0_Calculating_Heading_Elevation_Bank_Angle.pdf
[e] MATLAB, The MathWorks, Inc; Natick, MA
[f] Vicon-Motus 9.2, Vicon Motion Systems Inc, Centennial, CO
[g] STATA 11, StataCorp LP; College Station, TX

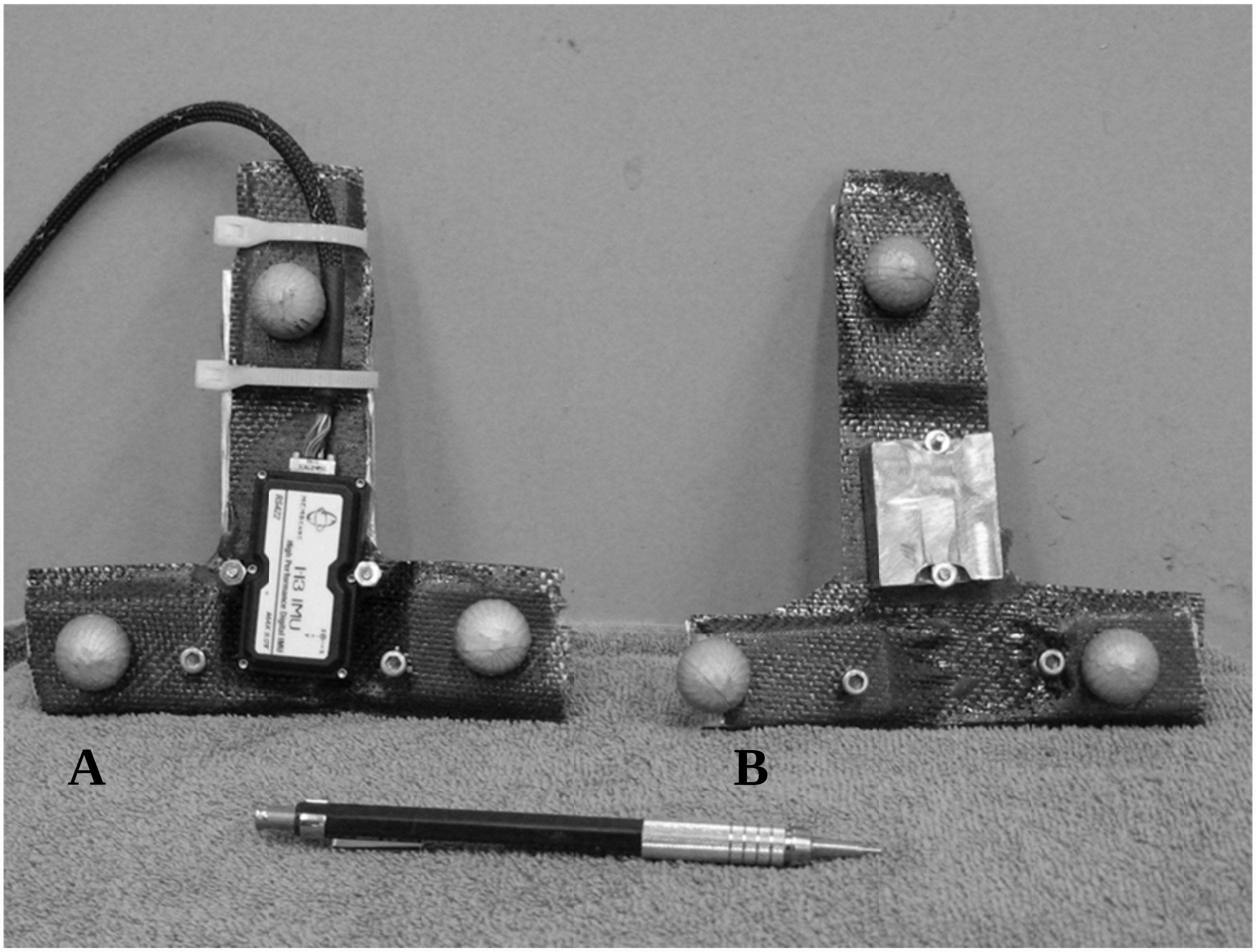

Figure 5.1 – Photograph of a marker triad with (A) an IMU attached and (B) a machined piece of metal with a similar mass to the IMU.

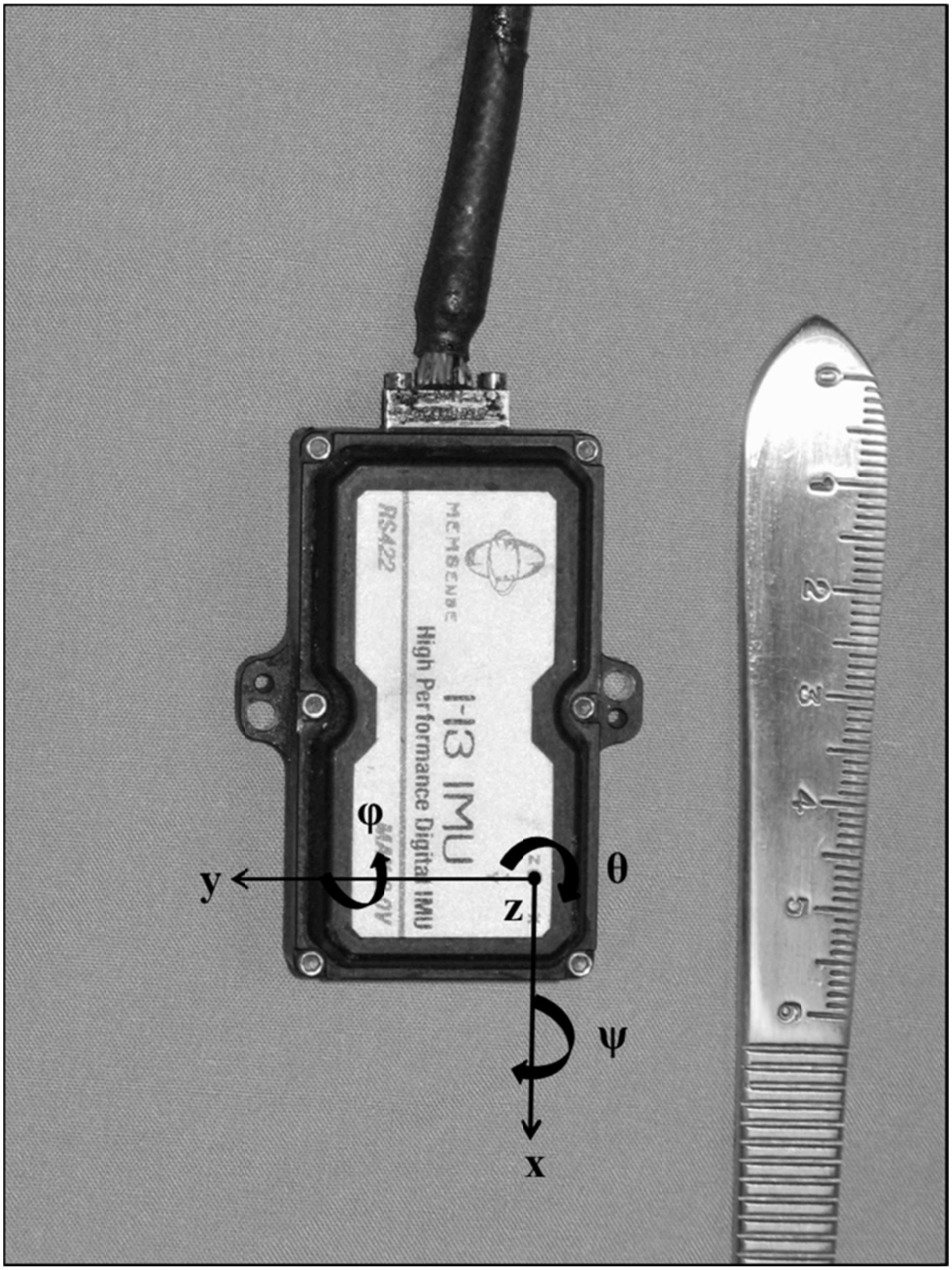

Figure 5.2 –Schematic of the local 3-D orientations of the IMU when mounted on an equine hoof. The cranial-caudal axis (y-axis) was positive in the caudal direction, the medial-lateral axis (z-axis) was positive medially, and the proximal-distal axis (x-axis) was positive in a distal direction when the hoof is flat on the ground. Rotation around the z-axis (Θ), y-axis (Φ), and x-axis (Ψ) are indicated. Rotation in all axes is positive in the counter-clockwise direction (right hand rule).

Table 5.1- Hoof orientation angles at the trot during stance and swing phases after lameness and peri-neural anesthesia (block). * indicates a significant difference from baseline (P<0.05). ** indicates a trend towards a significant difference from baseline (P<0.10). *Italics* indicate that data were ranked. ***Bold italics*** indicate that data were $\log_e$ transformed. ROM = range of motion

			Baseline		Grade 1		Grade 2		Grade 3		Block	
			mean/ median	st dev	mean/ median	st dev	mean/ median	st dev	mean/ median	st dev	mean/ median	st dev
Break-over	Psi – Ψ (°)	Max	42.6	6.7	47.9	4.9	45.4	5.2	43.6	6.4	47.5	6.2
		Min	-2.2	12.3	3.9**	6.8	5.2*	4.6	8.8*	5.3	3.3	8.7
		Avg	25.1	5.9	29.5	4.5	29.1	4.9	28.1	2.9	29.8	4.5
		ROM	44.8	10.4	44.0	9.9	40.2*	8.6	34.9*	9.2	44.2	12.8
	Phi – Φ (°)	Max	26.1	8.4	27.6	9.4	24.9	9.8	24.9*	12.6	26.5	8.6
		Min	-9.9		-9.1*		-9.0		-2.8		-7.9	
		Avg	10.1		13.0*		12.4*		14.9*		12.1**	
		ROM	32.6	4.3	34.1	3.8	31.7	5.4	29.5*	5.8	33.0	5.9
	Theta - Θ (°)	Max	62.1	13.1	56.1	10.5	49.4*	14.9	44.0*	15.3	57.3	21.1
		Min	-8.4	9.4	-10.1	6.2	-14.5	12.1	-15.2	9.1	-12.8	19.8
		Avg	17.7	9.1	15.2	8.2	8.7**	14.1	7.2*	12.6	11.5	20.7
		ROM	70.5	8.3	66.2	7.8	63.9*	9.0	59.2*	11.5	70.1	17.8
Swing	Psi – Ψ (°)	Max	23.8	17.3	30.8	12.6	31.7**	12.2	35.9*	13.9	32.2*	11.2
		Min	-80.3	8.0	-77.4	7.3	-76.7	8.2	-79.3	7.7	-77.3	7.4
		Avg	-36.1		-33.1		-26.7		-34.2		-28.0	
		ROM	104.2	14.1	108.2	15.4	108.4*	13.2	115.1*	14.8	109.4*	13.8
	Phi – Φ (°)	***Max***	114.4	1.1	113.2	1.1	112.4	1.1	112.4	1.1	110.1	1.1
		Min	-9.8		-12.6*		-11.2**		-11.0*		-10.7	
		Avg	40.9	1.3	39.6	1.4	38.8	1.3	41.4	1.3	35.8	1.3
		ROM	122.9	7.4	123.7	9.4	122.6	8.9	121.1	9.3	120.9	8.0
	Theta - Θ (°)	Max	102.8	7.1	100.9	9.1	109.5*	16.0	113.1*	15.0	121.5*	34.4
		Min	9.4	8.7	6.6	10.3	5.7	9.5	5.2	13.1	-6.2*	37.2
		Avg	57.1	7.5	57.1	8.7	56.7	9.3	57.8	8.3	59.6	14.8
		ROM	92.7	1.1	93.5	1.1	101.9*	1.2	106.1*	1.2	116.3*	1.5

Table 5.1 – Continued

			Baseline		Grade 1		Grade 2		Grade 3		Block	
			mean/ median	st dev	mean/ median	st dev	mean/ median	st dev	mean/ median	st dev	mean/ median	st dev
Initial Swing	Psi - Ψ (°)	Max	18.6	20.1	23.7	18.3	24.8	14.9	29.1	15.0	23.1	16.0
		Min	-42.5		-43.7**		-47.6*		-51.6*		-49.2*	
		Avg	-17.3	10.2	-16.7	10.4	-15.4	11.3	-16.2*	9.7	-14.4	10.4
		ROM	55.6	1.7	61.0**	1.7	62.5*	1.6	75.7*	1.5	60.7*	1.6
	Phi – Φ (°)	Max	35.0	21.4	40.5	21.9	39.0	19.7	45.3*	21.4	38.7*	18.7
		Min	-8.2		-10.0*		-9.7*		-9.5*		-9.3	
		Avg	11.4		9.2		11.0		12.6		12.1	
		ROM	41.1	16.4	47.0*	15.5	45.7*	15.1	51.6*	14.8	45.8*	14.1
	Theta - Θ (°)	Max	94.4	9.8	95.5	11.5	92.1	14.5	94.8	14.8	96.2	22.6
		Min	43.2	19.0	36.9	20.1	29.4*	22.8	25.2*	23.0	36.9*	21.3
		Avg	73.2	7.6	72.8	7.8	66.5	17.3	65.4	14.3	69.5	21.5
		ROM	51.2	25.1	58.7*	26.7	62.7*	21.3	69.7*	23.1	59.3*	22.0
Terminal Swing	Psi - Ψ (°)	Max	-19.9	16.1	-13.2	15.5	-14.5	18.1	-11.8	17.5	-9.4	12.8
		Min	-78.8	10.9	-77.0	7.4	-76.2	8.3	-78.8	7.7	-76.6	7.1
		Avg	-51.2		-47.9		-45.5		-48.5		-40.6	
		ROM	58.9	15.6	63.8	13.0	61.8	15.1	67.0	16.6	67.2	12.1
	Phi - Φ (°)	*Max*	109.4		105.7		107.8		112.0		106.4	
		Min	23.2	11.2	17.7	12.0	18.7	10.4	18.8*	8.2	14.4*	9.7
		Avg	72.6		68.7		58.4		65.8		55.4	
		ROM	89.9	15.0	94.2	16.3	92.0	16.1	93.8	14.5	95.4	11.0
	Theta - Θ (°)	***Max***	44.9	1.3	47.7	1.4	60.2*	1.7	63.4*	1.6	70.2*	1.7
		Min	10.7		9.7		9.7		11.6		10.3	
		Avg	25.4	1.4	27.0	1.5	31.5	1.8	36.6	1.6	31.3	1.7
		ROM	32.8	1.6	37.2	1.6	47.3*	1.9	50.9*	1.7	61.1*	2.1

Table 5.2 - Angular orientation of the hoof at the trot during specific hoof events after lameness and peri-neural anesthesia (block).

Events		Baseline mean/ median	Baseline st dev	Grade 1 mean/ median	Grade 1 st dev	Grade 2 mean/ median	Grade 2 st dev	Grade 3 mean/ median	Grade 3 st dev	Block mean/ median	Block st dev
Hoof Contact	Psi - Ψ (°)	-35.1	13.8	-34.2	20.7	-36.6*	16.9	-37.5	21.7	-35.6*	13.9
	Phi - Φ (°)	37.4	18.7	40.4	20.7	36.3	18.2	41.3	19.0	35.9	20.7
	Theta - Θ (°)	17.1	8.0	17.2	10.4	21.5	9.4	24.2	10.9	33.1*	34.0
Heel-Off	Psi – Ψ (°)	28.2	3.6	32.1	3.5	31.0	4.4	28.2*	4.0	30.4	5.9
	Phi - Φ (°)	12.1	10.0	12.1	10.3	10.8	11.2	9.2*	12.0	9.2	6.5
	Theta - Θ (°)	-7.7	8.6	-9.3	5.5	-13.6	10.7	-13.8	7.9	-12.3	19.2
Toe-Off	*Psi – Ψ (°)*	4.5		9.4*		8.1*		12.3*		7.8*	
	Phi - Φ (°)	-2.9		-4.8		-5.4		-2.4		-3.3	
	Theta - Θ (°)	56.0	22.7	46.6	23.9	42.1*	21.7	33.4*	24.8	50.1	17.1

Table 5.3 - Standard deviations of sagittal plane (Θ) orientation at the trot. All other conditions were compared to the peri-neural anesthesia (block) condition. The P-value is the test for homogeneity of variance, with significance at $P < 0.05$. * Indicates the blocked condition has a significantly larger standard deviation than a specific condition.

			P-value	Block st dev	Baseline st dev	Grade 1 st dev	Grade 2 st dev	Grade 3 st dev
Break-over	Theta - Θ (°)	Max	*0.005*	21.1	13.1*	10.5*	14.9*	15.3
		Min	*0.157*	19.8	9.4	6.2	12.1	9.1
		Avg	*0.058*	20.7	9.1	8.2	14.1	12.6
		ROM	*0.003*	17.8	8.3*	7.8*	9.0*	11.5*
Swing	Theta - Θ (°)	Max	*<0.001*	34.4	7.1*	9.1*	16.0*	15.0*
		Min	*<0.001*	37.2	8.7*	10.3*	9.5*	13.1*
		Avg	*0.036*	14.8	7.5*	8.7*	9.3*	8.3*
		ROM	*0.003*	68.7	11.0*	12.2*	21.0*	20.4*
Initial Swing	Theta - Θ (°)	Max	*0.013*	22.6	9.8*	11.5*	14.5*	14.8*
		Min	*0.419*	21.3	19.0	20.1	22.8	23.0
		Avg	*<0.001*	21.5	7.6*	7.8*	17.3	14.3*
		ROM	*0.440*	22.0	25.1	26.7	21.3	23.1
Terminal Swing	Theta - Θ (°)	Max	*0.002*	51.3	13.3*	15.8*	38.7	34.7*
		Min	*0.023*	37.5	8.1*	9.4*	10.0*	9.4*
		Avg	*0.027*	19.7	8.7	10.8	23.5	18.9
		ROM	*0.001*	79.8	14.8*	16.6*	37.0	32.99*
Hoof-Contact Theta - Θ (°)			*<0.001*	34.0	8.0*	10.4*	9.4*	10.9*
Heel-Off Theta - Θ (°)			*0.129*	19.2	8.6	5.5	10.7	7.9
Toe-Off Theta - Θ (°)			*0.456*	17.1	22.7	23.9	21.7	24.8

Table 5.4 - Standard deviations of Phi (Φ) orientation at the trot. All other conditions were compared to the peri-neural anesthesia (block) condition. The P-value is the test for homogeneity of variance, with significance at $P < 0.05$. * Indicates the blocked condition has a significantly larger standard deviation than a specific condition.

			P-value	Block st dev	Baseline st dev	Grade 1 st dev	Grade 2 st dev	Grade 3 st dev
Break-over	Phi - Φ (°)	Max	*0.191*	8.6	8.4	9.4	9.8	12.6
		Min	*0.083*	6.3	7.2	8.1	7.1	8.5
		Avg	*0.040*	5.0	6.2	6.0	6.7	7.9
		ROM	*0.076*	5.9	4.3	3.8	5.4	5.8
Swing	Phi - Φ (°)	Max	*0.493*	12.0	10.9	15.0	13.4	13.8
		Min	*0.827*	7.0	6.9	8.5	6.8	7.9
		Avg	*0.759*	11.1	10.8	13.5	10.7	11.2
		ROM	*0.425*	8.0	7.4	9.4	8.9	9.3
Initial Swing	Phi - Φ (°)	Max	*0.858*	18.7	21.4	21.9	19.7	21.4
		Min	*0.699*	6.8	7.3	8.5	7.8	8.9
		Avg	*0.955*	12.8	14.5	16.0	13.6	15.1
		ROM	*0.627*	14.1	16.4	15.5	15.1	14.8
Terminal Swing	Phi - Φ (°)	Max	*0.613*	11.9	10.9	13.8	13.0	13.3
		Min	*0.396*	9.7	11.2	12.0	10.4	8.2
		Avg	*0.707*	12.1	9.4	12.9	10.9	9.6
		ROM	*0.098*	11.0	15.0	16.3	16.1	14.5
Hoof-Contact Phi - Φ (°)			*0.760*	20.7	18.7	20.7	18.2	19.0
Heel-Off Phi - Φ (°)			*0.003*	6.5	10.0	10.3	11.2	12.0
Toe-Off Phi - Φ (°)			*0.451*	15.0	16.5	21.4	17.6	22.1

Table 5.5 - Standard deviations of Psi (Ψ) orientation at the trot. All other conditions were compared to the peri-neural anesthesia (block) condition. The P-value is the test for homogeneity of variance, with significance at $P < 0.05$. * Indicates the blocked condition has a significantly larger standard deviation than a specific condition.

			P-value	Block st dev	Baseline st dev	Grade 1 st dev	Grade 2 st dev	Grade 3 st dev
Break-over	Psi - Ψ (°)	Max	*0.491*	6.2	6.7	4.9	5.2	6.4
		Min	*0.000*	8.7	12.3	6.8	4.6	5.3
		Avg	*0.072*	4.5	5.9	4.5	4.9	2.9
		ROM	*0.025*	12.8	10.4	9.9	8.6*	9.2*
Swing	Psi - Ψ (°)	Max	*0.057*	11.2	17.3	12.6	12.2	13.9
		Min	*0.874*	7.4	8.0	7.3	8.2	7.7
		Avg	*0.139*	9.4	7.6	10.3	10.0	8.3
		ROM	*0.796*	13.8	14.1	15.4	13.2	14.8
Initial Swing	Psi - Ψ (°)	Max	*0.350*	16.0	20.1	18.3	14.9	15.0
		Min	*0.502*	18.7	17.3	20.9	20.3	20.1
		Avg	*0.939*	10.4	10.2	10.4	11.3	9.7
		ROM	*0.763*	27.8	31.3	35.6	29.6	31.3
Terminal Swing	Psi - Ψ (°)	Max	*0.212*	12.8	16.1	15.5	18.1	17.5
		Min	*0.397*	7.1	10.9	7.4	8.3	7.7
		Avg	*0.679*	10.9	13.3	12.3	13.4	10.5
		ROM	*0.454*	12.1	15.6	13.0	15.1	16.6
Hoof-Contact Psi - Ψ (°)			*0.040*	13.9	13.8	20.7	16.9	21.7
Heel-Off Psi - Ψ (°)			*0.016*	5.9	3.6*	3.5*	4.4	4.0*
Toe-Off Psi - Ψ (°)			*0.493*	18.1	22.3	20.8	16.2	18.9

Table 5.6 - Hoof orientation angles at the walk during stance and swing phases after lameness and peri-neural anesthesia (block).*See Table 5.1 for remainder of key*

			Baseline		Grade 1		Grade 2		Grade 3		Block	
			mean/ median	st dev	mean/ median	st dev	mean/ median	st dev	mean/ median	st dev	mean/ median	st dev
Break-over	Psi - Ψ $(^{o})$	***Max***	39.2	1.3	41.2	1.2	40.7	1.2	41.5	1.3	40.2	1.3
		Min	6.9		9.0		8.9		9.9		10.0*	
		Avg	19.4	4.5	21.3	1.7	20.9	2.1	20.5	2.9	20.7	3.7
		ROM	36.2	1.3	32.7**	1.3	30.7*	1.4	31.8*	1.5	30.2*	1.4
	Phi – Φ $(^{o})$	***Max***	20.5	1.8	15.9*	2.0	15.0*	2.1	14.2*	2.3	16.2*	2.0
		Min	-9.5		-10.7**		-10.4**		-9.3*		-8.0	
		Avg	6.5		0.6*		-1.2*		-2.1*		0.4*	
		ROM	30.1	1.3	27.2*	1.3	25.9*	1.5	26.0*	1.5	25.7*	1.4
	Theta - Θ $(^{o})$	Max	51.7	14.6	48.8	9.8	41.9	12.2	41.0	12.3	48.0	27.3
		Min	-2.5	8.4	-3.6	4.8	-3.6	7.0	-7.6	8.9	6.6*	30.4
		Avg	13.7	9.0	13.5	5.2	11.8	10.2	10.6	10.5	20.3	31.7
		ROM	54.2	9.2	52.4	9.5	45.5*	9.5	48.6*	10.2	41.5*	12.0
Swing	Psi - Ψ $(^{o})$	Max	37.7	18.4	41.8	15.8	43.4	16.4	44.7	15.0	44.2	11.8
		Min	-84.3		-77.8		-75.5		-76.8		-82.3	
		Avg	-33.8	7.0	-32.8	9.8	-33.2	8.8	-32.8	9.6	-31.8	8.6
		ROM	121.5	16.8	120.4	15.2	122.3	16.6	124.3	16.7	123.6	12.7
	Phi - Φ $(^{o})$	***Max***	102.9	1.2	106.1	1.1	106.8	1.2	104.5	1.1	103.0	1.1
		Min	-6.8		-8.9		-8.4		-8.7**		-5.5	
		Avg	42.0	8.3	45.8	9.7	46.0	7.0	45.1	9.3	44.0	9.9
		ROM	110.2	11.6	113.0	11.7	114.5	15.0	111.2	11.2	108.3	9.8
	Theta - Θ $(^{o})$	Max	98.1	7.7	98.4	5.1	101.0	6.9	104.4*	11.2	110.8*	16.3
		Min	-1.5		-2.7		-2.5		0.3		1.0	
		Avg	42.9		42.5		46.4**		43.9*		53.4*	
		ROM	102.8	1.2	102.0	1.1	103.7	1.1	108.8	1.2	104.5	1.2

Table 5.6 Continued –

			Baseline		Grade 1		Grade 2		Grade 3		Block	
			mean/ median	st dev	mean/ median	st dev	mean/ median	st dev	mean/ median	st dev	mean/ median	st dev
Initial Swing	Psi - Ψ (°)	Max	27.2	21.5	28.4	15.6	32.3	15.3	33.1	16.4	32.2	14.3
		Min	-60.2	14.7	-62.1	14.5	-64.3*	14.7	-64.6*	15.2	-67.5*	13.2
		Avg	-23.7	7.5	-23.8**	8.8	-23.3	7.3	-24.1	6.6	-25.1*	7.3
		ROM	87.4	33.8	90.6	27.4	96.6	26.9	97.7	30.2	99.7	25.2
	Phi – Φ (°)	*Max*	61.2		62.9		67.7*		65.5		70.5	
		Min	-6.2		-8.2		-6.9		-6.2		-2.7	
		Avg	29.3	1.7	35.3	1.4	37.5*	1.4	36.6	1.4	38.8*	1.3
		ROM	72.0	1.4	83.0	1.3	85.2	1.3	81.9	1.3	80.6	1.3
	Theta - Θ (°)	Max	97.7	8.0	98.2	5.3	100.2	6.3	102.7*	9.2	108.6*	14.4
		Min	34.1	24.6	38.2	17.2	32.7	15.0	27.1	24.4	38.9	21.1
		Avg	73.8	6.7	74.6	6.0	73.2	6.2	74.3	6.7	78.7*	12.1
		ROM	58.6	1.5	57.7	1.3	65.7	1.3	70.9*	1.4	66.8	1.4
Terminal Swing	Psi – Ψ (°)	Max	6.5	11.5	4.8	14.1	3.8	10.8	2.7	12.1	4.0	14.3
		Min	-82.8	9.0	-76.4	8.4	-77.3	7.9	-78.0	10.3	-77.3	8.4
		Avg	-44.4	9.1	-42.8	11.5	-45.5	11.0	-46.1	13.6	-43.2	13.7
		ROM	89.3	12.3	81.3	14.9	81.1	12.6	80.7	12.2	81.3	12.4
	Phi – Φ (°)	Max	98.1	9.1	99.6	7.8	98.4	7.5	98.9	8.5	98.7	8.2
		Min	5.8	10.1	9.9	13.5	11.0	11.8	10.3	10.8	8.5	13.2
		Avg	50.8	8.0	55.0	12.9	55.4	11.1	55.1	12.8	52.2	13.7
		ROM	92.3	9.6	89.7	12.1	87.4	12.4	88.6	10.4	90.1	12.5
	Theta - Θ (°)	***Max***	37.9	1.3	39.9	1.3	40.1	1.5	48.9*	1.5	63.2*	1.7
		Min	-1.3	7.0	-1.1	6.2	-1.5	9.2	-0.4	9.2	6.4*	20.1
		Avg	15.5	1.5	16.6	1.4	20.3*	1.7	23.5*	1.8	31.1*	2.1
		ROM	39.2	1.2	40.6	1.3	40.4	1.6	46.7**	1.7	59.3*	1.6

Table 5.7 - Angular orientation of the hoof at the walk during specific hoof events after lameness and peri-neural anesthesia (block).

Events		Baseline mean/ median	Baseline st dev	Grade 1 mean/ median	Grade 1 st dev	Grade 2 mean/ median	Grade 2 st dev	Grade 3 mean/ median	Grade 3 st dev	Block mean/ median	Block st dev
Hoof Contact	*Psi – Ψ (°)*	-14.1		-17.0		-19.7		-15.2		-26.9*	
	Phi - Φ (°)	22.1		38.3*		46.0*		42.2*		49.5*	
	Theta - Θ (°)	5.2		6.7		8.6		8.4		8.7*	
Heel-Off	Psi – Ψ (°)	11.7	4.2	14.0	2.7	13.3	2.8	13.5	3.6	12.9	3.3
	Phi – Φ (°)	0.6	6.8	-1.6*	6.1	-2.7*	6.0	-2.3*	6.4	-3.0*	4.2
	Theta - Θ (°)	-1.6		-2.5		-3.6		-3.9		-4.5	
Toe-Off	*Psi - Ψ (°)*	15.1		21.4		20.8**		24.8*		22.0*	
	Phi - Φ (°)	-2.9		-5.1**		-4.3		-2.6		3.9	
	Theta - Θ (°)	44.9	25.1	41.9	19.1	36.8	16.7	29.8*	25.1	43.0	19.7

Table 5.8 – Standard deviations of sagittal plane (Θ) orientation at the walk. All other conditions were compared to the peri-neural anesthesia (block) condition. The P-value is the test for homogeneity of variance, with significance at P < 0.05. * Indicates the blocked condition has a significantly larger standard deviation than a specific condition.

			P-value	Block st dev	Baseline st dev	Grade 1 st dev	Grade 2 st dev	Grade 3 st dev
Break-over	Theta - Θ (°)	Max	*< 0.001*	27.3	14.6*	9.8*	12.2*	12.3*
		Min	*< 0.001*	30.4	8.4*	4.8*	7.0*	8.9*
		Avg	*< 0.001*	31.7	9.0*	5.2*	10.2*	10.5*
		ROM	*0.757*	11.9	9.2	9.5	9.5	10.2
Swing	Theta - Θ (°)	Max	*< 0.001*	16.3	7.7*	5.1*	6.9*	11.2*
		Min	*0.083*	19.7	14.4	6.9	8.5	11.5
		Avg	*< 0.001*	23.0	5.5*	7.7*	11.7*	15.0*
		ROM	*0.170*	16.6	18.2	8.4	13.0	19.9
Initial Swing	Theta - Θ (°)	Max	*< 0.001*	14.4	8.0*	5.3*	6.3*	9.2*
		Min	*0.198*	21.1	24.6	17.2	15.0	24.4
		Avg	*< 0.001*	12.1	6.7*	6.0*	6.2*	6.7*
		ROM	*0.113*	20.6	28.1	19.1	16.12	27.9
Terminal Swing	Theta - Θ (°)	Max	*< 0.001*	38.7	8.2*	9.6*	21.5*	25.1*
		Min	*< 0.001*	20.1	7.0*	6.2*	9.2*	9.2*
		Avg	*< 0.001*	30.2	6.4*	6.6*	15.7*	18.8*
		ROM	*0.002*	30.6	8.1*	10.7*	27.9	32.6
Hoof Contact Theta - Θ (°)			*< 0.001*	46.6	9.2*	8.9*	11.5*	9.2*
Heel-Off Theta - Θ (°)			*< 0.001*	31.3	8.8*	5.2*	6.7*	7.3*
Toe-Off Theta - Θ (°)			*0.197*	19.7	25.1	19.1	16.7	25.1

Table 5.9 – Standard deviations of Phi (Φ) orientation at the walk. All other conditions were compared to the peri-neural anesthesia (block) condition. The P-value is the test for homogeneity of variance, with significance at P < 0.05. * Indicates the blocked condition has a significantly larger standard deviation than a specific condition.

			P-value	Block st dev	Baseline st dev	Grade 1 st dev	Grade 2 st dev	Grade 3 st dev
Break-over	Phi - Φ (°)	Max	*0.958*	15.4	15.3	15.4	17.0	20.9
		Min	*0.335*	5.7	7.5	6.8	6.1	8.9
		Avg	*0.724*	7.0	7.9	8.1	7.4	9.5
		ROM	*0.843*	11.4	9.4	10.0	13.0	13.6
Swing	Phi - Φ (°)	Max	*0.669*	10.2	15.1	13.0	15.6	14.1
		Min	*0.509*	8.8	7.6	9.6	6.8	9.6
		Avg	*0.345*	9.9	8.3	9.7	7.0	9.3
		ROM	*0.527*	9.8	11.6	11.7	15.0	11.2
Initial Swing	Phi - Φ (°)	Max	*0.856*	23.2	34.7	30.4	31.3	29.4
		Min	*0.944*	11.2	11.0	12.5	10.2	12.2
		Avg	*0.645*	11.6	16.5	15.0	13.8	14.1
		ROM	*0.966*	22.3	27.5	26.7	28.5	24.2
Terminal Swing	Phi - Φ (°)	Max	*0.900*	8.2	9.1	7.8	7.5	8.5
		Min	*0.498*	13.2	10.1	13.5	11.8	10.8
		Avg	*0.010*	13.7	8.0*	12.9	11.1	12.8
		ROM	*0.438*	12.5	9.6	12.1	12.4	10.4
Hoof Contact Phi - Φ (°)			*0.375*	21.1	27.0	32.0	27.4	27.3
Heel-Off Phi - Φ (°)			*0.011*	4.2	6.8	6.1	6.0	6.4
Toe-Off Phi - Φ (°)			*0.989*	21.5	23.0	22.2	22.7	27.0

Table 5.10 - Standard deviations of Psi (Ψ) orientation at the walk. All other conditions were compared to the peri-neural anesthesia (block) condition. The P-value is the test for homogeneity of variance, with significance at $P < 0.05$. * Indicates the blocked condition has a significantly larger standard deviation than a specific condition.

			P-value	Block st dev	Baseline st dev	Grade 1 st dev	Grade 2 st dev	Grade 3 st dev
Break-over	Psi -Ψ (°)	Max	*0.502*	10.3	10.9	8.1	9.0	11.5
		Min	*0.005*	4.2	10.1	4.2	3.8	4.6
		Avg	*0.000*	3.7	4.5	1.7*	2.1*	2.9
		ROM	*0.505*	10.6	9.8	8.6	11.0	13.7
Swing	Psi - Ψ (°)	Max	*0.102*	11.8	18.4	15.8	16.4	15.0
		Min	*0.457*	6.0	8.5	6.7	6.9	8.4
		Avg	*0.244*	8.6	7.0	9.8	8.8	9.6
		ROM	*0.422*	12.7	16.8	15.2	16.6	16.7
Initial Swing	Psi - Ψ (°)	Max	*0.028*	14.3	21.5	15.6	15.3	16.4
		Min	*0.992*	13.2	14.7	14.5	14.7	15.2
		Avg	*0.533*	7.3	7.5	8.8	7.3	6.6
		ROM	*0.342*	25.2	33.8	27.4	26.9	30.2
Terminal Swing	Psi - Ψ (°)	Max	*0.548*	14.3	11.5	14.1	10.8	12.1
		Min	*0.446*	8.4	9.0	8.4	7.9	10.3
		Avg	*0.086*	13.7	9.1	11.5	11.0	13.6
		ROM	*0.950*	12.4	12.3	14.9	12.6	12.2
Hoof Contact Psi - Ψ (°)			*0.543*	19.3	19.4	21.1	23.4	20.5
Heel-Off Psi - Ψ (°)			*0.267*	3.3	4.2	2.7	2.8	3.6
Toe-Off Psi - Ψ(°)			*0.183*	15.5	24.1	17.2	15.8	17.6

References

1. USDA. National animal health monitoring system equine study. Part I: baseline reference of 1998 equine health and management. Fort Collins, CO: USDA, APHIS, Veterinary Services. 1998.

2. Kaneene JB, Ross WA, Miller RA. The Michigan equine monitoring system. II. Frequencies and impact of selected health problems. Prev Vet Med 1997; 29:277-292.

3. Gaughan EM. Skeletal origins of exercise intolerance in horses. Vet Clin North Am Equine Pract 1996: 12:517-535.

4. Parente EJ, Russau AL, Birks EK. Effects of mild forelimb lameness on exercise performance. Equine Vet J Suppl 34 2002: 34: 252-256.

5. McCracken MJ, Krammer J, Keegan KG, et al. Comparison of an inertial sensor system of lameness quantification with subjective lameness evaluation. Equine Vet J 2012; 44: 652-656.

6. Arkell M, Archer RM, Guitian FJ, et al. Evidence of bias affecting the interpretation of the results of local anesthetic nerve blocks when assessing lameness in horses. Vet Rec 2006; 159: 346-349.

7. Fuller CJ, Bladon BM, Driver AJ, et al. The intra- and inter-assessor reliability of measurement of functional outcome by lameness scoring in horses. The Vet J 2006; 171: 281-286.

8. Hewetson M, Christley RM, Hunt ID, et al. Investigations of the reliability of observational gait analysis for the assessment of lameness in horses. Vet Rec 2006; 158: 852-858.

9. Keegan KG, Dent EV, Wilson DA, et al. Repeatability of subjective evaluation of lameness in horses. Equine Vet J 2010; 42: 92-97.

10. Ishihara A, Bertone AL, Rajala-Schultz PJ. Association between subjective lameness grade and kinetic gait parameters in horses with experimentally induced forelimb lameness. Am J Vet Res 2005; 66: 1805-1815.

11. Buchner HHF, Savelberg HHCM, Schamhardt HC, et al. Limb movement adaptations in horses with experimentally induced fore- or hindlimb lameness. Equine Vet J 1996; 28: 63-70.

12. Galisteo AM, Cano MR, Morales JL, et al. Kinematics in horses at the trot before and after an induced forelimb supporting lameness. Equine Vet J Suppl 23 1997; 29: 97-101.

13. Keegan KG, Wilson DA, Smith BK, et al. Changes in kinematic variables observed during pressure-induced forelimb lameness in adult horses trotting on a treadmill. Am J Vet Res 2000; 61: 612-619.

14. Moorman VJ, Reiser RF, Peterson ML, et al. The effect of equine forelimb lameness on hoof kinematics at the trot. Am J Vet Res 2013; **In Press.**

15. Moorman VJ, Reiser RF, Peterson ML, et al. The effect of equine forelimb lameness on hoof kinematics at the walk. Am J Vet Res 2013; **In Press.**

16. van Weeren PR, van den Bogert, Barneveld A. Correction models for skin displacement in equine kinematic gait analysis. J Equine Vet Sci 1992; 12: 178-192.

17. Clayton HM, Sha DH, Stick JA, et al. 3D kinematics of the interphalangeal joints in the forelimb of walking and trotting horses. Vet Comp Orthop Traumatol 2007; 20:1-7.

18. Keegan KG, Yonezawa Y, Pai PF, et al. Evaluation of a sensor-based system of motion analysis for detection and quantification of forelimb and hind limb lameness in horses. Am J Vet Res 2004; 65: 665-670.

19. Pfau T, Robilliard JJ, Weller R, et al. Assessment of mild hindlimb lameness during over ground locomotion using linear discriminant analysis of inertial sensor data. Equine Vet J 2007; 39: 407-413.

20. Moorman VJ, Reiser RF, McIlwraith CW, et al. Validation of an equine inertial measurement unit system in clinically normal horses during walking and trotting. Am J Vet Res 2012; 73: 1160-1170.

21. Marshall JF, Lund DG, Voute LC.Use of a wireless, inertial sensor-based system to objectively evaluate flexion tests in the horse.Equine Vet J Suppl *43* 2012; 44: 8-11.

22. Keegan KG, MacAllister CG, Wilson DA, et al. Comparison of an inertial sensor system with a stationary force plate for evaluation of horses with bilateral forelimb lameness. Am J Vet Res 2012; 73: 368-374.

23. Rouhani H, Favre J, Crevoisier X, et al. Measurement of multi-segment foot joint angles during gait using a wearable system. J Biomech Eng 2012; 134: 061006.

24. Chateau H, Degueurce C, Jerbi H, et al. Normal three-dimensional behavior of the metacarpophalangeal joint and the effect of uneven foot bearing. Equine Vet J Suppl 33 2001; 33: 84-88.

25. American Association of Equine Practitioners. Guide for veterinary service and judging of equestrian events. 4th ed. Lexington, Ky: American Association of Equine Practitioners, 1991;19.

26. Chateau H, Degueurce C, Denoix J-M. Evaluation of three-dimensional kinematics of the distal portion of the forelimb in horses walking in a straight line. Am J Vet Res 2004; 65: 447-455.

27. Degueurce C, Chateau H, Jerbi H, et al. Three-dimensional kinematics of the proximal interphalangeal joint: effects of raising the heels or the toe. Equine Vet J Suppl 33 2001; 33: 79-83.

28. Peham C, Licka T, Girtler D, et al. The influence of lameness on equine stride length consistency. The Vet J 2001; 162: 153-157.

29. Clayton HM, White AD, Kaiser LJ, et al. Short-term habituation of equine limb kinematics to tactile stimulation of the coronet. Vet Comp Orthop Traumatol 2008; 21: 211-214.

30. Mazza C, Donati M, McCamley J, et al. An optimized Kalman filter for the estimate of trunk orientation from inertial sensors data during treadmill walking. Gait Posture 2012; 35: 138-142.

Summary and Conclusions

In summary, this group of studies successfully utilized two different IMU systems mounted to the hoof of the horse to collect meaningful data at the walk and the trot. In the first study, we found that the equine IMU could produce accurate linear and angular data in the sagittal plane compared to the 3-D optical capture system on a front and hind hoof in clinically normal horses. The linear and angular data in frontal and transverse planes had the same general appearance to the optical system, but the values were significantly different. Clinically it is not crucial for the IMU and 3-D optical to produce identical data, as long as the two systems are not used to collect kinematics interchangeably.

The outcome of this first study was very promising, leading to further investigation of a hoof mounted IMU. This particular IMU, which was developed for equine applications, had several positive attributes, as it could handle high accelerations (up to ± 125 g), was light-weight (80 grams), and was wireless. However, there were some negative attributes of this sensor system, including its inability to capture hoof contact data and that the programming set all variables to zero during stance. As we believe that hoof contact is a critical phase of the stride, it was important to find an appropriate system to capture this hoof event. This led to the investigation of a different IMU for the second set of experiments. This IMU could handle high accelerations (± 200 g), was very light-weight (55 grams), but required a wired connection to a data logging device (handheld computer). Following data collection, this IMU did not produce realistic linear accelerations at the walk and trot; the accelerations appeared too low compared to previously collected data at the walk and trot. Angular orientations in the sagittal plane (Θ) appeared realistic in magnitude, but the ranges of Φ and Ψ appeared larger than expected.

The second IMU showed significant changes in angular orientation in all three rotations during both stance and swing phases and during specific hoof events at both the walk and trot following the induction of lameness. In addition, the variability in sagittal plane rotation (Θ) increased from baseline and lameness following peri-neural anesthesia. It needs to be noted that there were only six horses in the second set of experiments, and IMU data could not be collected from all horses for all lameness conditions. While these data appear promising, there still needs to be more work performed in a larger number of horses before these findings can be extrapolated to the larger equine population, especially considering the larger ranges in Φ and Ψ rotations. Additionally, as an experimental weight-bearing lameness was induced in this group of horses, it is unknown if other sources of lameness may result in slightly different hoof kinematics. Examining a large number of horses with clinical lameness would be warranted to ensure that the parameters identified in this study can be extrapolated to the population. However, before any of this is evaluated, the IMU requires more testing to determine the error in the three planes of motion, as well as improving the processing to address any offsets and drift originating from the gyroscopes.

While a hoof-mounted IMU has been shown to have attributes for use in lameness diagnosis, a hoof-mounted IMU may also hold other applications. These may include the examination of corrective farriery, examining the influence of surface on hoof kinematics, as well as looking at the influence of other movements, such as turning, backing, or going up or down an incline. With this knowledge, we may be able to better dictate treatments for specific horses if we know movements that might be detrimental to their recovery from injury.

Since the IMU does not require the constraints of a gait analysis laboratory, it should be investigated for its use in a clinical setting. This also requires the investigation of other hoof attachment methods, which could be easily and quickly be attached to a clinical case. In addition, the development of software to quickly and easily process the IMU kinematic data is crucial to its continued development as a motion analysis system. This would move the IMU from a pure research instrument to a potential clinical tool.

Thus, the IMU appears to have utility in detecting hoof kinematics in both clinically normal horses, as well as in multiple grades of experimental lameness. It requires further research and development before it can be utilized clinically. At this time, it is unknown which IMU system might be best suited to examine the kinematics of the hoof.

Appendix I

Definitions of Linear and Angular Variables

Table I.1 – Linear kinematic variables used for comparison of IMU and 3-D optical capture systems for analysis of horses during walking and trotting

Variable	**Maximum**	**Minimum**
X direction position	Displacement of the hoof cranially (ie, swing length)	Most caudal position relative to start of the swing phase
X direction velocity	Peak cranial velocity of the hoof	Lowest cranial velocity of the hoof (caudal velocity if negative)
X direction acceleration	Peak cranial acceleration of the hoof	Lowest acceleration of the hoof in the cranial direction (caudal direction if negative)
Y direction position	Peak displacement of the hoof medially relative to the start of the swing phase	Most lateral displacement of the hoof relative to the start of the swing phase
Y direction velocity	Peak velocity of the hoof medially	Lowest velocity of the hoof medially (laterally if negative)
Y direction acceleration	Peak acceleration of the hoof medially	Lowest acceleration of the hoof medially (laterally if negative)
Z direction position	Maximum 1: First proximally vertical peak displacement of the hoof relative to start of the swing phase Maximum 2: Second proximally vertical peak displacement of the hoof relative to start of the swing phase	Lowest displacement of the hoof vertically relative to start of the swing phase (below start of the swing phase if negative)
Z direction velocity	Peak proximally vertical velocity of the hoof	Lowest proximally vertical velocity of the hoof (distally if negative)
Z direction acceleration	Peak proximally vertical acceleration of the hoof	Lowest proximally vertical acceleration of the hoof (distally if negative)

Table I.2 – Angular kinematic variables used for comparison of IMU and 3-D optical capture systems for analysis of horses during walking and trotting

Variable	**Maximum**	**Minimum**
Θ Orientation	Peak counter-clockwise angle of the hoof about the y-axis (ie, toe down)	Lowest counter-clockwise angle of the hoof about the y-axis (toe up if negative)
Θ Angular velocity	Peak counter-clockwise velocity of the hoof about the y-axis (ie, toe down)	Lowest counter-clockwise velocity of the hoof about the y-axis (toe up if negative)
Θ Angular acceleration	Peak counter-clockwise acceleration of the hoof about the y-axis (ie, toe down)	Lowest counter-clockwise acceleration of the hoof about the y-axis (toe up if negative)
Φ Orientation	Peak counter-clockwise angle of the hoof about the x'-axis (ie, medial edge elevated relative to lateral edge of hoof)	Lowest counter-clockwise angle of the hoof about the x'-axis (lateral edge elevated relative to medial edge of hoof if negative)
Φ Angular velocity	Peak counter-clockwise velocity of the hoof about the x'-axis (ie, medial edge elevated)	Lowest counter-clockwise velocity of the hoof about the x'-axis (lateral edge elevated if negative)
Φ Angular acceleration	Peak counter-clockwise acceleration of the hoof about the x'-axis (ie, medial edge elevated)	Lowest counter-clockwise acceleration of the hoof about the x'-axis (lateral edge elevated if negative)
Ψ Orientation	Peak counter-clockwise angle of the hoof about the z"-axis (ie, toe in)	Lowest counter-clockwise angle of the hoof about the z"-axis (toe out if negative)
Ψ Angular velocity	Peak counter-clockwise velocity of the hoof about the z"-axis (ie, toe in)	Lowest counter-clockwise velocity of the hoof about the z"-axis (toe out if negative)
Ψ Angular acceleration	Peak counter-clockwise acceleration of the hoof about the z"-axis (ie, toe in)	Lowest counter-clockwise acceleration of the hoof about the z"-axis (toe out if negative)

Appendix II

Acceleration vs. Time Curves

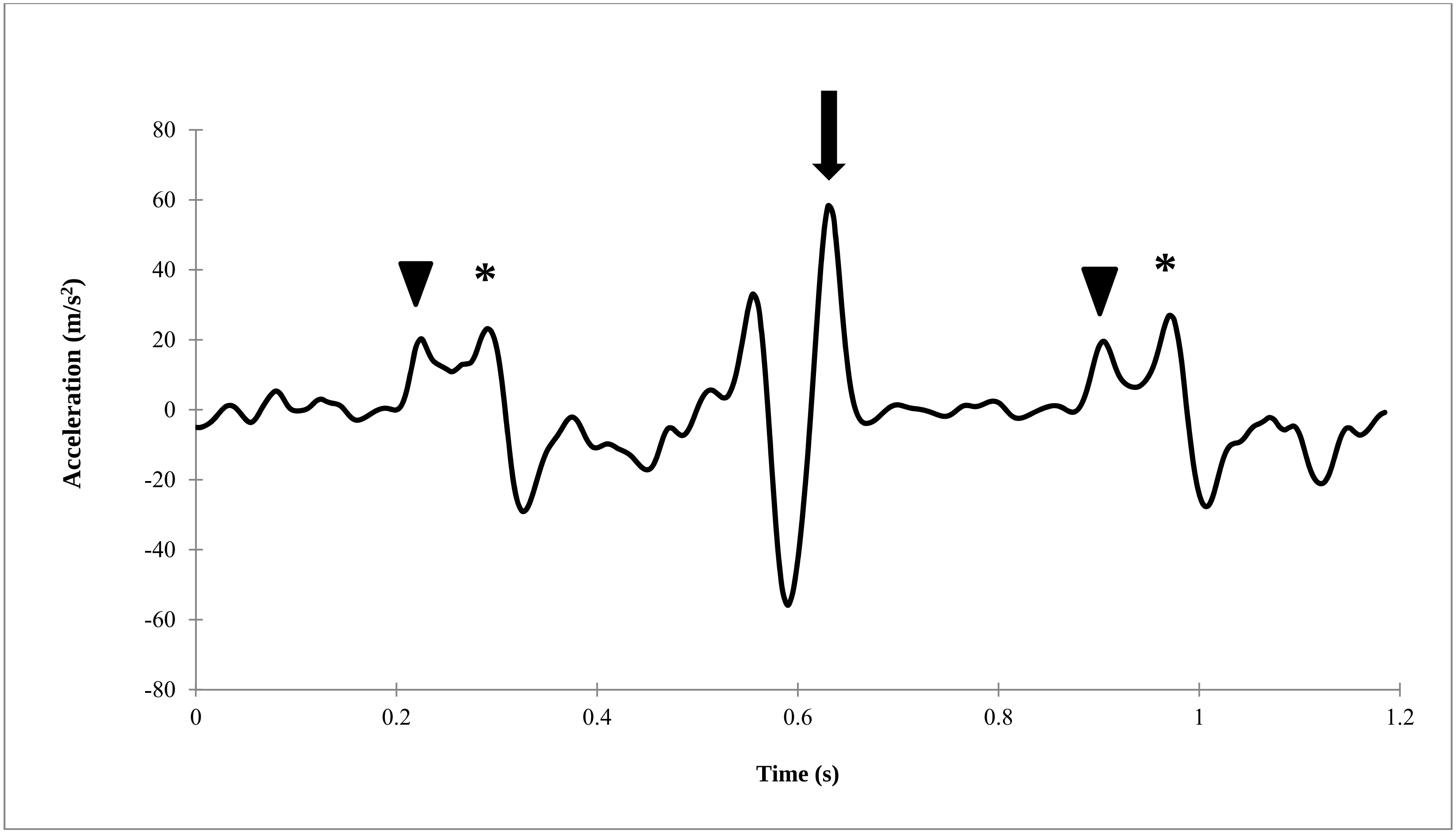

Figure II.1 - Vertical acceleration vs. time curve from the optical capture system used to determine hoof events in order to segment the stride into sections. Heel-off is marked by a black arrowhead. Toe-off is marked by a star (*). Hoof-contact is marked with a black arrow.

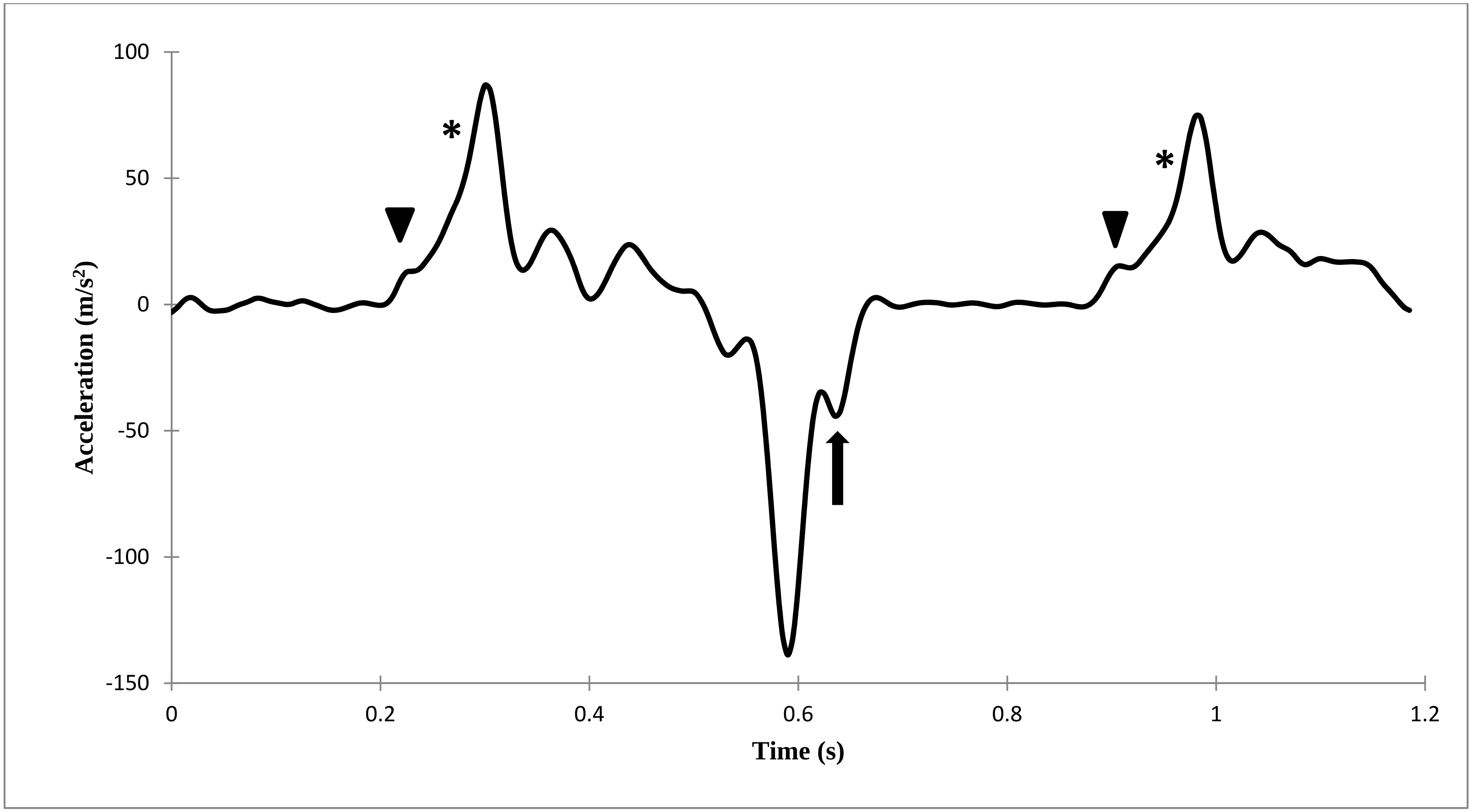

Figure II.2 - Cranial-caudal acceleration vs. time curve from the IMU used to determine hoof events in order to segment the stride into sections. Heel-off is marked by a black arrowhead. Toe-off is marked by a star (*). Hoof-contact is marked with a black arrow.

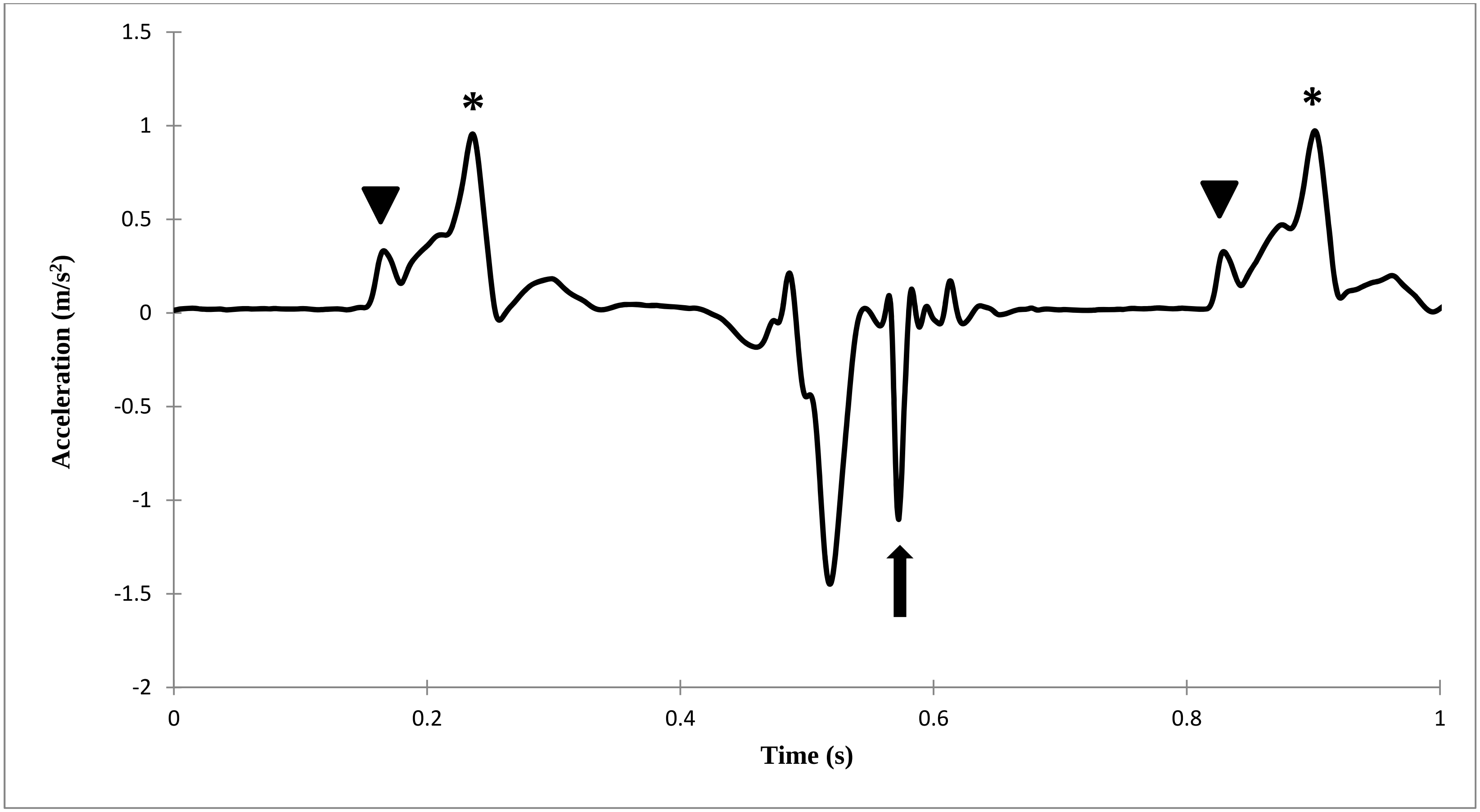

Figure II.3: Vertical acceleration vs. time curve from the IMU used to determine hoof events in order to segment the stride into sections. Heel-off is marked by a black arrowhead. Toe-off is marked by a star (*). Hoof-contact is marked with a black arrow.

Appendix III

Optical Kinematics of the Fore Hoof at the Trot

Table III.1 - Cranial-caudal (X) movement of the fore hoof during break-over at the trot. * indicates a significant inter-limb difference at a specific lameness grade (P < 0.05). † indicates a significant intra-limb difference between that lameness grade and baseline (P < 0.05).

Break-over			Baseline		Grade 1		Grade 2		Grade 3		After Block	
			mean	st dev	mean	st dev	mean	st dev	mean	st dev	mean	st dev
X position (m)	Min	L	-0.05*	0.01	-0.05*	0.01	-0.04†	0.01	-0.04*	0.01	-0.04†	0.01
		NL	-0.04*	0.01	-0.04*†	0.01	-0.04	0.01	-0.04*	0.01	-0.04	0.01
	Avg	L	-0.03*	0.01	-0.03*	0.01	-0.03†	0.00	-0.03*	0.00	-0.03†	0.01
		NL	-0.03*	0.01	-0.03*†	0.01	-0.03	0.01	-0.03*	0.00	-0.03	0.01
X velocity (m/s)	Max	L	1.71*	0.20	1.76*	0.19	1.69*	0.22	1.70*	0.20	1.66*	0.20
		NL	1.53*	0.25	1.59*†	0.19	1.57*†	0.22	1.52*†	0.19	1.50*	0.17
	Min	L	0.25	0.07	0.26	0.07	0.26	0.07	0.26	0.07	0.26	0.04
		NL	0.25	0.06	0.26	0.06	0.27†	0.07	0.26	0.07	0.24	0.08
	Avg	L	0.87*	0.14	0.89*	0.12	0.86	0.13	0.85*†	0.13	0.84*	0.11
		NL	0.81*	0.10	0.83*†	0.09	0.83†	0.13	0.82*	0.11	0.79*	0.09
X acceleration (m/s^2)	Max	L	45.8	12.71	48.73*†	12.91	49.11*†	16.06	51.77*	13.99	48.78*	11.33
		NL	44.5	14.26	47.84*	15.09	44.80*	13.59	42.91*	11.63	44.39*	13.45
	Min	L	16.2*	5.51	16.39*	4.99	16.43*	5.24	16.07†	5.33	15.02*	3.78
		NL	13.5*	5.04	14.75*	4.66	14.97*†	5.22	15.71	5.24	11.43*†	7.97
	Avg	L	27.7*	6.51	28.82*	6.02	28.41*†	7.47	28.60*†	6.19	27.55*	4.42
		NL	24.8*	6.65	26.20*	6.55	25.26*†	6.55	25.14*†	5.38	23.47*†	4.44

Table III.2 - Vertical (Z) movement of the fore hoof during break-over at the trot. *See Table III.1 for remainder of key.*

Break-over			Baseline		Grade 1		Grade 2		Grade 3		After Block	
			mean	st dev	mean	st dev	mean	st dev	mean	st dev	mean	st dev
Z position (m)	Min	L	-0.03*	0.00	-0.04*	0.00	-0.04*	0.00	-0.04*†	0.00	-0.04*	0.00
		NL	-0.03*	0.01	-0.03*	0.01	-0.03*	0.01	-0.03*	0.01	-0.03*	0.01
	Avg	L	-0.02*	0.00	-0.02*	0.00	-0.02*	0.00	-0.02*†	0.00	-0.02*	0.00
		NL	-0.02*	0.01	-0.02*	0.01	-0.02*	0.00	-0.02*	0.00	-0.02*	0.01
Z velocity (m/s)	Max	L	0.87*	0.21	0.90*	0.21	0.93†	0.24	0.99*	0.17	0.98*	0.19
		NL	0.85*	0.25	0.88*	0.28	0.88†	0.24	0.86*	0.25	0.82*	0.22
	Min	L	0.32*	0.08	0.33*	0.07	0.34*	0.08	0.33*	0.09	0.34*	0.06
		NL	0.24*	0.12	0.24*	0.12	0.27*†	0.11	0.25*	0.08	0.17*†	0.13
	Avg	L	0.64*	0.13	0.65*	0.11	0.67*	0.13	0.70*	0.11	0.69*	0.08
		NL	0.55*	0.19	0.55*	0.20	0.57*†	0.17	0.56*	0.16	0.49*†	0.14
Z acceleration (m/s^2)	Max	L	21.54*	5.02	21.33*	4.80	21.87*	5.83	22.91*	4.25	23.95	8.91
		NL	24.25*	5.76	24.90*	5.71	23.49*	5.15	24.67*	6.81	26.61	9.91
	Min	L	2.89	6.50	3.08	6.48	4.57	6.51	6.09	5.61	4.12*	8.53
		NL	2.17	10.84	4.87	10.18	3.73	11.03	4.77	7.37	0.43*	12.00
	Avg	L	11.10*	4.64	11.40	4.84	12.23†	5.57	13.38	3.96	13.07*	5.18
		NL	12.02*	4.85	13.26†	5.71	12.28	4.75	12.83	5.19	11.66*	4.50

Table III.3 - Cranial-caudal (X) movement of the fore hoof during the initial 25% of swing at the trot. *See Table III.1 for remainder of key.*

Initial Swing			Baseline		Grade 1		Grade 2		Grade 3		After Block	
			mean	st dev	mean	st dev	mean	st dev	mean	st dev	mean	st dev
X position (m)	Max	L	0.38	0.05	0.38	0.04	0.38	0.06	0.39*	0.05	0.38*	0.04
		NL	0.38	0.06	0.39	0.05	0.38	0.06	0.37*†	0.04	0.37*†	0.04
	Avg	L	0.16*	0.02	0.17	0.02	0.17	0.03	0.17*	0.02	0.16*	0.02
		NL	0.16*	0.03	0.17	0.02	0.16	0.03	0.16*†	0.02	0.16*†	0.02
X velocity (m/s)	Max	L	5.17	0.41	5.27*	0.45	5.20	0.51	5.27	0.38	5.17	0.41
		NL	5.20	0.44	5.37*†	0.51	5.26	0.47	5.24	0.36	5.17	0.40
	Min	L	1.73*	0.22	1.79*	0.18	1.72*	0.22	1.76*	0.29	1.70*	0.20
		NL	1.56*	0.26	1.64*†	0.25	1.57*	0.22	1.54*†	0.18	1.52*	0.16
	Avg	L	3.87	0.38	3.95	0.37	3.90	0.50	3.98	0.39	3.87*	0.34
		NL	3.87	0.45	4.00	0.44	3.90	0.45	3.88	0.35	3.78*	0.33
X acceleration (m/s^2)	Max	L	70.29*	15.25	71.65*	15.80	72.52*	18.54	76.04	16.33	72.62	12.78
		NL	77.87*	13.58	79.82*	14.32	77.02*	13.35	78.78	14.85	74.05†	13.32
	Min	L	13.56*	4.29	13.83*	5.47	12.58	7.56	13.68	4.48	13.77	3.84
		NL	8.17*	8.92	10.38*	6.35	13.04†	5.61	11.70†	5.67	10.97†	8.22
	Avg	L	35.21*	4.82	36.21*	4.59	35.81*	4.40	36.25*	3.75	35.87*	4.75
		NL	37.30*	4.07	38.50*	5.57	37.94*	3.78	38.16*	3.44	37.37*	4.47

Table III.4 - Vertical (Z) movement of the fore hoof during the initial 25% of swing at the trot. *See Table III.1 for remainder of key.*

Initial Swing			Baseline		Grade 1		Grade 2		Grade 3		After Block	
			mean	st dev	mean	st dev	mean	st dev	mean	st dev	mean	st dev
Z position (m)	Max	L	0.08*	0.02	0.08	0.02	0.08	0.021	0.08	0.02	0.08*	0.02
		NL	0.07*	0.02	0.08	0.02	0.08†	0.017	0.08	0.02	0.07*	0.01
	Avg	L	0.05*	0.01	0.05	0.01	0.05	0.011	0.05	0.01	0.05*	0.01
		NL	0.04*	0.01	0.04	0.01	0.05†	0.009	0.05	0.01	0.04*	0.01
Z velocity (m/s)	Max	L	1.27	0.25	1.27	0.19	1.29	0.30	1.35	0.22	1.35*	0.20
		NL	1.22	0.24	1.29	0.24	1.30†	0.24	1.33	0.33	1.19*	0.23
	Min	L	0.46	0.22	0.41	0.24	0.40	0.28	0.41	0.24	0.38	0.23
		NL	0.39	0.23	0.38	0.25	0.42	0.23	0.41	0.29	0.29	0.25
	Avg	L	0.84*	0.21	0.80	0.20	0.81	0.22	0.86	0.20	0.85*	0.21
		NL	0.77*	0.17	0.81	0.16	0.82†	0.17	0.82	0.23	0.70*	0.15
Z acceleration (m/s^2)	Max	L	22.82	10.87	22.65*	6.69	24.60	17.31	22.77*	6.65	24.95	6.17
		NL	25.16	5.46	27.19*	6.58	26.47	4.85	29.09*	7.17	28.19	9.80
	Min	L	-28.72*	12.30	-30.83*	9.74	-30.96*	12.47	-33.92*	12.53	-35.55	9.14
		NL	-34.39*	14.29	-35.53*	15.80	-35.49*	14.43	-37.41*	16.89	-35.81	13.98
	Avg	L	-2.75*	2.22	-3.39*	2.55	-2.90*	2.87	-3.30*	2.55	-2.86*	2.58
		NL	-1.50*	2.79	-2.13*	2.41	-1.64*	2.81	-1.50*†	3.00	-1.67*†	2.48

Table III.5 - Cranial-caudal (X) movement of the fore hoof during the terminal 25% of swing at the trot. *See Table III.1 for remainder of key.*

Terminal Swing			Baseline		Grade 1		Grade 2		Grade 3		After Block	
			mean	st dev	mean	st dev	mean	st dev	mean	st dev	mean	st dev
X position (m)	Max	L	1.92	0.15	1.95	0.14	1.97	0.18	1.97	0.18	1.93	0.13
		NL	1.93	0.15	1.98	0.18	1.93	0.15	1.91	0.14	1.89	0.09
	Min	L	1.59	0.14	1.61	0.11	1.63*†	0.16	1.62	0.16	1.59	0.12
		NL	1.61	0.16	1.64†	0.16	1.58*	0.13	1.57	0.12	1.56	0.10
	Avg	L	1.81	0.14	1.83	0.12	1.85	0.17	1.84	0.17	1.81	0.12
		NL	1.82	0.15	1.86†	0.17	1.81	0.14	1.79	0.12	1.78	0.09
X velocity (m/s)	Max	L	6.44	0.45	6.57*	0.54	6.55*	0.31	6.51*	0.30	6.41	0.38
		NL	6.54	0.46	6.80*†	0.63	6.78*†	0.35	6.63*†	0.28	6.55	0.57
	Min	L	0.68	0.35	0.80†	0.40	0.76†	0.41	0.79†	0.45	0.78†	0.40
		NL	0.68	0.34	0.83†	0.39	0.79†	0.40	0.82†	0.47	0.79†	0.36
	Avg	L	3.42	0.44	3.57	0.43	3.57*†	0.37	3.56†	0.39	3.50*†	0.41
		NL	3.56	0.47	3.70	0.47	3.73*†	0.34	3.62	0.34	3.72*†	0.36
X acceleration (m/s^2)	Max	L	-8.40	12.55	-7.98	14.01	-5.45	15.69	-8.83	16.33	-6.52	18.80
		NL	-7.06	14.78	-6.07	15.42	-4.17	15.03	-8.00	10.01	-4.26	15.20
	Min	L	-112.15	19.93	-111.77*	18.59	-111.20*	18.74	-108.43*†	21.06	-107.88*†	18.83
		NL	-115.65	21.33	-117.05*	21.28	-117.81*	18.52	-115.52*	17.55	-120.98*	21.79
	Avg	L	-57.77	7.10	-58.79*	8.12	-58.24*	6.29	-57.66*	6.37	-56.62	6.93
		NL	-59.32	7.49	-60.59*	9.27	-61.04*	7.35	-59.28*	6.51	-58.01	7.34

Table III.6 - Vertical (Z) movement of the fore hoof during the terminal 25% of swing at the trot. *See Table III.1 for remainder of key.*

Terminal Swing			Baseline		Grade 1		Grade 2		Grade 3		After Block	
			mean	st dev	mean	st dev	mean	st dev	mean	st dev	mean	st dev
Z position (m)	Max	L	0.05	0.01	0.05	0.01	0.05*	0.01	0.05	0.01	0.05*	0.01
		NL	0.05	0.01	0.05	0.01	0.05*†	0.01	0.05	0.01	0.04*†	0.01
	Avg	L	0.03	0.01	0.03	0.01	0.03*	0.01	0.03	0.00	0.03*†	0.01
		NL	0.03	0.00	0.03	0.01	0.03*†	0.00	0.03	0.01	0.03*†	0.01
Z velocity (m/s)	Max	L	0.36	0.42	0.35*	0.33	0.39	0.38	0.32*	0.33	0.48*	0.35
		NL	0.41	0.34	0.45*	0.35	0.48	0.34	0.46*	0.34	0.54*	0.27
	Min	L	-1.11*	0.29	-1.06*	0.26	-1.07*	0.26	-1.08*†	0.21	-1.11	0.23
		NL	-1.20*	0.22	-1.20*	0.26	-1.17*	0.26	-1.24*	0.26	-1.13†	0.22
	Avg	L	-0.49	0.25	-0.45	0.17	-0.44	0.18	-0.47†	0.17	-0.42*†	0.14
		NL	-0.44	0.13	-0.42	0.13	-0.41	0.14	-0.42	0.14	-0.33*†	0.12
Z acceleration (m/s^2)	Max	L	53.19	11.56	50.10*	12.56	53.39	17.93	49.47	10.45	54.92	14.23
		NL	53.46	13.01	54.35*	15.32	54.86	14.48	53.68	12.09	52.34	11.31
	Min	L	-57.88	22.19	-57.59	21.61	-57.56*	20.66	-56.25*	18.65	-65.73	25.57
		NL	-62.06	22.32	-60.26	26.24	-66.65*†	24.99	-62.17*	18.73	-63.67	22.85
	Avg	L	-0.54	5.40	0.45	4.23	0.32	4.14	0.74	4.04	0.45	3.63
		NL	-0.12	4.21	0.56	3.90	0.44	3.66	-0.72	4.84	-0.30	3.03

Table III.7 - Cranial-caudal (X) movement of the fore hoof during total swing at the trot.*See Table III.1 for remainder of key.*

Swing			Baseline		Grade 1		Grade 2		Grade 3		After Block	
			mean	st dev	mean	st dev	mean	st dev	mean	st dev	mean	st dev
X position (m)	Max	L	1.91	0.14	1.94	0.14	1.97	0.18	1.95	0.19	1.93*	0.13
		NL	1.91	0.16	1.96	0.17	1.93	0.14	1.90	0.14	1.90*	0.12
	Avg	L	0.97	0.08	0.98	0.07	1.00*†	0.10	0.99	0.10	0.97	0.07
		NL	0.97	0.10	1.00	0.09	0.97*	0.08	0.96	0.08	0.96	0.07
X velocity (m/s)	Max	L	6.90*	0.44	6.99*	0.48	7.02*†	0.40	6.88*	0.35	6.90*	0.39
		NL	7.07*	0.34	7.33*†	0.51	7.17*†	0.34	7.12*	0.37	7.00*	0.39
	Min	L	0.63	0.31	0.71	0.35	0.74	0.43	0.79	0.46	0.82*	0.41
		NL	0.67	0.38	0.71	0.38	0.69	0.32	0.70	0.42	0.61*	0.27
	Avg	L	4.91	0.33	5.00*	0.34	5.00	0.34	5.00	0.33	4.96*	0.27
		NL	4.98	0.26	5.16*†	0.41	5.05†	0.27	5.05	0.32	4.87*	0.30
X acceleration (m/s^2)	Max	L	69.50*	15.71	69.65*	15.58	79.16†	26.25	76.33	16.14	73.93	13.24
		NL	78.40*	13.61	81.03*	14.45	75.21	11.39	74.35	14.06	74.12†	14.35
	Min	L	-115.70	20.55	-115.50	19.53	-111.40	19.08	-107.81†	19.79	-109.72†	18.32
		NL	-117.89	26.11	-119.07	24.06	-120.39	21.08	-119.57	18.87	-112.72	23.31
	Avg	L	-2.70	0.68	-2.63	1.22	-2.26	1.26	-2.47	1.38	-2.27	1.18
		NL	-2.25	0.92	-2.40	0.97	-2.26	0.80	-2.75	1.90	-2.30	0.86

Table III.8: Vertical (Z) movement of the fore hoof during total swing at the trot. *See Table III.1 for remainder of key.*

Swing			Baseline		Grade 1		Grade 2		Grade 3		After Block	
			mean	st dev	mean	st dev	mean	st dev	mean	st dev	mean	st dev
Z position (m)	Max	L	0.11	0.02	0.11	0.02	0.11	0.02	0.11*	0.02	0.11*	0.02
		NL	0.11	0.02	0.10	0.01	0.10	0.02	0.10*	0.02	0.09*†	0.02
	Avg	L	0.06*	0.01	0.06	0.01	0.06*	0.01	0.06*	0.01	0.06*	0.01
		NL	0.06*	0.01	0.06	0.01	0.05*	0.01	0.06*	0.01	0.05*†	0.01
Z velocity (m/s)	Max	L	1.30	0.26	1.33	0.18	1.34†	0.28	1.40	0.20	1.40*	0.18
		NL	1.31	0.24	1.37†	0.18	1.32	0.14	1.32	0.24	1.25*	0.20
	Min	L	-1.10*	0.26	-1.10*	0.27	-1.08*	0.29	-1.11*	0.22	-1.15	0.28
		NL	-1.21*	0.27	-1.22*	0.31	-1.29*	0.32	-1.33*	0.29	-1.10†	0.27
	Avg	L	0.00*	0.00	0.00*	0.00	0.00*	0.00	0.00*	0.00	0.00*†	0.00
		NL	0.00*	0.00	0.00*	0.00	0.00*	0.00	0.00*	0.00	0.00*	0.00
Z acceleration (m/s^2)	Max	L	57.83	10.39	52.24*	12.08	59.70	24.14	52.27	18.43	57.15	18.39
		NL	54.50	13.20	57.09*	16.81	60.33	13.55	57.78	13.45	52.88	17.56
	Min	L	-64.87	20.02	-64.34	22.43	-62.27*	19.10	-59.88*†	17.75	-72.14	28.07
		NL	-68.43	19.21	-68.60	27.22	-76.09*†	26.39	-70.49*†	16.10	-64.82	15.51
	Avg	L	-3.20	0.54	-3.18	0.57	-3.04	0.79	-3.32	0.61	-3.20*	0.58
		NL	-3.13	0.72	-3.16	0.76	-3.23	0.82	-3.25	0.59	-2.86*	0.81

Table III.9 - Sagittal plane orientation of the fore hoof at the trot. *See Table III.1 for remainder of key.*

			Baseline		Grade 1		Grade 2		Grade 3		After Block	
			mean	st dev	mean	st dev	mean	st dev	mean	st dev	mean	st dev
Break-over Orientation (°)	Max	L	-3.6	1.5	-3.5	1.6	-4.0	1.1	-3.5*	1.1	-4.1†	1.0
		NL	-3.9	1.5	-3.9	1.4	-3.9	1.0	-4.2*	1.2	-4.3	1.5
	Min	L	-45.7	6.0	-44.8*	5.2	-44.0*	3.7	-43.3*	3.8	-43.6*	5.5
		NL	-47.0	7.6	-48.6*†	6.9	-47.9*	5.8	-47.1*	5.0	-49.3*	5.4
	Avg	L	-20.3*	2.6	-19.8*	2.3	-20.0	1.9	-19.3*	1.8	-20.1*	2.2
		NL	-21.3*	3.7	-21.7*	3.2	-21.5	2.8	-21.4*	2.5	-22.7*	3.8
Initial Swing Orientation (°)	Max	L	-45.0	6.4	-44.8*	5.3	-44.2*	3.8	-44.3*	5.9	-43.8*	4.5
		NL	-47.2	7.3	-49.2*	6.9	-46.8*	5.8	-47.2*	4.8	-48.6*	5.4
	Min	L	-108.6	5.7	-110.0*	4.5	-110.0	5.1	-109.9*	5.2	-110.0*	4.1
		NL	-109.4	4.9	-111.2*†	4.8	-110.6†	5.9	-111.4*	3.8	-112.1*†	5.2
	Avg	L	-92.6	5.2	-93.4*	3.5	-93.1*	3.9	-93.3*	4.7	-93.1*	3.5
		NL	-93.8	4.9	-95.7*†	4.3	-94.5*	4.6	-95.2*	3.4	-95.8*	3.9
Terminal Swing Orientation (°)	Max	L	-0.3*	2.9	-0.1*	3.2	-0.3*	3.3	0.6	2.4	0.5	3.4
		NL	1.1*	3.6	2.5*†	3.4	1.7*	4.1	2.0†	5.1	-0.3	2.5
	Min	L	-39.4	8.9	-39.7	9.3	-40.0	9.9	-39.4	7.9	-38.7*	8.4
		NL	-40.6	7.0	-39.9	6.6	-40.8	6.5	-39.0	5.7	-44.1*	6.6
	Avg	L	-13.9	3.7	-13.7	4.7	-14.1	4.5	-13.4	3.6	-13.2*	3.9
		NL	-14.0	3.7	-12.6	4.5	-13.5	4.3	-13.9	6.7	-16.4*	3.8
Total Swing Orientation (°)	Max	L	-0.3	2.9	-1.2*	2.7	-0.1	3.4	0.2	2.5	0.8*	3.1
		NL	0.2	4.6	1.8*	3.3	0.2	3.7	0.4	8.4	-1.3*	3.2
	Min	L	-113.5	6.3	-113.4	5.2	-114.6	5.6	-114.4	5.5	-113.4	4.9
		NL	-113.9	6.5	-115.1	6.3	-114.2	5.7	-114.2	11.1	-114.7	11.3
	Avg	L	-72.6	3.7	-73.6	4.0	-73.8	3.1	-74.5†	3.6	-73.4*†	3.9
		NL	-73.3	2.6	-73.7	3.4	-74.2	3.0	-73.1	4.2	-75.2*†	3.8

Table III.10 - Hoof-contact at the trot. *See Table III.1 for remainder of key.*

Hoof Contact		Baseline		Grade 1		Grade 2		Grade 3		After Block	
		mean	st dev	mean	st dev	mean	st dev	mean	st dev	mean	st dev
X position (m)	L	-0.05*	0.01	-0.06	0.01	-0.05	0.01	-0.05	0.01	-0.05	0.01
	NL	-0.05*	0.01	-0.06†	0.01	-0.05†	0.01	-0.05	0.01	-0.05	0.01
Z position (m)	L	-0.04*	0.01	-0.04*	0.01	-0.04*	0.00	-0.04*†	0.01	-0.04*†	0.00
	NL	-0.03*	0.01	-0.03*	0.01	-0.03*	0.01	-0.03*	0.01	-0.03*†	0.01
X velocity (m/s)	L	0.61	0.35	0.74†	0.40	0.75†	0.40	0.79*†	0.45	0.80†	0.41
	NL	0.68	0.35	0.78†	0.38	0.74†	0.37	0.77*†	0.41	0.72†	0.38
Z velocity (m/s)	L	-0.46	0.18	-0.45	0.17	-0.43*	0.14	-0.40*†	-0.38	0.14*†	0.14
	NL	-0.48	0.18	-0.45	0.15	-0.49*	0.24	-0.49*	0.17	-0.46*	0.17
X acceleration (m/s^2)	L	-40.35	10.07	-45.11*†	15.10	-45.81*†	12.10	-46.68†	9.76	-42.93*†	10.97
	NL	-38.21	10.22	-41.07*	13.91	-41.83*†	12.23	-38.57	13.39	-38.87*†	11.86
Z acceleration (m/s^2)	L	43.75*	11.82	42.14*	10.85	41.91*	10.67	42.43*	8.62	44.45	13.14
	NL	47.84*	14.40	47.12*	13.98	47.43*	15.08	51.48*	12.35	45.94	13.13
Orientation (^{o})	L	-1.4	2.3	-1.3*	2.6	-1.2*	2.7	-0.4*	2.4	-0.5	2.60
	NL	-0.8	2.9	0.2*†	2.2	0.1*†	2.6	0.2*†	2.7	-0.9	2.32

Table III.11: Stride durations of the fore hoof at the trot. *See Table III.1 for remainder of key.*

Durations		Baseline		Grade 1		Grade 2		Grade 3		After Block	
		mean	st dev	mean	st dev	mean	st dev	mean	st dev	mean	st dev
Stance (s)	L	0.32*	0.02	0.31*	0.03	0.31*†	0.02	0.32*	0.03	0.33*	0.03
	NL	0.32*	0.03	0.32*	0.03	0.32*†	0.02	0.32*	0.03	0.34*	0.03
Break-over (s)	L	0.06	0.01	0.05	0.01	0.05†	0.01	0.05	0.01	0.05†	0.01
	NL	0.05	0.01	0.05	0.01	0.05	0.01	0.05	0.01	0.05	0.01
Swing (s)	L	0.38	0.02	0.38*	0.02	0.39*	0.02	0.39	0.02	0.39	0.02
	NL	0.38	0.02	0.38*	0.02	0.38*	0.02	0.37	0.02	0.39	0.02
Initial Swing (s)	L	0.10	0.00	0.10†	0.00	0.10	0.01	0.10*	0.01	0.10	0.00
	NL	0.10	0.01	0.10	0.00	0.10	0.01	0.10*	0.00	0.10	0.00
Terminal Swing (s)	L	0.10	0.00	0.10†	0.00	0.10*	0.01	0.10*	0.01	0.10	0.00
	NL	0.10	0.01	0.10	0.00	0.10*	0.01	0.10*	0.00	0.10	0.00

Table III.12: Range of motion of the fore hoof at the trot. *See Table III.1 for remainder of key.*

Range of Motion		Baseline		Grade 1		Grade 2		Grade 3		After Blocking	
		mean	st dev	mean	st dev	mean	st dev	mean	st dev	mean	st dev
Break-over (^{o})	L	42.1	5.5	41.4*	5.1	40.1*†	3.5	39.8*†	3.78	39.6*†	5.4
	NL	43.1	7.4	44.7*†	6.8	44.0*	5.8	43.0*	4.9	44.8*	5.1
Initial Swing (^{o})	L	63.6	8.4	65.2*	8.0	65.7*†	7.3	65.6	7.5	66.1*†	6.2
	NL	62.3	7.8	62.0*	8.4	63.8*	8.4	64.3	5.8	63.5*	7.5
Terminal Swing (^{o})	L	39.2	9.5	39.6	9.0	39.8	9.3	39.9	7.8	39.1*	9.7
	NL	41.6	7.6	42.4	7.1	42.5	7.8	41.0	6.9	43.8*	6.2
Swing (^{o})	L	113.2	7.8	112.2*	6.0	114.5	8.1	114.4	7.3	114.1*	7.2
	NL	114.0	7.8	116.8*	7.4	113.8	6.1	114.5	11.6	109.1*	3.8

Appendix IV

Optical Kinematics of the Fore Hoof at the Walk

Table IV.1 - Cranial-caudal (X) movement of the fore hoof during break-over at the walk. * indicates a significant inter-limb difference at a specific lameness grade (P < 0.05). † indicates a significant intra-limb difference between the specific lameness grade and baseline (P < 0.05).

Break-over			Baseline		Grade 1		Grade 2		Grade 3		After Block	
			mean	st dev	mean	st dev	mean	st dev	mean	st dev	mean	st dev
X Position (m)	Min	L	-0.05	0.01	-0.05*	0.01	-0.05*	0.01	-0.04*	0.01	-0.04*	0.01
		NL	-0.04	0.01	-0.04*	0.01	-0.04*	0.01	-0.04*†	0.01	-0.04*†	0.01
	Avg	L	-0.03	0.01	-0.03*	0.01	-0.03*	0.01	-0.03*	0.01	-0.03*†	0.01
		NL	-0.03	0.01	-0.03*	0.01	-0.03*	0.01	-0.03*	0.01	-0.03*†	0.01
X Velocity (m/s)	Max	L	1.40*	0.18	1.40*	0.16	1.40*	0.17	1.35*	0.19	1.38*	0.18
		NL	1.26*	0.18	1.28*	0.17	1.28*	0.13	1.23*	0.14	1.21*†	0.15
	Min	L	0.14*	0.03	0.13*†	0.03	0.14*	0.03	0.13*	0.03	0.13*	0.03
		NL	0.11*	0.04	0.11*	0.05	0.11*	0.04	0.12*	0.04	0.11*	0.05
	Avg	L	0.52*	0.08	0.51*	0.06	0.51*	0.07	0.49	0.07	0.49*	0.07
		NL	0.47*	0.08	0.48*	0.08	0.47*	0.07	0.46	0.07	0.44*†	0.06
X Acceleration (m/s^2)	Max	L	39.16*	5.24	41.08*	6.26	42.56*†	7.09	41.63*	6.41	44.05*†	7.11
		NL	37.29*	8.41	37.89*	7.82	38.88*	7.45	38.06*	6.45	38.11*	6.89
	Min	L	2.72*	1.04	3.10	1.44	2.36	1.72	2.53	1.61	2.45	1.49
		NL	1.57*	3.20	2.41	3.35	2.05	2.68	2.33	1.58	1.67	2.89
	Avg	L	14.35*	2.69	14.22*	2.67	13.99*	2.69	13.63†	2.67	14.28*	2.10
		NL	12.54*	2.43	13.39*	2.72	13.15*	2.71	13.04	2.88	12.56*	2.00

Table IV.2 - Vertical (Z) movement of the fore hoof during break-over at the walk. *See Table IV.1 for the remainder of the key.*

Break-over			Baseline		Grade 1		Grade 2		Grade 3		After Block	
			mean	st dev	mean	st dev	mean	st dev	mean	st dev	mean	st dev
Z Position (m)	Min	L	-0.038*	0.006	-0.038*	0.006	-0.040*	0.006	-0.040*	0.007	-0.041*	0.004
		NL	-0.033*	0.008	-0.032*	0.009	-0.034*†	0.007	-0.033*	0.006	-0.033*	0.007
	Avg	L	-0.023*	0.004	-0.023*	0.004	-0.024*	0.004	-0.024*	0.006	-0.025*	0.003
		NL	-0.020*	0.005	-0.019*	0.005	-0.021*†	0.004	-0.020*	0.004	-0.020*	0.004
Z Velocity (m/s)	Max	L	0.697*	0.140	0.714*	0.173	0.729*	0.174	0.774*	0.102	0.801*†	0.101
		NL	0.625*	0.157	0.615*	0.168	0.659*	0.143	0.620*	0.145	0.645*	0.135
	Min	L	0.181*	0.033	0.170*	0.042	0.176*	0.042	0.191*	0.048	0.178*	0.081
		NL	0.127*	0.082	0.126*	0.091	0.141*	0.069	0.132*	0.088	0.141*	0.061
	Avg	L	0.418*	0.063	0.418*	0.075	0.426*	0.079	0.446*	0.048	0.456*†	0.041
		NL	0.350*	0.093	0.355*	0.098	0.371*†	0.075	0.356*	0.075	0.365*	0.060
Z Acceleration (m/s^2)	Max	L	10.530	4.587	11.555	5.585	11.028	4.689	11.322	2.769	12.428	3.395
		NL	12.124	5.244	11.563	5.355	11.631	5.916	12.363	7.240	12.268	5.386
	Min	L	-0.137	7.868	-0.134	5.375	-0.298	5.732	1.347	3.055	0.579	7.402
		NL	-2.195	9.612	0.203	4.734	0.501	5.011	0.681	3.668	-0.602	8.727
	Avg	L	5.576	1.996	5.845	2.805	5.687	2.542	6.359*	1.687	6.527*	2.444
		NL	4.977	2.006	5.451	2.357	5.478	2.199	5.461*	2.288	5.465*	1.686

Table IV.3 - Cranial-caudal (X) movement of the fore hoof during the initial 25% of swing at the walk. *See Table IV.1 for the remainder of the key.*

Initial Swing			Baseline		Grade 1		Grade 2		Grade 3		After Block	
			mean	st dev	mean	st dev	mean	st dev	mean	st dev	mean	st dev
X Position (m)	Max	L	0.341	0.022	0.349	0.020	0.351†	0.022	0.339	0.018	0.339	0.019
		NL	0.340	0.030	0.348	0.024	0.347	0.020	0.338	0.022	0.337	0.028
	Avg	L	0.149	0.010	0.153	0.009	0.154†	0.011	0.149	0.009	0.151	0.009
		NL	0.147	0.016	0.150	0.014	0.151	0.010	0.146	0.010	0.146	0.013
X Velocity (m/s)	Max	L	3.908	0.250	4.004	0.294	3.984	0.266	3.822	0.198	3.771	0.191
		NL	3.948	0.234	4.069	0.267	3.947	0.225	3.858	0.162	3.846	0.187
	Min	L	1.348*	0.165	1.376	0.159	1.378*	0.155	1.314*	0.199	1.370*	0.172
		NL	1.255*	0.185	1.299	0.232	1.292*	0.135	1.200*	0.105	1.225*	0.156
	Avg	L	3.078	0.166	3.162	0.210	3.150	0.196	3.029	0.188	3.033	0.159
		NL	3.077	0.228	3.146	0.173	3.101	0.163	3.012†	0.129	3.011	0.194
X Acceleration (m/s^2)	Max	L	52.815*	5.005	56.105	8.365	55.826	7.372	56.046	6.104	55.846	6.403
		NL	57.185*	9.437	57.666	8.324	55.526†	7.390	55.961	8.828	55.531	9.903
	Min	L	0.613	3.159	-0.227	3.928	-2.423†	8.084	-1.714	2.984	-1.485	2.519
		NL	-0.257	4.364	-1.015	5.641	-1.916	5.534	-0.619	4.346	-2.494	5.125
	Avg	L	23.136*	2.721	23.874	2.926	23.342	2.219	22.438*	2.001	21.687*	2.444
		NL	24.188*	2.323	24.840	4.228	23.517†	2.467	23.570*	1.975	23.067*	1.964

Table IV.4 - Vertical (Z) movement of the fore hoof during the initial 25% of swing at the walk. *See Table IV.1 for the remainder of the key.*

Initial Swing			Baseline		Grade 1		Grade 2		Grade 3		After Block	
			mean	st dev	mean	st dev	mean	st dev	mean	st dev	mean	st dev
Z Position (m)	Max	L	0.057	0.011	0.055	0.015	0.056	0.012	0.057	0.013	0.059	0.013
		NL	0.051	0.011	0.051	0.011	0.050	0.011	0.047	0.012	0.049	0.011
	Avg	L	0.032*	0.007	0.031*	0.008	0.031*	0.007	0.033*	0.010	0.033*	0.007
		NL	0.027*	0.007	0.027*	0.007	0.027*	0.007	0.025*	0.008	0.027*	0.006
Z Velocity (m/s)	Max	L	0.817	0.125	0.823	0.183	0.858*	0.175	0.879*	0.124	0.934*†	0.110
		NL	0.752	0.174	0.779	0.135	0.762*	0.119	0.764*	0.154	0.765*	0.137
	Min	L	0.203	0.217	0.180	0.197	0.173*	0.218	0.132	0.276	0.153	0.263
		NL	0.155	0.177	0.141	0.199	0.107*†	0.184	0.046†	0.185	0.082	0.182
	Avg	L	0.518	0.106	0.511	0.149	0.513*	0.108	0.504*	0.123	0.544*	0.121
		NL	0.466	0.100	0.472	0.099	0.458*	0.099	0.430*	0.108	0.448*	0.096
Z Acceleration (m/s^2)	Max	L	15.220	11.779	17.098	7.234	17.872	11.900	19.461	16.192	20.760	9.043
		NL	18.172	6.445	19.963	8.360	18.986	6.700	19.727	5.812	19.521	8.150
	Min	L	-20.895	8.084	-22.533	7.416	-26.414†	13.169	-25.442	7.698	-27.844†	11.881
		NL	-23.302	10.070	-23.221	8.091	-25.091	8.831	-26.979†	9.733	-25.873	9.459
	Avg	L	-1.852*	2.158	-1.780*	1.827	-1.717*	1.688	-1.682*	2.287	-1.522*	2.279
		NL	-0.521*	1.533	-0.948*	1.965	-1.180*	1.639	-0.711*	1.470	-0.854*	1.654

\

Table IV.5 - Cranial-caudal (X) movement of the fore hoof during the terminal 25% of swing at the walk. *See Table IV.1 for the remainder of the key.*

Terminal Swing			Baseline		Grade 1		Grade 2		Grade 3		After Block	
			mean	st dev	mean	st dev	mean	st dev	mean	st dev	mean	st dev
X Position (m)	Max	L	1.542	0.091	1.575	0.079	1.578†	0.082	1.549	0.079	1.540	0.106
		NL	1.559	0.099	1.578	0.089	1.581	0.090	1.565	0.093	1.561	0.120
	Min	L	1.288	0.085	1.321†	0.083	1.311	0.064	1.288	0.055	1.269	0.080
		NL	1.313	0.090	1.332	0.055	1.326	0.067	1.309	0.072	1.309	0.090
	Avg	L	1.455	0.085	1.487†	0.076	1.485	0.069	1.457	0.061	1.443	0.089
		NL	1.475	0.094	1.496	0.072	1.494	0.077	1.478	0.081	1.475	0.104
X Velocity (m/s)	Max	L	4.299	0.260	4.332	0.472	4.398	0.281	4.214	0.302	4.249	0.275
		NL	4.260	0.253	4.400	0.314	4.361	0.286	4.243	0.275	4.271	0.236
	Min	L	0.280	0.279	0.256	0.284	0.319	0.275	0.338	0.325	0.408†	0.284
		NL	0.294	0.182	0.262	0.215	0.265	0.232	0.301	0.241	0.313	0.262
	Avg	L	2.320	0.385	2.321	0.435	2.413	0.395	2.346	0.454	2.435	0.399
		NL	2.248	0.277	2.283	0.385	2.302	0.320	2.293	0.319	2.308	0.330
X Acceleration (m/s^2)	Max	L	-4.535*	11.712	-3.174	12.510	-5.795	12.634	-6.235	13.068	-6.790	12.711
		NL	-8.381*	7.871	-7.620	7.322	-7.821	8.432	-3.890	10.032	-6.765	10.751
	Min	L	-59.543	10.151	-59.089*	10.760	-59.537	10.961	-57.812	14.505	-61.984	17.089
		NL	-60.528	11.116	-65.118*	9.718	-60.453	9.025	-61.544	12.071	-60.812	12.073
	Avg	L	-35.444	2.902	-36.122	5.134	-35.657	3.237	-33.778	2.302	-33.449	3.121
		NL	-35.342	2.951	-37.034	4.120	-35.915	3.360	-34.439	2.479	-34.782	2.923

Table IV.6 - Vertical (Z) movement of the fore hoof during the terminal 25% of swing at the walk. *See Table IV.1 for the remainder of the key.*

Terminal Swing			Baseline		Grade 1		Grade 2		Grade 3		After Block	
			mean	st dev	mean	st dev	mean	st dev	mean	st dev	mean	st dev
Z Position (m)	Max	L	0.036*	0.011	0.038	0.010	0.036	0.009	0.037*	0.008	0.037	0.011
		NL	0.029*	0.007	0.032	0.008	0.032	0.005	0.030*	0.006	0.033	0.007
	Avg	L	0.021*	0.005	0.022*	0.004	0.021	0.004	0.022	0.003	0.022	0.006
		NL	0.017*	0.004	0.019*	0.004	0.020	0.003	0.019	0.004	0.021	0.005
Z Velocity (m/s)	Max	L	-0.051*	0.138	-0.043*	0.180	-0.032*	0.123	-0.031*	0.169	0.013*	0.159
		NL	0.069*	0.157	0.079*	0.200	0.035*	0.149	0.101*	0.156	0.063*	0.159
	Min	L	-0.606*	0.173	-0.643	0.156	-0.607	0.194	-0.624	0.178	-0.670	0.310
		NL	-0.534*	0.122	-0.575	0.121	-0.589	0.084	-0.599†	0.132	-0.615†	0.140
	Avg	L	-0.317*	0.099	-0.340*	0.109	-0.315*	0.088	-0.325*	0.081	-0.321*	0.106
		NL	-0.241*	0.072	-0.255*	0.079	-0.267*	0.064	-0.237*	0.060	-0.262*	0.078
Z Acceleration (m/s^2)	Max	L	29.815	6.624	30.785	7.436	30.116	7.835	30.329	6.461	31.067	10.099
		NL	25.357	7.630	28.169	9.023	28.656	6.083	29.007†	6.629	26.989	6.414
	Min	L	-17.372*	9.261	-18.892	10.322	-18.229*	10.361	-19.548*	13.966	-23.843	20.442
		NL	-22.061*	8.995	-25.939	10.715	-22.858*	7.741	-25.331*†	12.133	-22.724	9.470
	Avg	L	0.691*	3.092	0.733	3.252	1.199*	3.079	0.665*	2.958	1.103*	2.885
		NL	-0.915*	2.264	-0.649	2.809	-0.751*	2.180	-0.884*	1.961	-1.026*	2.213

Table IV.7 - Cranial-caudal (X) movement of the fore hoof during swing at the walk. *See Table IV.1 for the remainder of the key.*

Swing			Baseline		Grade 1		Grade 2		Grade 3		After Block	
			mean	st dev	mean	st dev	mean	st dev	mean	st dev	mean	st dev
X Position (m)	Max	L	1.542	0.091	1.575†	0.079	1.578†	0.082	1.549	0.079	1.540	0.106
		NL	1.551	0.095	1.571	0.088	1.568	0.089	1.551	0.092	1.534	0.108
	Avg	L	0.802	0.046	0.824†	0.045	0.820†	0.038	0.803	0.031	0.795	0.047
		NL	0.812	0.055	0.821	0.040	0.821	0.040	0.806	0.044	0.798	0.054
X Velocity (m/s)	Max	L	4.701*	0.360	4.759	0.249	4.739	0.219	4.587*	0.141	4.583	0.216
		NL	4.776*	0.321	4.875	0.343	4.781	0.231	4.673*	0.163	4.641	0.184
	Min	L	0.298	0.284	0.262	0.296	0.319	0.275	0.338	0.325	0.407*†	0.280
		NL	0.304	0.244	0.254	0.211	0.235	0.241	0.263	0.257	0.268*	0.246
	Avg	L	3.514	0.212	3.545	0.200	3.567*	0.176	3.446	0.167	3.455	0.178
		NL	3.529	0.227	3.579	0.219	3.503*	0.198	3.462	0.162	3.439	0.166
X Acceleration (m/s^2)	Max	L	53.020*	5.090	56.902	8.078	55.826	7.372	56.046	6.104	55.817	5.863
		NL	57.666*	9.618	57.556	8.488	55.459†	7.377	55.961	8.828	55.531	9.903
	Min	L	-59.985	10.508	-60.742	12.405	-59.537	10.961	-57.812*	14.505	-61.984	17.089
		NL	-59.213	10.023	-64.121	9.499	-59.000	7.801	-63.085*	12.862	-60.635	11.616
	Avg	L	-2.277	0.648	-2.308	0.717	-2.249	0.710	-2.048	0.842	-2.030	0.671
		NL	-2.093	0.533	-2.238	0.682	-2.192	0.649	-1.952	0.603	-2.023	0.609

Table IV.8 - Vertical (Z) movement of the fore hoof during swing at the walk. *See Table IV.1 for the remainder of the key.*

Swing			Baseline		Grade 1		Grade 2		Grade 3		After Block	
			mean	st dev	mean	st dev	mean	st dev	mean	st dev	mean	st dev
Z Position (m)	Max	L	0.074*	0.022	0.075*	0.022	0.074*	0.021	0.076*	0.022	0.079*†	0.022
		NL	0.063*	0.015	0.064*	0.014	0.061*	0.013	0.060*	0.015	0.062*	0.012
	Avg	L	0.043*	0.011	0.044*	0.012	0.043*	0.011	0.044*	0.011	0.045*	0.012
		NL	0.035*	0.009	0.035*	0.009	0.034*	0.008	0.033*	0.010	0.034*	0.008
Z Velocity (m/s)	Max	L	0.823	0.128	0.844	0.165	0.858*	0.175	0.900*	0.171	0.958*†	0.152
		NL	0.791	0.190	0.776	0.133	0.759*	0.120	0.768*	0.152	0.770*	0.133
	Min	L	-0.631	0.177	-0.703	0.240	-0.664	0.245	-0.694	0.229	-0.722	0.296
		NL	-0.589	0.179	-0.650	0.182	-0.661	0.163	-0.620	0.134	-0.691	0.239
	Avg	L	0.003	0.001	0.003	0.001	0.003*	0.001	0.000	0.018	0.004*	0.001
		NL	0.002	0.002	0.002	0.001	0.002*	0.001	0.002	0.001	0.002*	0.001
Z Acceleration (m/s^2)	Max	L	31.271	8.502	34.220	9.483	33.461	14.103	35.189	14.748	35.357	16.337
		NL	27.987	7.436	33.678	10.122	32.241	9.049	32.085	6.939	32.873	11.536
	Min	L	-25.108*	8.416	-31.349	14.343	-32.890†	14.470	-34.035	16.599	-38.968†	19.198
		NL	-32.462*	8.278	-36.122	13.541	-33.785	10.407	-35.605	7.969	-39.996	15.612
	Avg	L	-1.913	0.335	-1.985*	0.418	-1.891	0.380	-1.998*	0.334	-1.946	0.555
		NL	-1.800	0.551	-1.690*	0.353	-1.822	0.327	-1.728*	0.325	-1.821	0.355

Table IV.9 - Sagittal plane orientation of the fore hoof at the walk. *See Table IV.1 for the remainder of the key.*

			Baseline		Grade 1		Grade 2		Grade 3		After Block	
			mean	st dev	mean	st dev	mean	st dev	mean	st dev	mean	st dev
Break-over Orientation (°)	Max	L	-5.14	1.43	-4.83	1.25	-5.02	1.98	-4.67	1.49	-4.77	1.71
		NL	-4.72	1.45	-4.92	1.59	-4.80	1.19	-4.28	1.04	-4.54	1.20
	Min	L	-45.49*	4.99	-45.44*	4.50	-45.63*	4.31	-45.55*	4.61	-45.13*	4.37
		NL	-48.78*	4.55	-48.64*	5.47	-49.72*	5.10	-48.80*	5.25	-48.85*	6.02
	Avg	L	-19.20*	2.11	-18.92*	1.68	-19.18*	2.02	-19.00	1.89	-19.04*	1.73
		NL	-20.12*	2.47	-20.00*	2.22	-20.24*	2.17	-19.60	1.97	-19.99*	2.53
Initial Swing Orientation (°)	Max	L	-44.83*	5.01	-45.51*	4.12	-45.87*	4.03	-45.12	5.24	-45.52*	4.25
		NL	-47.77*	4.65	-49.31*	6.51	-49.58*	5.40	-47.40	4.60	-48.76*	6.38
	Min	L	-103.98	3.76	-104.42	3.05	-105.06	2.64	-103.33	2.27	-103.87	2.81
		NL	-103.06	5.08	-105.37†	4.61	-104.47	3.48	-104.47	2.40	-105.08†	4.44
	Avg	L	-88.69	3.71	-89.26*	2.74	-89.99	2.51	-88.29*	2.79	-89.21	2.59
		NL	-89.47	4.38	-91.21*†	3.90	-90.89†	2.61	-90.09*	2.50	-90.87	4.19
Terminal Swing Orientation (°)	Max	L	1.81	3.44	1.28	3.44	1.39*	3.11	0.91*	2.17	2.49	2.89
		NL	2.65	4.44	2.57	4.62	2.85*	3.71	2.79*	3.79	2.08	4.00
	Min	L	-37.79	3.91	-38.01	5.32	-39.13	4.93	-37.61	5.11	-39.18	5.37
		NL	-35.85	4.09	-36.63	6.62	-36.73	4.54	-36.04	4.07	-36.91	5.16
	Avg	L	-14.78	3.56	-15.31	4.14	-16.01*	3.97	-15.40	3.71	-16.10	4.06
		NL	-13.08	3.88	-13.13	4.60	-13.56*	3.89	-14.15	5.26	-15.49	4.99
Swing Orientation (°)	Max	L	2.02	3.56	1.39	3.54	1.39	3.11	0.91*	2.17	2.49	2.89
		NL	2.02	3.89	1.81	4.59	2.09	3.64	2.83*	3.50	1.63	3.92
	Min	L	-104.04	3.94	-104.18	3.65	-105.13	2.80	-103.86	2.22	-104.14	2.58
		NL	-104.55	5.44	-105.69	4.78	-104.28	3.37	-104.15	2.49	-105.10	4.12
	Avg	L	-64.70	3.36	-64.78	3.24	-66.53*†	3.29	-64.91	2.42	-66.07†	3.27
		NL	-64.57	3.98	-64.98	3.93	-64.57*	2.60	-63.99	3.29	-65.40	2.80

Table IV.10 - Hoof Contact at the walk. *See Table IV.1 for the remainder of the key.*

Hoof Contact		Baseline		Grade 1		Grade 2		Grade 3		After Block	
		mean	st dev	mean	st dev	mean	st dev	mean	st dev	mean	st dev
X position (m)	L	-0.0535*	0.0111	-0.0529*	0.0115	-0.0534*	0.0107	-0.0514*	0.0101	-0.0524*	0.0110
	NL	-0.0496*	0.0088	-0.0483*	0.0093	-0.0484*	0.0081	-0.0480*	0.0092	-0.0455*†	0.0102
Z position (m)	L	-0.0406*	0.0064	-0.0410*	0.0067	-0.0428*†	0.0075	-0.0435*	0.0082	-0.0451*†	0.0053
	NL	-0.0344*	0.0096	-0.0327*	0.0105	-0.0362*†	0.0078	-0.0339*	0.0087	-0.0336*	0.0091
X velocity (m/s)	L	0.3090	0.2905	0.2966	0.2933	0.2858	0.2829	0.3268	0.3047	0.3849	0.2900
	NL	0.3033	0.2098	0.2698	0.1955	0.2919	0.2418	0.3422	0.2470	0.3139	0.2661
Z velocity (m/s)	L	-0.2271	0.1109	-0.2275	0.0992	-0.2246	0.1217	-0.2059	0.1061	-0.2064	0.1569
	NL	-0.2397	0.0986	-0.2160	0.1595	-0.2625	0.0860	-0.2271	0.0929	-0.2434	0.1213
X acceleration (m/s^2)	L	-15.5272	11.7425	-14.8915	12.0815	-14.6547	9.7871	-17.7829	10.4144	-17.0348	10.6494
	NL	-14.6258	9.7982	-15.0141	8.9920	-12.8101	10.3054	-14.7131	9.5305	-15.9019	10.3813
Z acceleration (m/s^2)	L	22.8850	10.3413	24.5776	10.4013	24.9560	10.3359	23.8412	10.7967	25.6413	13.3807
	NL	20.6313	10.9220	22.1919	11.5877	26.4036	9.2750	22.3835	12.4416	22.1126	13.8755
Orientation (^{o})	L	0.6962	3.1649	0.6058	2.9047	0.5768*	2.4973	0.3689*	1.9621	1.5399†	2.8322
	NL	1.2022	2.7236	0.8101	2.7307	1.4062*	2.4221	1.8395*†	2.7232	1.1913	2.9598

Table IV.11 - Stride durations of the fore hoof at the walk. *See Table IV.1 for the remainder of the key.*

Durations		Baseline		Grade 1		Grade 2		Grade 3		After Block	
		mean	st dev	mean	st dev	mean	st dev	mean	st dev	mean	st dev
Stance (s)	L	0.804	0.051	0.786	0.068	0.799	0.067	0.831†	0.069	0.840†	0.047
	NL	0.819	0.046	0.792	0.065	0.805	0.064	0.840	0.065	0.838	0.050
Break-over (s)	L	0.092*	0.013	0.094†	0.015	0.095†	0.013	0.093†	0.012	0.092	0.010
	NL	0.096*	0.012	0.091	0.015	0.094	0.015	0.094	0.015	0.091	0.014
Swing (s)	L	0.439	0.022	0.440	0.022	0.439	0.014	0.446	0.015	0.442	0.017
	NL	0.437	0.015	0.436	0.020	0.444	0.016	0.444	0.018	0.442	0.018
Initial Swing (s)	L	0.110	0.006	0.110	0.005	0.111	0.003	0.111	0.004	0.111	0.004
	NL	0.110	0.004	0.110	0.005	0.111	0.004	0.111	0.005	0.111	0.005
Terminal Swing (s)	L	0.110	0.004	0.110	0.005	0.111	0.004	0.111	0.004	0.111	0.004
	NL	0.110	0.004	0.109	0.006	0.111	0.004	0.111	0.005	0.111	0.004

Table IV.12 - Sagittal plane range of motion of the fore hoof at the walk. *See Table IV.1 for the remainder of the key.*

Range of Motion		Baseline		Grade 1		Grade 2		Grade 3		After Block	
		mean	st dev	mean	st dev	mean	st dev	mean	st dev	mean	st dev
Break-over (°)	L	40.35*	4.66	40.61*	4.25	40.62*	4.16	40.88*	4.22	40.36*	4.08
	NL	44.06*	4.35	43.73*	5.53	44.93*	4.71	44.10*	4.62	44.33*	5.89
Initial Swing (°)	L	59.14*	5.29	58.91	5.10	59.19*	4.46	58.22	5.21	58.36	4.49
	NL	55.29*	5.59	56.06	7.65	54.89*	6.85	57.07	5.08	56.31	6.34
Terminal Swing (°)	L	39.61	5.17	39.28	6.60	40.52	5.52	38.52	6.19	41.67†	6.95
	NL	38.50	4.36	39.20	6.72	39.59	4.45	38.83	3.38	38.99	5.83
Swing (°)	L	106.07	4.81	105.58	4.01	106.52	3.74	104.77*	2.71	106.63	3.37
	NL	106.49	5.72	107.36	5.14	106.61	4.35	106.49*	3.46	106.20	4.47